Soil water regime and evapotranspiration of sites with trees and lawn in Moscow

Thesis committee

Thesis supervisor	Prof. dr. ir. P.C. Struik Professor of Crop Physiology Wageningen University
Thesis co-supervisors	Prof. dr. Olga V. Makarova-Kormilitsyna Head of the Soil Science Group Moscow State Forest University
	Dr. ir. A.J. Koolen Associate Professor Farm Technology Group Wageningen University

Other members

Prof. dr. ir. R. Rabbinge	Wageningen University
Prof. dr. ir. R.A. Feddes	Wageningen University
Dr. G.B.M. Pedroli	Alterra, Wageningen University and Research Centre
Prof. dr. M.C. Krol	Wageningen University

This research was conducted under the C.T. de Wit Graduate School:
Production Ecology and Resource Conservation.

Soil water regime and evapotranspiration of sites with trees and lawn in Moscow

Vasily V. Bondarenko

Thesis

submitted in partial fulfilment of the requirements for the degree of doctor

at Wageningen University

by the authority of the Rector Magnificus

Prof. dr. M.J. Kropff,

in the presence of the

Thesis Committee appointed by the Doctorate Board

to be defended in public

on Tuesday 1 December 2009

at 1.30 PM in de Aula.

Vasily V. Bondarenko (2009)
Soil water regime and evapotranspiration of sites with trees and lawn in Moscow, 171 pp.
PhD thesis, Wageningen University. With summaries in English and Dutch
ISBN: 978-90-8504-767-4

To my loved

ABSTRACT

Vasily V. Bondarenko, 2009. Soil water regime and evapotranspiration of sites with trees and lawn in Moscow. PhD thesis, Wageningen University, Wageningen, The Netherlands, 171 pp., with summaries in English and Dutch.

Situations where tree groups of the species *Tilia cordata* grow together with lawn grass (trees overlapping grass) were studied on five locations in Moscow, Russia, during six periods of the growing season of 2004. The measurements included: detailed descriptions of the soil profiles, tree and lawn dimensions, and, for each period, leaf area index (LAI), soil water content, and soil electric conductivity (EC). LAI was determined through taking photos with a digital camera and processing the photos with a digital image processing program. Using weather and LAI data and vegetation dimensions, the values of potential evapotranspiration of the vegetation combinations were calculated. These calculations followed FAO guidelines for computing crop water requirements. The reference evapotranspiration was also calculated according to Makkink's radiation model. The results resembled the values of the FAO reference. The measured values of soil water content were used to identify sites and periods with reduced evapotranspiration due to water stress. It appeared that incidence of water stress was very common. The measured soil water content values were transformed into ratios of actual evapotranspiration and potential evapotranspiration: so-called water stress factors. Using these factors, the actual evapotranspiration was calculated from the potential evapotranspiration values. The water regimes of each object and period were analysed. Deep percolation occurred in early spring and late autumn. The possibilities for rainwater to infiltrate the soil were very limited, due to degeneration of soil structure. The water balance of the root zones indicated that the root-zone volumes were smaller than in average forest conditions, and that runoff was extremely high.

Keywords: Urban vegetation, *Tilia cordata*, linden, lawn, grass, Leaf Area Index, LAI, digital image processing, evapotranspiration, water stress, electric conductivity, salinity stress, Makkink's radiation model, deep percolation, water infiltration, runoff, modelling

Contents

INTRODUCTION

Problem statement

Moscow, the capital of Russia, is one of the largest cities in the world. Its green areas include trees, lawns and shrubs. Trees are often small leaved Linden (*Tilia cordata*), growing in lawn and planted in groups. During recent decades, the condition of the vegetation was often very suboptimal.

A Russian measure to express the condition of trees is the “percentage of wilted leaves”, which ranges from 0 to over 75 for individual, living trees. A survey from Makarova (2003) showed that this percentage was more than 25 for half of the Linden stock in Moscow during 1999. This value may be compared with other cities, e.g. with The Hague, the governmental residence of The Netherlands.

A German measure to express tree condition uses four vitality phases (Roloff, 1989): exploration, degeneration, stagnation, and surrender to the dying process (resignation). Kareva (2005) assessed trees in the centre of The Hague according to this system. She found that in that environment almost all trees were in the exploration phase, i.e. in the highest vitality class.

Makarova (2003) studied whether tree condition and tree environment in Moscow were connected. The study included a wide range of environmental and physiological factors: contents of heavy metals in soil and leaf, nutrient contents in soil and leaf, abundance of de-icing salt, soil texture and structure, soil water content and transpiration of trees. Makarova concluded that water stress was a main cause for the suboptimal tree condition. This scientific result compares well with observations by the Urban Greening Department of the Moscow municipality, showing that the state of the trees in Moscow is better in years with wetter growing seasons than in years with drier conditions.

This thesis therefore elaborates the evapotranspiration of sites with trees and lawn and analyses the causes of the water stress.

Scientific background and assumptions

Key factors in the analysis of water stress are:

- potential and actual evapotranspiration of the vegetation and the soil;
- water stored in the root zone;
- rainfall;

- runoff of rainwater from the soil surface; and
- deep percolation of soil water from the root zone.

Measuring all these quantities individually under "undisturbed", in situ, urban conditions is very difficult. This especially holds true for actual evapotranspiration, runoff, and deep percolation. For such variables, predictions on the basis of well calibrated and validated models are necessary. In order to collect the necessary information on the key factors for water stress, it is therefore assumed that:

1. the amount of rainfall and soil water content can be measured accurately;
2. the potential and actual evapotranspiration can be calculated from climate and weather data, soil data, and measured leaf areas using appropriate models;
3. deep percolation and runoff can be estimated or derived from the balance equation for the water regime of the root zone.

It is further assumed that detailed knowledge on the above-mentioned key factors will allow development of measures that reveal the water stress. However, this aspect is subject of another project.

Aims of the studies

The objectives of the study were:

1. to study existing models for the estimation of evapotranspiration, with respect to use for Moscow city.
2. to define water stress for trees-lawn combinations using the chosen evapotranspiration model and characteristics of the urban climate, leaf area index (LAI) of the vegetation, and water characteristics of soil in the city conditions.
3. to assess principal reasons for water stress of the trees-lawn combinations and identify possible changes of water regime of the urban soil.

Thus the current thesis:

- reviews potential models to be used;
- identifies the most appropriate model;
- obtains accurate estimates for the key factors of water stress; and
- applies the most appropriate model to calculate the potential and actual evapotranspiration, water regimes, and water stress in tree-lawn combinations.

Approach

Site demands. The study was made for a range of selected sites in Moscow. The sites were selected so that they represented for Moscow:

- a common range of tree conditions;
- of the most frequent vegetation type;
- on the most frequent soil type;
- at medium tree age.

Selection was done by local experts.

The vegetation of each site consisted of a group of *Tilia cordata* trees that grew together with lawn. Throughout the thesis this vegetation type will be referred to by: trees-lawn combinations.

Model demands. The potential evapotranspiration of the selected sites will be calculated from climate and regular weather data using existing evapotranspiration models. The potential models should therefore be able to deal with:

- combinations of plant species (trees with lawn);
- high vegetation (trees); and
- non-pristine, sparse vegetation (low and unusual leaf area indices).

Moreover, the potential models:

- should already have been verified and widely accepted;
- do not need to model temperature regimes or growth and dry matter production;
- for experimental reasons, the time steps in the calculation should not be very short;
- do not need to provide detailed simulation.

It is preferred that the final models identified can be fully understood by the user (transparency wish). The thesis provides the basic theory for this understanding. It is also preferred that the user can implement and run the models using a standard spreadsheet. Calculation procedures will be described in such a way that they can be reproduced by the reader.

Calculations. The actual evapotranspiration of the selected objects will be calculated from the potential evapotranspiration values and the water content levels of the root zones. The amount of deep percolation from the root zone will be estimated from the soil water content at the bottom of the root zone. The rainfall data, the actual evapotranspiration and the amount of deep percolation will be inserted in a water balance of the root zone for each object in each period. This water balance diagnoses the water stress and will reveal the factors that are responsible for a suboptimal water regime. Thereafter, strategies to diminish the water stress problem are proposed.

Outline of the thesis

Chapter 1 sketches the relevant conditions in Moscow. The reader finds details on the climate, weather and atmosphere, as well as on soil genesis, hydrology and arboriculture.

Chapter 2 is devoted to modelling evapotranspiration and provides a detailed, logical, complete introduction into the commonly accepted theory of evapotranspiration. It is included in so much detail to comply with the transparency wish and to allow the reader to fully understand the background of the calculations and predictions. It starts with a classification of models according to Shuttleworth (1991), presents mechanistic models that are especially developed for trees with varying dimensions and canopy parameters, and concludes with a section on modelling evapotranspiration of non-pristine, sparse vegetation according to FAO guidelines (Allen et al., 1998). Based on accuracy considerations these guidelines will be followed in the further part of the thesis.

Chapter 3 is the "materials and methods" section. It describes characteristics and surroundings of the objects with *Tilia cordata* and lawn that are selected for the evapotranspiration and water regime research. It includes site descriptions, the results of a detailed soil survey, the methods that were used for measuring water contents and electric conductivities of the root zones at a number of points in time, and a quick and convenient procedure to find values of leaf area index (LAI) and fraction of ground cover of trees and lawn.

Chapter 4 presents collected data and the results of basic data processing. The chapter starts with the identification of growth stages of the Linden trees and the division of the 2004 growing season into six evapotranspiration periods. Then, for each period, the reference evapotranspiration of a reference surface is calculated from meteorological data of Moscow. The LAI values of the individual trees and lawn areas are presented, and combined in order to obtain values of the crop factor (potential object evaporation relative to a reference evaporation) for each of the objects and periods. In agrohydrology, such transformation factors are named "crop factors" even if the vegetation is not a crop. Finally, the reference evapotranspiration values are multiplied with the respective crop factors in order to find the potential evapotranspiration for each object and period.

Chapter 5 introduces the concepts of water stress and salinity stress, and water stress and salinity stress factors. The stress factors are calculated from the measurements of the water contents and electric conductivities of each object and period. Multiplying the potential evapotranspiration values with the respective stress factors gives the actual evapotranspiration of each object and period.

Chapter 6 is devoted to rainfall interception.

Chapter 7 uses the rainfall values, the actual evapotranspiration values, and the water content of the root zone in order to analyse the water regime of each object in each period. The analysis uses soil physical characteristics in order to establish the likelihood of the occurrence of percolation of root-zone water to deeper soil layers and runoff of rainwater from the surface of the objects.

Chapters 8 and 9 present discussion and conclusions, respectively.

CHAPTER 1. CLIMATE, SOIL AND VEGETATION IN MOSCOW

1.1. Location

Moscow is located between 55° and 56° northern latitude, and between 37° and 38° eastern longitude, between the rivers Oka and Volga. The area of the city is 1081 km^2. The population of the municipality Moscow amounts to 10.407 million persons. Moscow is divided into 10 administrative districts and 123 regions.

1.2. Climate

The climate of Moscow is moderately continental, but the degree of continentality is much higher relative to other large European cities. The annual temperature amplitude is in Moscow 28 °C, in Warsaw 22 °C, in Berlin 19 °C, and in Paris 16 °C. On average, the first frosts are observed on September, 29, and the last frosts are on average on May, 10; this means that the frost-free period is, on average, 141 days. This frost-free period, however, ranges between 98 and 182 days.

In Moscow, the vegetative period, *i.e.* the period with an average daily temperature of at least + 5 °C, is 175 days and extends from April, 18 until October, 11. On average, stable frosts begin on November, 24 and end on March, 10. Thaws in January and February are within 5–7 days after the start of a frost period, in December within 8–9 days, in November and March within 17–18 days. The average temperature in January is –9.4 °C and in July it is +18.4 °C. These have been considered to be stable reference values between 1961 and 1990 (norm). During recent years the mean annual air temperature has increased by 0.8 °C in comparison with the 1961–1990 norm and equals 5.8 °C. The mean winter temperature has increased by 2.2 °C, and in other seasons, the means increased by 0.4–0.5 °C (NN, 2005).

Arising above the big city is «the island of heat» (Barry and Chorley, 2003), which is formed in Moscow rather clearly. As a result the temperature in the city as a whole is 1.5–2.0 °C higher than in the vicinities. Throughout the year, the city centre is on average 1–2 °C warmer than the suburbs. In the city centre, frosts begin 2 weeks later and come to an end earlier. Consequently, the frost-free period in the centre is approximately a month longer than in the suburbs. In clear frosty nights, outside the city, it is sometimes 4–5 °C colder than in the city centre (10–12 years back: 2–3 °C). For 80 years, the mean annual temperature at the borders of the city did not change (3.8 °C). But in the central part of the city the temperature showed a remarkable increase during the past few decades. In 1976, the average temperature was 4.6 °C, in 1990 it was 4.8 °C, and in 1995 it had increased to 5.6 °C. And it still shows an increasing trend (Isaev, 2002; Hromov and Petrosynz, 2001).

The quantity of precipitation in Moscow usually equals 540–650 mm per year. On average there are per year in total 184 days with precipitation of at least 0.1 mm. On average for the last five years the annual quantity of precipitation equaled 760 mm, which is 1.2 times the long-term norm (644 mm). The maximum quantities of precipitation in these last five years were in July, August and October, the minimum quantity was observed in April. The majority of the total quantity of precipitation comes down during the warm period (75%). Rainstorms in the centre occurred 1.5 times more often than in the suburbs or out of the city. For the Moscow region, the quantity of precipitation typically decreases from the northwest to the southeast and the east. But in the city of Moscow, the quantity of precipitation increases by up to 190–220 mm (Isaev, 2002). More detailed information about air temperature and precipitation is presented in Table 1.1 and Figure 1.1.

A stable snow cover is established on about November, 26 (extremes: October, 31 and January, 9), and finally disappears by April, 11 (extremes: March, 23 and April, 27). The height of snow cover reaches on average 30–35 cm by the end of winter.

The greatest quantity of clouds in Moscow is observed from October until January, when the cloudiness of the sky averages 75–85%. For the last forty-years period in Moscow cloudiness has increased 10–17%. In the warm period of the year (April – September) cloudiness decreases to 48–60%. It can be connected with an increase in the frequency of an atmospheric, cyclonic-type, circulation in the cold period of year, and with the urban influence promoting an increase of the moisture content in the atmosphere. During the last 10 years high air relative humidity (> 70%) and rather high winter air temperature (> 0 °C) occurred more often.

Average monthly pressure of air from October until February does almost not vary and equals 748 mm, in summer months (June–August) 746 mm.

Winds in Moscow are possible in all directions. In the cold period of the year western, southwest and southern winds, caused by the general atmospheric circulation, prevail. Since May frequency of northwest and northern winds increases. One of the important meteorological characteristics is wind speed, especially its low values (0–1 m/s). Monthly average wind speed is 1.8–2.2 m/s. Frequency of wind speed 0–1 m/s (38%) and calms (18%)

Table 1.1. Air temperature and precipitation in Moscow

Months	Air temperature, °C			Precipitation, mm		
	mean (norm)	max	min	mean (norm)	max	min
January	–9.4	–5.8	–11.7	43	98	5
February	–7.7	–4.5	–11.2	37	94	2
March	–2.2	1.2	–6.1	34	88	6
April	5.8	10.5	1.6	44	110	3
May	13.1	18.1	7.3	49	160	2
June	16.6	21.9	11.6	62	190	5
July	18.4	23.2	13.4	83	295	8
August	16.4	21.5	12.1	75	270	1
September	11.0	15.5	7.2	54	200	7
October	5.1	8.1	2.1	49	185	2
November	–1.2	0.6	–3.9	58	140	4
December	–6.1	–3.5	–8.4	56	112	13
Year	5.0	9.0	1.3	644	883	397

has increased as compared with the long-term norm. The greatest frequency of weak winds for these years was observed in May–June (51%). Thus, we can observe a tendency of decrease of wind speed in the city (in comparison with suburbs), which is most likely connected with growth of urban territory and increase of surface area and of the number of stories of buildings. The largest frequency of calms and low wind speeds between apartment blocks occurred in extended zones that were generated in the north, the south and in the centre of Moscow.

The natural cycle of temperature, distribution of precipitations, air humidity, solar light and other meteorological factors considerably changed in connection with intensive increase of the area of city buildings and with development of the collecting system that quickly drains off rain water. This is connected with the large quantity of stone constructions and the large areas of roofs and asphalt coverings. In the process of growth of the city and growth of the difference between the climates of Moscow and the Moscow suburbs each of these factors became more significant.

More and more often, thaws and more frequent negative combinations of temperature and humidity create discomfort and negatively influence conditions of vegetation, roads, buildings, and communications.

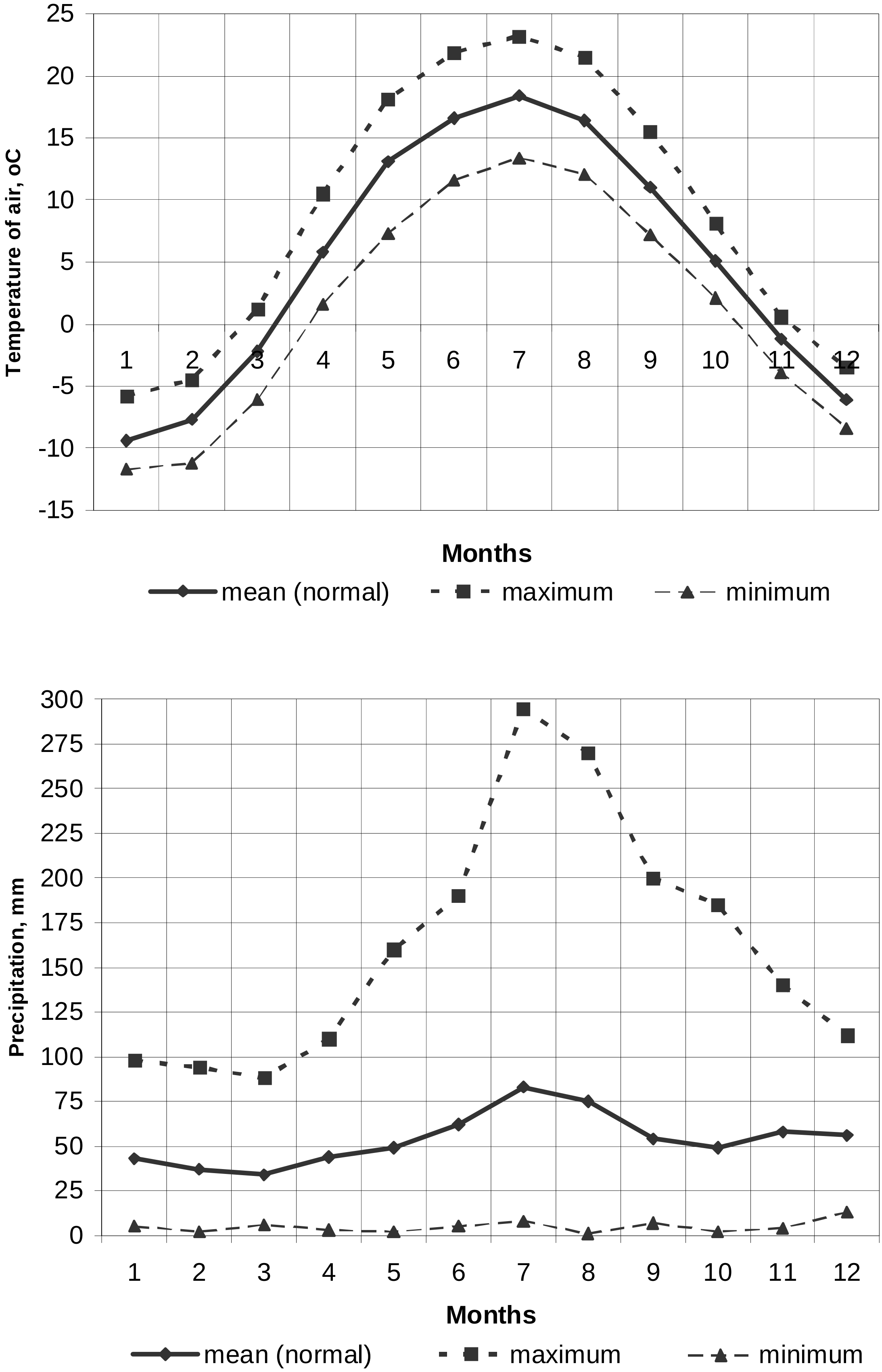

Fig. 1.1. Air temperature and precipitation in Moscow

1.3. Hydrological conditions

The hydrographic network of the city of Moscow represents a complex of water objects consisting of more than 140 rivers and streams and more than 430 natural and artificial reservoirs. The basic rivers of the city territory are the Moscow-river and its large inflows Yausa, Setun, and Shodnya, which each have lengths of more than 25 km in Moscow (Zubov, 1998).

The Moscow River, the main waterway of the city, crosses Moscow from northwest to southeast. The length of the river part within the city equals almost 80 km. The air regime of the central part of the city and valley of the Moscow River has special temperature and geomorphologic conditions. Due to a difference of temperatures (1–1.5 ^{o}C), air streams go from periphery to city centre.

Water objects of the city experience big anthropogenic influence, which is related to their use for industry aims and power engineering, cultural and community water consumption and recreation, and also to runoff removal, groundwater and sewage.

1.4. Geomorphologic conditions

Moscow is located on three physiographic areas (Lihacheva, 1996):

1. Smolensko-Moscowskaya moraine height, located in the northwestern part of Moscow. It includes smoothed relief forms with absolute heights of 175–185 m above sea level.

2. Moscvorecko-Okskaya, a moraine-erosive plane coming into the city from the south and named «Teplostanskaya height». It represents an erosive surface with absolute heights of 200–250 m. It is deeply cut by ravines.

3. Mescherskaya zandrovaya, lowland, located in the east-city parts. It represents flat sandy lowland with separate moraine raisings and superficial depositions of Jurassic clay and Carbonic lime stones covered with water-glacial sand and sandy loams. Absolute relief has heights up to 160 m. Pine woods on sandy sod-podzol soils are widely distributed. On separate sites are well-developed peat-podzol soils.

The territory of the city is located at a height of 150 m above sea level, with a height of 30–35 m relative to the level of the Moscow River. About 30% of the territory of the city is occupied by a valley of the Moscow River which includes floodlands and terraces. East and southeast are the lowest parts of the city (Mescherskaya plane).

The modern relief of Moscow is substantially formed by sediments of the glacial epoch (Moscowskaya and Dneprovskaya moraines) and erosive activity of the rivers. However, as a result of economic and building activities there is a change of relief of the city territory: ravines and floodlands are covered with earth; hills and slopes are leveled; rivers and streams go to underground collectors (Stroganova et al., 1997). Thus, modern anthropogenic sediments which have depths from 3 to 20 m form a rather significant area. In these conditions, parts of the mother bed remained natural, and parts of the motherbed became also a cultural layer, banked, and with alluvial material.

1.5. Urban soil

As a result of the anthropogenic influence, there is an intensive transformation of natural peat soil, floodplane soil, and podzolic and sod-podzol soils with different degrees of podzolic and gley processes and organic mater contents into specific soil: anthropogenic, surface reformed natural soil («urbo-soil»); anthropogenic, deeply reformed soil («urbanozem»); «technozem».

«Urbo-soil» combines the top layer created as a result of human activity ("urbic", a non-agricultural layer) having a depth less than 50 cm with the undisturbed middle and bottom parts of soil profiles.

«Urbanozem» has an "urbic" layer, consisting of one or several layers (U_1, U_2, etc.), with a depth of more than 50 cm, that originated by mixing, covering, or pollution with urban materials, including debris (Bockheim, 1974; Gerasimova et al., 2003). The profile of «urbanozem» is characterized by the absence of natural genetic horizons down to depths of 50 cm and more. Mechanically (physically) and chemically transformed soils exist.

«Technozem» are artificially created and designed surface formations (soils; grounds; substrates), enriched with organic layers and consisting of one or several layers.

According to research studies (Makarova, 2003), the soils of the Moscow region are exposed to a washing water regime and under actions of a podsolic process. As a result of migration of clay particles downwards in the profile, dust particles always concentrate in the top part of the soil. In the anthropogenic conditions of Moscow these processes are maintained, but accumulation of dust particles occurs in higher amounts, due to deflation of these particles from bare soil surfaces and due to significant initial contents of dust particles in soil substrates for plants. Change of the soil texture and soil structure also changes the physical, chemical and biological properties of the soil. So, for example, when there is a destruction of the structure of a top layer, its density is increased and thus its porosity and water penetration decrease. The organic matter content in the root zone can change from 2–7% up to 15–25% and more. The pH_{KCl} reaches values of 6.9–7.8; the concentrations of some exchange cations and nutrient elements are on average equal to: Ca^{2+}: 20–50 mg-equivalent/100 g soil; Mg^{2+}: 2 mg-equivalent/100 g soil; P_2O_5: 5–27 mg/100 g soil; K_2O: 10–21 mg/100 g soil. These values are in excess of values that are typical for natural soils (Stroganova and Agarkova, 1992).

Moreover, relevant factors are the high contents of heavy metals in soils (Pb, As, Cu, Zn, Cd, Ni) and the salinization of the soil (NaCl, $CaCl_2$, etc.) as a result of using de-icing mixes in the winter period, because their high concentration can have a negative effect on the condition of various components of the environment (Lihacheva and Smirnova, 1994).

1.6. Urban vegetation

The total size of the green areas of the city (trees, shrubs, lawns) equals about 16785.8 ha. The most widespread species are: *Tilia cordata* – 19.5%; *Acer platanoides* – 9.7%; *Populus balsamifera* – 6.7%; *Fraxinus pennsylvanica* – 6.0%; *Acer negundo* – 5.6% (NN, 2004).

According to a monitoring of the condition of urban vegetation during 1999–2004 (NN, 2003; NN, 2004; NN, 2005), more than 90% of the *Tilia cordata* trees have categories 1; 2; 3; 4 (Table 1.3, Fig. 1.2). The classification of tree state categories is presented in Table 1.2. (Mozolevskaya et al., 1996; cited in Makarova, 2003).

Occasional improvement of the condition of plants was also reported, which was explained by a favourable combination of climatic factors, the use of less dangerous new-generation de-icing mixes in the winter period, and /or improvement of the maintenance of plants.

More than 77% of the plantings along highways are linear planting, and about 53% of the plantings in the streets are alleys and tree groups. In most sites there is a combination of trees and lawn.

In conditions of such a large megalopolis, as the city Moscow, a large number of various natural and anthropogenic factors influence the vegetation. So, for example, the industry of Moscow includes more than 10,000 industrial enterprises placed on an area of 1080 km^2 with a volume of emissions of about 91,000 tons per year; the number of cars is

Table 1.2. Classification of tree state categories

№ of category	Tree state categories (visual estimation)
0	No signs of weakening
1	Trees with less than 25% of leaves wilting
2	Trees with 25–50% of leaves wilting
3	Trees with 50–75% of leaves wilting
4	Trees with over 75% of leaves wilting
5	Dead wood of the current year
6	Dead wood of previous years

more than 3,000,000 units (NN, 2005). A detailed description of the factors influencing the condition of the city vegetation is presented in the research report of Makarova (2003): ecological conditions of the city; technologies of planting and maintenance of plants; the state of the soil; anthropogenic (accidental) factors; cost of planting.

Table 1.3. Distribution of trees (*Tilia cordata*) by Tree State Categories in Moscow during 1999–2004

Year	Distribution of trees (*Tilia cordata*) by Tree State Categories, %						
	0	1	2	3	4	5	6
1999	0.6	36.5	39.8	18.0	4.4	0.5	0.2
2000	0.6	27.3	35.6	26.6	8.6	0.9	0.4
2001	3.9	24.1	38.0	26.1	5.9	1.6	0.4
2002	5.9	37.6	40.6	11.1	3.0	1.3	0.5
2003	0.4	32.6	45.0	15.9	4.4	1.2	0.5
2004	0.2	40.7	37.7	18.7	2.0	0.4	0.3

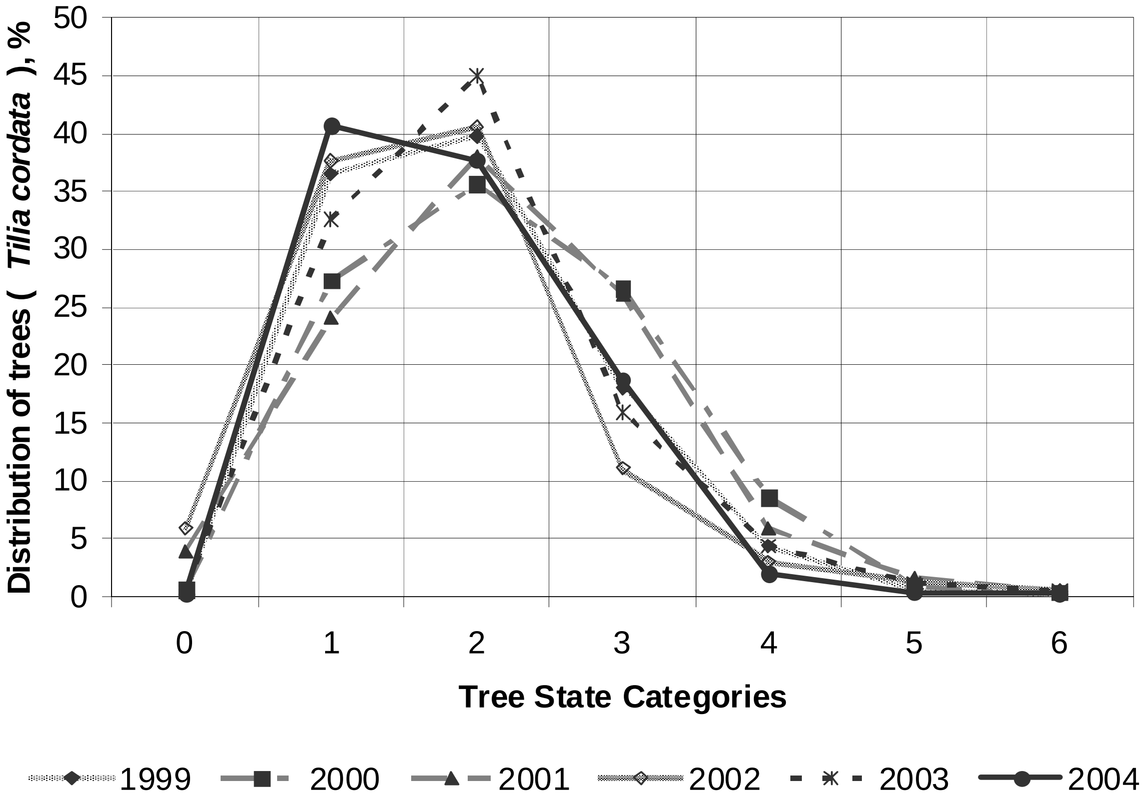

Fig. 1.2. Distribution of trees (*Tilia cordata*) by Tree State Categories in Moscow during 1999–2004

1.7 Conclusion

The significance of the above information in connection with the thesis may be summarized as follows.

The climate of Moscow is not only determined by a high continentality, but also by strong effects of the city. Relative to the surroundings, these urban influences increase Moscow temperature, cloudiness and air relative humidity and decrease wind speed, all playing roles in the level of evapotranspiration.

The soils of Moscow often have high organic mater content (especially in the top part of a profile), contain a large amount of dust particles and often have bad structure. This structure is very sensitive to damaging actions (NN, 1965; Schachtschabel et al., 1989), which often are very intensive under urban conditions.

Tilia cordata is the most important planting of Moscow. The thesis concentrates on this species. Janson (1994) classifies *Tilia cordata* as a tree that has little demands to the soil.

CHAPTER 2. EVAPOTRANSPIRATION.
REVIEW, MODELS AND MODEL SELECTION

2.1. Introduction

Results of scientific research on hydrometeorological aspects of trees-lawn combinations under urban conditions are very scarce. Therefore, we studied literature on similar vegetation categories:

- stand-alone trees;
- mixed vegetation in agroforestry;
- forest with transpiring understorey;
- orchards and vineyards.

Stand-alone trees. Literature on the transpiration of stand-alone trees may throw the reader in confusion. On one hand, a common opinion is that, in urban conditions, trees transpire more than comparable forest trees, due to stronger winds, drier air, and light reflection by buildings and pavements. On the other hand, it may be reasoned that the micro-climate in the crown of a stand-alone tree resembles the climate remote from the tree rather than a condition that would exist if the tree was close to similar trees (forest situation). Generally, the micro-climate of surfaces without trees induces a lower transpiration potential than the micro-climate of forested surfaces, because the roughness of forest produces stronger air turbulence (Eagleson, 2002). The micro-climate in streets of villages, towns, and small- and medium-sized cities may be totally different from that of a large city like Moscow (see Chapter 1). Landsberg and McMurtrie (1984) assessed whether water use by isolated trees can be calculated from weather data, and the consequences of water uptake in terms of soil drying patterns. Landsberg and McMurtrie presented concepts. Vrecenak and Herrington (1984) modelled transpiration from urban trees in 75 litre containers. The frequency of measuring data collection was 1 $hour^{-1}$. The conditions of an individual urban tree often interact with those of neighbouring trees. In order to deal with this problem, Eagleson (2002) started from two extreme situations. One extreme was a tree spacing that was comparable with a forest situation. The other extreme situation included only one tree, on an infinitely large, not transpiring, surface. Eagleson derived the transpiration of the latter situation from the former situation through very rough approximations. He calculated the transpiration of situations between both extremes (sparse vegetation of trees on a not-transpiring surface) through linear interpolation between the two extremes. Combinations of alleys or groups of trees and lawn grass areas are even more complicated because the lawn grass also contributes to the evapotranspiration. McMurtie and Wolf (1983) explored conditions for the coexistence of trees and grass using a mathematical model describing plant competition for radiation, water and nutrients. The model describes growth of both species in terms of key physiological processes (radiation interception, photosynthesis, respiration, grazing, litterfall, assimilate partitioning, nutrient uptake and water use). They used the model to demonstrate how species compete by depriving each other of resources essential for growth. Changes of growth parameters are shown to lead to shifts in species composition (e.g. through replacement of one species by another). Scholes and Archer (1997) reviewed literature on tree-grass interactions in savannas. These authors state that the coexistence of apparent competitors can be accounted for ("modelled") in different ways. A first way is that competitors avoid competition by using resources that are slightly different, obtained from different places, or obtained at different times (niche separation by depth or by phenology). A second way is balanced competition: balancing through increasing negative effects for the species that is in a period of winning the competition. If no balance is possible under normal conditions, incidental events/disasters may occur that suppress the stronger species, fires being a classic example.

Agroforestry is a farming system that integrates crops and/or livestock with trees and shrubs. The resulting biological interactions provide multiple benefits, including diversified income sources, increased biological production, better water quality, and improved habitat for both humans and wildlife. Farmers adopt agroforestry practices for two reasons. They want to increase their economic stability and they want to improve the management of natural resources under their care. Agroforestry systems, especially for temperate climates, have not traditionally received much attention from either the agricultural or the forestry research communities (Beetz, 2002). One can find proceedings of a number of scientific meetings and monographs devoted to modelling for agroforestry (NN, 1994; Sinoquet and Cruz, 1995; Auclair and Dupraz, 1999). They do not include comprehensive, robust, models. Mayus (1998) modelled transpiration and growth of millet in windbreak-shielded fields in the Sahel. Her simulation results showed good agreement with the experimental data from an experimental field in Niger.

Forest with transpiring understorey. The understorey of forest trees often accounts for a significant proportion of forest evapotranspiration. Black and Kelliher (1989) discuss the role of the understorey radiation regime, and the aerodynamic and stomatal conductance characteristics of the understorey in understorey evapotranspiration. Values of a so-called decoupling coefficient for the understorey in Douglas-fir stands indicated considerable coupling between the understorey and the atmosphere above the overstorey. Kelliher et al. (1986) estimated the effects of understorey removal from a Douglas-fir forest using a two-layer canopy evapotranspiration model (Shuttleworth and Wallace, 1985). The model used meteorological data measured hourly at different heights above the canopy and in the tree crowns, and meteorological measurements near a salal understorey taken at a frequency of 0.1 s^{-1}. There was generally good agreement between modelling and experimental results. Using a similar approach, Spittlehouse and Black (1982) determined, in a Douglas-fir forest with salal, the evapotranspiration of the Douglas-fir overstorey and the evapotranspiration of the salal understorey separately.

Orchards and vineyards have great importance for economy of many countries. Much research has been done in order to analyse and predict accurately their water requirements. This research is based on lysimeter experiments and detailed measurements of weather and soil water contents, in different climates. It resembles agricultural research for other crops. A group of experts worked during 8 years to update the FAO Irrigation and Drainage Paper No. 24, published in 1977 (Allen et al., 1998). The update distinguishes a large number of agricultural crop categories, among them vineyards and orchards. It treats also “natural, non-typical and non-pristine vegetation”. The paper refers to over 300 research publications. It is the prediction method described in this paper that is followed in our research. The method is described thoroughly later in this chapter. First, sections follow that are needed for understanding and judging the FAO method, and putting it in a right perspective.

A main aim of the thesis is the calculation of potential evapotranspiration of selected sites with trees and lawn in Moscow. The calculation should only use regular weather data and canopy parameters. The modelling should be able to deal with non-pristine, sparse, tall, vegetation, and produce reproducible results. It should be based on existing models that already have been verified and does not need to model temperature regimes or growth and dry matter production. For experimental reasons, the time steps in the calculation should not be very short. Detailed simulation is not intended. Many mechanistic models exist. Such models often suffer from inaccuracy and need a vast amount of input data. But they provide much insight. Evapotranspiration calculations for practical purposes often follow empirical-analytical methods. They often combine empirical crop factors with a mechanistic model like the Penman-Monteith equation. Section 2.2 classifies evapotranspiration models according to a scheme that is developed by Shuttleworth (1991), and reviews significant models and submodels. Section 2.3 lists the mathematical procedures for the application of two empirical-analytical methods: Makkink's radiation model and the computation according to FAO guidelines. Section 2.4 justifies the use of the FAO guidelines in the further part of the thesis.

2.2. Review of models: model types – models – submodels

2.2.1. Model types. Classification of evaporation models according to Shuttleworth

Many evaporation models exist. A description of many models is presented in NN (1996a). Shuttleworth (1991) classified evaporation models, mainly through the meteorological input they require and the type of evaporation they provide (e.g. actual evapotranspiration, potential evapotranspiration, transpiration E_T, evaporation of a reference crop E_{RC}, potential evaporation E_0). Now his reasoning follows.

Simulation models

When one aims at estimation of actual evaporation, a logical approach is to build a model that tries to simulate the physical and physiological processes that actually occur in the real situation.

Usually these models are built in one dimension, and attempt to simulate evaporation from vegetation by including all the information available for the vegetation stand under study, e.g. its structure and form, and submodels of its stomatal behaviour in response to meteorological parameters. The model must also be supplied with short-term measurements of the meteorological conditions above the canopy as input, and then simultaneously solves all the equations describing the canopy using these as a boundary condition. In doing so, it generates simulated profiles of temperature, vapour pressure and the heat fluxes.

Generally, the vegetation is divided into a finite number of horizontal layers. About 10 layers are usually used, and for each layer the interception of solar and thermal radiation is calculated, and partitioned into sensible heat, latent heat, and photochemical energy. Iterative procedures are used until an energy balance is achieved for all foliage layers.

Such models must be considered the best available method of predicting actual evaporation, given extremely high data availability; and providing the required submodels are available.

Single source models

Single source or "big leaf" models of plant canopies consider the overall effect of the whole canopy reasonably approximated by a model that assumes all the component elements of the vegetation are exposed to the same microclimate. In the general model, the sensible heat and latent heat from the vegetation are assumed to be generated at one and the same height (the so-called "effective source sink height") in the canopy, and are merged with those from the soil beneath. They then pass through additional resistances to reach some level above the canopy, "the screen height", at which measurements of temperature and vapour measurements are made.

Although simulation and single source models are superior to all other techniques, in that they provide a direct estimate of actual evaporation, their use is inhibited by the current lack of short-term meteorological data sets, and the submodels of stomata resistance required for their implementation.

Intermediate models

The prior section treated single source models. The section after the section under discussion (intermediate models) will treat energy balance models. Between the single source models and energy balance models a group of intermediate models may be distinguished. The energy balance models provide estimates of the evaporation of a reference crop E_{RC}, the evaporation of a water surface E_o, or the evaporation of a saturated land surface. In order to increase the applicability of energy balance models beyond E_{RC} and E_o, energy balance models have been extended with submodels. The extended energy balance methods provide estimates of crop transpiration E_T. An example of such an extension is the inclusion of a relationship that can predict the aerodynamic resistance against upward transport of heat and vapour, not only from the wind velocity at screen height but also from canopy parameters. Another example is the inclusion of distinct submodels for "dry crop" transpiration and for evaporation of rainfall that was intercepted by the canopy. Section 2.3.2 (FAO guidelines) is an example of an intermediate model.

Energy balance models

The Penman equation is the original and typical example of energy balance models. It calculates the energy used for evaporation from a free water surface (E_o) as the difference between the net radiation energy received by the free water surface and the energy lost by the free water surface in the form of sensible heat. The energy used for evaporation from the free water surface is equal to the amount of evaporation (upward vapour transport from the water surface to screen height) multiplied by λ, the latent heat of vaporization per unit mass of liquid water. The net radiation energy received by the free water surface is equal to the sum of the total incoming solar (shortwave) radiation and downward longwave radiation, minus the sum of the reflected solar (shortwave) radiation and the upward longwave radiation (heat fluxes in the water under the water surface are usually neglected). The energy lost by the free water surface in the form of sensible heat is equal to the temperature difference between the water surface and the temperature at screen height, multiplied by the amount of upward air transport from the water surface to screen height, and multiplied by the specific heat of air. The rate of upward vapour and air transport depends on turbulent movements in the boundary layer of the atmosphere, in such a way that the rate of upward (vertical) transport increases with increasing (horizontal) wind velocity at screen height. This dependency is modelled by a so-called wind function $f(u)$.

Following the above reasoning for a reference crop, a model for the calculation of the potential evaporation of the reference crop E_{RC} is obtained.

Radiation models

Penman's elaboration of his model led to an equation showing that the rate of evaporation consists of two parts: a part that is proportional to the net radiation, and a part that is proportional to the vapour pressure deficit at screen height (the saturated vapour pressure at screen height minus the actual vapour pressure at screen height). It appears that an empirical relationship exists between the two parts. Moreover, the first part is commonly four to five times larger than the second. Both facts explain why simple models exist stating that, albeit evaporation energy is not equal to the net radiation energy, evaporation energy of a reference crop is proportional to the net radiation energy. In a number of cases, the energy which is used for evaporation appeared to be near equal to the net radiation. Makkink's model, described in Section 2.3.1., is an example of a radiation model.

Humidity models

Although it may be expected that evaporation correlates less with vapour pressure deficit than with net radiation (see above), models exist that assume proportionality between crop evaporation and vapour pressure deficit at screen height. The proportionality factor may be a wind speed dependent empirical expression.

Temperature models

Several empirical formulas exist which relate reference crop evaporation to temperature. The physical basis for them is that both the net radiation and the vapour pressure deficit are likely to have some, albeit ill-defined, relationship with temperature. The only real justification for using models of this type is that an estimate of evaporation is required on the basis of existing data, and temperature is the only measurement available.

2.2.2. Penman model and Penman-Monteith model

Penman model

Literature shows that the well-known Penman model for the evaporation from a free water surface can be derived in many ways (Penman 1948; Penman 1963; Goudriaan, 1977; Frere, 1979; Frere and Popov, 1979). The next derivation follows Van Keulen and Wolf (1986). Penman assumed that the air close to the water surface is always saturated, and wrote, for the energy balance at the evaporating free water surface,

$$R_N = H + LE = h_u (T_s - T_a) + \frac{h_u}{\gamma}(e_s - e_a)$$

R_N = net radiation [J m^{-2} day^{-1}],

H = sensible heat loss [J m^{-2} day^{-1}],

LE = energy used for evaporation (L = latent heat of vaporization of water; E = rate of water loss at the surface) [J m^{-2} day^{-1}],

h_u = sensible heat transfer coefficient [J m^{-2} day^{-1} ^{o}C^{-1}],

T_s, T_a are air temperature at the surface and air temperature at screen height, respectively [ºC],

γ = the psychrometer constant, expressing the physical connection between sensible heat transport and vapour transport by the moving air [mbar ºC^{-1}],

e_s, e_a are vapour pressure at the surface and vapour pressure at screen height, respectively [mbar].

When, in addition to E, the quantities T_s and e_s are also unknown, the above equation can still calculate E using the Penman linearization of the temperature – saturated vapour pressure curve (see Fig. 2.1.):

$$e_s - e_a = \Delta(T_s - T_d)$$

T_d = the dewpoint of the air at screen height, i.e., the temperature at which the vapour in the air at screen height would start to condense or, in other words, the temperature at which the actual vapour pressure in the air at screen height would be the saturated vapour pressure [ºC],

Δ = slope of saturation vapour pressure curve [kPa ºC^{-1}].

After substituting this linearization into the first equation, making T_s explicit, and combining with

$$R_N = H + LE \qquad \text{and} \qquad H = h_u(T_s - T_a)$$

we obtain the well-known Penman equations for the evaporation from a free water surface:

$$LE = \frac{\Delta}{\Delta + \gamma}(R_N + h_u(T_a - T_d))$$

or, using in addition the linearization $T_a - T_d = (e_d - e_a)/\Delta$

$$LE = \frac{1}{\Delta + \gamma}(\Delta R_N + h_u(e_d - e_a))$$

e_d = the saturation vapour pressure at the air temperature at screen height, i.e., the vapour pressure at screen height if the air at screen height would be saturated [mbar].

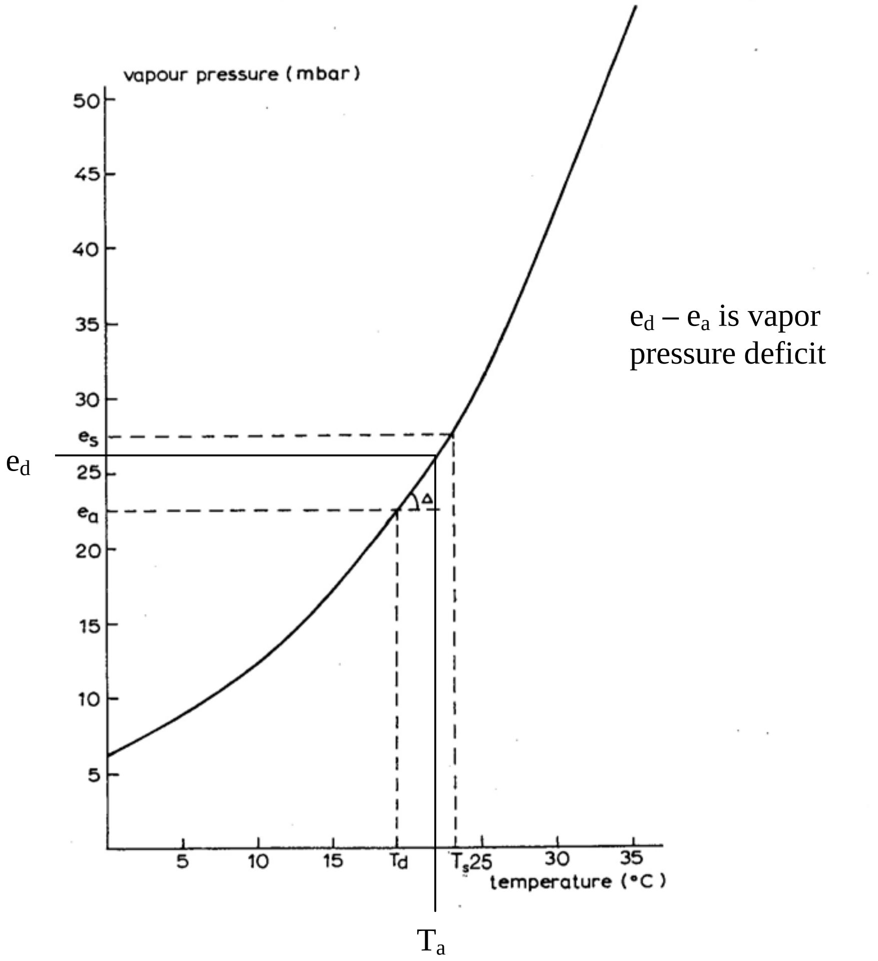

Fig. 2.1. The relation between temperature and saturated vapour pressure.

The figure is obtained by elaboration of Fig. 22 from Van Keulen and Wolf (1986). T_a = air temperature at screen height, T_s = surface temperature, e_a = actual vapour pressure at screen height, e_s = saturated vapour pressure prevailing at the surface, T_d = the dewpoint of the air at screen height, e_d = the saturation vapour pressure at the air temperature at screen height.

The sensible heat coefficient h_u can be considered as a conductivity, and its reciprocal $(1/h_u)$ as a resistance. Often, h_u is substituted using

$$h_u = \rho\, c_p / r_a$$

in which:

r_a = atmospheric or aerodynamic resistance (with units "time divided by length") [d m^{-1}],

ρ = air mass density [kg m^{-3}],

c_p = specific heat of air [J kg^{-1} ^{o}C^{-1}], Substitution of $h_u = \rho\, c_p / r_a$ in the last Penman equation gives the most widely used form of the Penman model:

$$LE = \frac{1}{\Delta + \gamma}(\Delta R_N + \rho\, c_p (e_d - e_a)/r_a)$$

Penman's model is not only suitable for free water surfaces, but also for closed short canopies that are well supplied with water from the roots. This is because under these conditions the evaporation from the wet inner surfaces of the very many leaf stomata is similar to the evaporation of a free water surface. The model can also successfully be applied to saturated bare soil surfaces.

<u>Penman-Monteith model</u>

Experiments have shown that the above form of the Penman equation is less suitable for vegetated surfaces when the water supply from the roots is limited and/or when the canopy is not closed and short. For these conditions, Monteith combined the Penman equation with theory on canopy resistance against evaporation from the wet inner surfaces of the stomata. This combination is known as the Penman-Monteith model (Monteith, 1965; Rauner, 1976; Monteith, 1981).

We consider a canopy that supplies sensible heat and water vapour to the atmosphere above the canopy. Sensible heat is transferred from the canopy surfaces to the air surrounding the canopy parts. The surrounding air is transported upwards to screen height by turbulent flow. The upward transport of sensible heat is proportional to the mass of upward air transport and to the temperature difference between canopy and screen height. The upward transport, from canopy to screen height, of an air volume in the turbulent air movements takes some time. From a physical point of view, this time dependency can be considered to be similar to the concept of "resistance" that is used for electric currents or fluid flows. So, we may say that the upward transport of air volumes encounters resistances, during their movement through the canopy, and during their movement between the canopy top and screen height. In the Penman-Monteith model, both resistances are combined in the so-called aerodynamic resistance r_a.

The transport of vapour from the neighborhoods of the leaves to screen height is also connected with the turbulent air movements, which implies that the aerodynamic resistance for vapour is very similar to the aerodynamic resistance for sensible heat. But the water vapour has to overcome an additional resistance, namely the resistance encountered during its movement from the wet inner stomata walls, through the stomata openings, to the air surrounding of the leaves: the so-called canopy resistance r_c. Therefore, Monteith assumed that the movement of water vapour from the evaporating inner stomata walls to screen height encounters the resistance $r_a + r_c$. The combination of this concept with the Penman model is known as the Penman-Monteith model.

The form of the Penman-Monteith model can be derived in many ways. In this section, we follow the reasoning in Rowntree (1991). Rowntree wrote, for the energy balance at a vegetated surface,

$$R_N = H + LE = \frac{\rho\, c_p}{r_a}(T_s - T_a) + \frac{\rho\, c_p}{\gamma\,(r_a + r_c)}(e_s - e_a)$$

Following similar mathematical procedures as for the derivation of the Penman model, the last equation can be transformed into the Penman-Monteith model:

$$LE = \frac{\Delta R_N + \rho\, c_p (e_d - e_a)/r_a}{\Delta + \gamma\,(1 + r_c / r_a)}$$

It can be seen from the equations that the Penman-Monteith model may be obtained from the Penman model by replacing γ by $\gamma\,(1 + r_c / r_a)$. The ratio r_c / r_a is known as the resistance ratio. For wet canopy, $r_c = 0$. Then, the Penman equation and the Penman-Monteith equation are the same. When the canopy is dry and the stomata are closed, the value of r_c is infinitely large. Then, the above equation predicts that the evaporation is zero. It should be noted that the derivation of the Penman-Monteith equation may be based on different physical reasoning.

E.g. Eagleson uses the same form although he neglects the stomata resistance in calculating the canopy resistance (Eagleson, 2002, p. 140 and p. 145).

2.2.3. A range of submodels

Wind profile

The height-dependent wind velocity near the earth surface plays a large role in evaporation. The horizontal wind velocity at a certain height above the earth surface varies with height and depends on the wind velocity at screen height, canopy properties and properties of the earth surface. Fig. 2.2 (from Brutsaert, 1982) is a definition sketch for the relevant quantities.

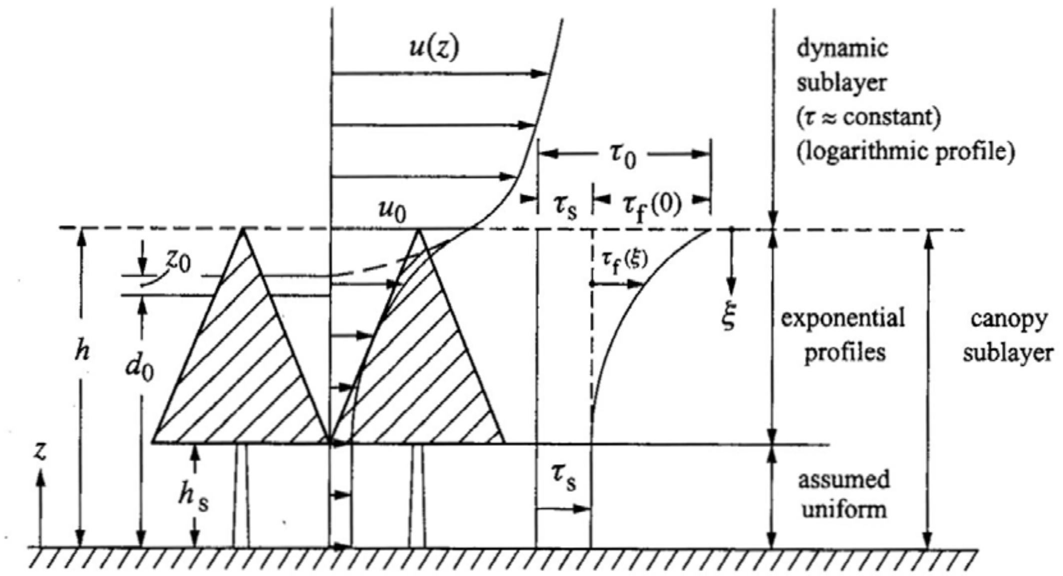

Fig. 2.2. Quantities defining the wind profile in and above a canopy of trees

(Brutsaert, 1982).

Various heights are distinguished (Eagleson, 2002):

- wind velocity at heights above the trees,
- wind velocity and shear stress at the top of the tree crowns,
- wind velocity within the tree crowns,
- wind velocity below the tree crowns.

Wind velocity at heights above the trees

In 1930, von Kármán presented his well-accepted logarithmic law describing the vertical distribution of the mean horizontal wind velocity in the boundary layer of the earth atmosphere. The wind speed above a canopy follows this law:

$$u(z) = \frac{u_*}{k} \ln\left(\frac{z - d_0}{z_0}\right)$$

in which

$u(z)$ = mean horizontal wind velocity at height z [m s^{-1}],

k = von Kármán’s constant [-],

u_* = shear velocity (explained below) [m s^{-1}],

d_0 = zero-plane displacement height [m],

z_0 = surface roughness length [m].

Note that $u(z)$ refers to heights above the top of the trees, while d_0 refers to heights lower than the canopy top. Eagleson (2002, p. 101 and p. 107) presents equations and graphs allowing the determination of d_0 and z_0 from canopy properties. When d_0 and z_0 are known, and one value of $u(z)$ at a height z is available (e.g., a measuring value), the shear velocity and the wind speed at any height above the canopy can be calculated using the above equation.

Wind velocity and shear stress at the top of the tree crowns

At the top of the canopy the gradient of the wind velocity with depth is very high. Therefore, very significant shear stress occurs between the air above the canopy and the air in the canopy. This shear stress τ_0 at the top of the canopy increases with the wind speed u_0 at the top of the canopy. The physical quantity u_* describes conditions at the top of the canopy and is connected to the shear stress τ_0 as well as to the velocity u_0. It depends on properties of the canopy. Because u_* has the dimensions of length per time, it is called shear velocity. The shear velocity is defined by

$$u_* = \sqrt{\tau_0 / \rho} = C_f^{1/2}\ u_0$$

in which

u_* = shear velocity [m s^{-1}],

τ_0 = shear stress at top of canopy [N m^{-2}],

ρ = fluid mass density [kg m^{-3}],

C_f = foliage surface drag coefficient [-].

The foliage surface drag coefficient C_f depends on canopy parameters as follows:

$$C_f = (k\ (\frac{h - d_0}{h - h_s})\ m\ n\ \beta\ L_t)^2$$

in which

h = tree height [m],

h_s = height of crown base above surface [m],

m = exponent relating shear stress on foliage to horizontal wind velocity and having the nominal value 0.5 for the foliage elements of trees [-],

n = number of sides of each foliage element producing surface resistance to wind and having the nominal value 2 for the foliage elements of trees [-],

β = momentum extinction coefficient = cosine of angle leaf surface makes with horizontal [-],

L_t = foliage area index = upper-sided area of all foliage elements per unit of basal area (foliage includes leaves, branches and stem) [-].

Both last equations may be combined giving the form

$$\frac{u_*}{ku_0} = (\frac{h - d_0}{h - h_s})\ m\ n\ \beta\ L_t$$

This form relates u_0 to u_* through canopy properties.

Wind velocity within the tree crowns

Many observations have shown that, within the canopy, the extinction of wind velocity with depth has an exponential form, according to

$$\frac{u(\xi)}{u_0} = \exp(-m\,n\,\beta\,L_t\,\xi)$$

with

$$\xi = \frac{h - z}{h - h_s}$$

The quantity ξ varies from 0 at the top of the canopy to 1 at the bottom of the crowns.

Wind velocity below the tree crowns

Here, it is assumed that the wind velocity u does not vary with height, and has the value of the wind velocity at the bottom of the crowns. From the last two equations, with $\xi = 1$, it follows that

$$u = u_0 \exp(-m\,n\,\beta\,L_t)$$

This assumption implies the assumption that the shear stress on the surface is zero. This is allowed because observations showed that, for $L_t > 1$, "the shearing stress transmitted to the ground surface is essentially zero".

Atmospheric, or aerodynamic resistance

The literature shows that the atmospheric resistance is modelled in different ways. The various models predict different r_a values for the same input values. E.g. the model of Eagleson, which follows now, predicts rather low values. After Eagleson's model, models will be described that predict higher values. Atmospheric resistance is also called: aerodynamic resistance (Shaw and Pereira, 1982).

Equivalent atmospheric resistance according to Eagleson (2002)

For the conditions between the reference height and the top of the canopy we can use an analogy with Ohm's law (Eagleson, 2002, p. 133). Ohm's law for an electric current in a wire states that “the difference in electric potential V between the wire ends is equal to the electric current i in the wire multiplied by the resistance R of the wire”, or:

$$R = \frac{V}{i}$$

By analogy we may assume that

R = the aerodynamic (or atmospheric) resistance r_a between screen height and canopy top,

V = the difference between momentum concentration ρu [kg m^{-2} s^{-1}] at screen height and momentum concentration ρu at the top of the canopy,

i = the shear stress τ (flux of momentum [kg m^{-1} s^{-2}]) in the layer between screen height and canopy top. This shear stress does not vary with height so that it equals τ_0, the shear stress at canopy height.

Substituting these quantities into Ohm’s law gives:

$$r_a = \frac{\rho u_2 - \rho u_0}{\tau_0}$$

where index 2 refers to screen height and index 0 to height of canopy top. Because usually $u_2 >> u_0$ this may be approximated as

$$r_a = \frac{\rho u_2}{\tau_0}$$

Using the von Kármán equation $u_2 = \frac{u_*}{k} \ln(\frac{z_2 - d_0}{z_0})$ with z_2 is screen height, and the definition of shear velocity $u_* = \sqrt{\tau_0 / \rho}$, this can be transformed into

$$r_a = \frac{\ln^2(\frac{z_2 - d_0}{z_0})}{k^2 u_2}$$

This is the aerodynamic resistance for the transport of momentum. But we need for our evaporation models the aerodynamic resistance for vapour transport. Eagleson assumes that the aerodynamic resistance for vapour transport can be approximated by the aerodynamic resistance for momentum transport (Eagleson, 2002). This is only partly true because the vapour transport is merely a diffusion process, and momentum is also transported by pressure differences (aerodynamic resistance for vapour transport is larger than for momentum transport).

A widely accepted model for aerodynamic resistance

Like the wind speed distribution, the variation of the air specific humidity q with height may well be approximated by a logarithmic function (Brutsaert, 1982, p. 61):

$$q_s - q(z) = \frac{E}{a_v \; k \; u_* \; \rho} \ln\left(\frac{z - d_0}{z_{0h}}\right)$$

with

q_s = saturation air specific humidity, at the surface (mass of water vapour per unit mass of dry air) [-],

$q(z)$ = air specific humidity at height z [-],

E = vapour flux (mass of water vapour per unit of surface per unit of time) [kg m^{-2} s^{-1}],

α_v = ratio of the von Kármán constants for water vapour and momentum, ≈ 1 ,

z_{0h} = roughness length for vapour and heat [m].

The equation has been developed from similitude considerations, dimensional analysis and experimental results. The u_* can be eliminated from this equation by using the equation for the logarithmic wind profile (z_{0m} = roughness length for momentum [m])

$$u = \frac{u_*}{k} \ln\left(\frac{z - d_0}{z_{0m}}\right) \quad \text{or} \quad \frac{1}{u_*} = \frac{1}{k\,u} \ln\left(\frac{z - d_0}{z_{0m}}\right)$$

so that, with $\alpha_v = 1$,

$$q_s - q(z) = \frac{E}{k^2 \rho} \ln\left(\frac{z - d_0}{z_{0h}}\right) \ln\left(\frac{z - d_0}{z_{0m}}\right)$$

This equation can be inserted in the Ohm's analogy for vapour transport:

$$r_a = \frac{\rho\,(q_s - q(z))}{E}$$

resulting in the widely accepted equation for calculating aerodynamic resistance for vapour transport from wind speed measurements and humidity measurements:

$$r_a = \frac{\ln\left(\frac{z_m - d_0}{z_{0m}}\right) \ln\left(\frac{z_h - d_0}{z_{0h}}\right)}{k^2 u}$$

where:

z_m = height of wind speed measurements [m],

z_h = height of temperature and humidity measurements [m],

u = measured wind speed [m s^{-1}].

Allen et al. (1989) and Allen et al. (1998) state that

$d_0 = \frac{2}{3}\, h_{crop}$

$z_{0m} = 0.123\, h_{crop}$

$z_{0h} = 0.1 z_{0m} = 0.0123\, h_{crop}$

h_{crop} = crop height [m].

It can be seen that, if wind speed and humidity are measured at the same height, the above equation and the equation for the equivalent aerodynamic resistance according to Eagleson are the same if z_{oh} would be equal to z_{om}. But, as mentioned a few sentences before, Allen et al. (1989) and Allen et al. (1998) state that $z_{0h} = 0.1 z_{0m}$ or $z_{0h} / z_{om} = 1/10$. Brutsaert (1982, p. 124) writes that this ratio "appears to be of the order of 1/7 to 1/12, but for tall trees it is probably of the order of 1/3 to1/2, but not much larger.” This remark suggests that the difference between both equations is less for tall trees than for short trees.

It may be noted that Eagleson (2002, p. 101 and p. 107) also uses different relations between d_0, z_{0m}, and plant height. He refers to measurements showing that the relations he presented are more appropriate for trees than the relations

$$d_0 = \frac{2}{3} h_{crop}$$

$$z_{0m} = 0.123\, h_{crop}$$

presented by Allen et al. (1989) and Allen et al. (1998).

Model in Mohren (1987)

Mohren (1987) specifies that the equation of r_a for the transport of momentum applies to the momentum transport from reference height to a plane at height $z_0 + d_0$ inside the canopy, the level at which the logarithmic wind profile would predict zero wind speed. In the case of a canopy of considerable roughness, differences between aerodynamic resistance to momentum and resistance to vapour and heat exchange must be taken into account. Resistances to vapour and heat exchange will be larger because these traits cannot be transferred by pressure interactions in the air between the ever-moving leaves. This can be taken into account by adding an excess resistance r_{ex} to the turbulent resistance for the transport of momentum calculated from the wind profile. Mohren follows results from Chen and uses

$$r_{ex} = 4 / u_*$$

where u_* = shear velocity [m s^{-1}]. This value of r_{ex} [s m^{-1}] should be added to the value of r_a calculated like Eagleson did (see above).

Model in Van Keulen and Wolf (1986)

The example calculations in Van Keulen and Wolf (1986) all use aerodynamic resistances that apply to “a smooth land surface” (empirical results from Frere and Popov, see p. 70 of Van Keulen and Wolf (1986). Variations in the wind profile with vegetation parameters are not accounted for.

Concluding remarks

It may be concluded from the above, that Eagleson's model provides relatively low r_a values. Complicating factors are that:

- Eagleson calculates the wind profile from, amongst others, β, the momentum extinction coefficient = cosine of angle leaf surface makes with horizontal. It appears that r_a is very sensitive to β. An appropriate value for β is not easy to find.
- Later, when calculating canopy transpiration, Eagleson uses relatively low values for the canopy resistance r_c, which may enlarge the effect of a relatively low r_a value on the calculated transpiration.

Canopy resistance

When considering the vapour transport between the wet inner walls of stomata to the atmosphere above the canopy, it is common to define the resistance against this transport as the canopy resistance. The water that evaporates from the saturated inner walls of the stomata has to overcome several component resistances before it leaves the upper boundary of the canopy;

- water tension at the wet inner walls of the stomata, which is connected to the water tension in the soil,
- intercellular resistance, controlling the flow within the stomatal cavity,
- stomatal resistance, a physiological "valve" regulating plant water loss and carbon dioxide assimilation,
- leaf boundary layer resistance (resistance during transport through a thin, relatively stable, air layer around the leaf),
- interleaf resistance in the air layers between the leaves with their boundary layers, during the labyrinthic atmospheric pathway through the crown.

Physically, the vapour transport in the canopy is a gas diffusion process obeying Fick's diffusion law. For plants it is common to use a simplified form of this law (Larcher, 1995, p. 75):

Flux = concentration difference/resistance

This equation is very similar to Ohm's law for electrical currents. The various resistances may act "in series" or "parallel". E.g., leaf stomatal resistance and leaf boundary layer resistance act "in series", resistances of individual stomata act "in parallel". Many authors proposed models that estimate canopy resistance. These models differ with respect to the specific component resistances they neglect. E.g., Eagleson (2002) neglects in a large part of his book: leaf epidermis resistance, intercellular resistance, stomatal resistance, leaf boundary layer resistance. However, neglecting stomatal resistance may give unrealistic results. Other authors consider the interleaf resistance being a part of the aerodynamic resistance, and not a component of the canopy resistance.

In many models the single stomatal resistance plays a central role. The resistance of an individual stoma may increase with temperature, vapour pressure deficit and/or soil water tension. Therefore, the use of a so-called minimum stomatal resistance is meaningful.

Canopy resistance according to Spittlehouse and Black (1982)

Spittlehouse and Black (1982) do not consider the interleaf resistance and state that the stomatal resistance + boundary layer resistance of each leaf layer (layer with leaf area index = 1) should be connected "in parallel" in order to find the bulk stomatal resistance [s m^{-1}] of the canopy:

$$r_c = \frac{r_{ls} + r_{lb}}{L}$$

where:

r_{ls} = stomatal resistance per unit area of leaf surface [s m^{-1}],

r_{lb} = leaf boundary layer resistance per unit area of leaf surface [s m^{-1}],

L = leaf area index [-].

Eagleson (2002, p. 32) presents foliage area indices of a range of deciduous trees, suggesting that an average value for L is 4. Feddes et al. (2003) give a minimum value $r_c = 125$ s/m for forest. Substituting both values in the above equation gives a minimum $r_{ls} + r_{lb} = 500$ s/m. This value compares well with resistance measurements in an oak forest in The Netherlands (Ogink-Hendriks, 1995). Spittlehouse and Black (1982) present, for a

Douglas-fir stand, a minimum value r_{ls} = 428 s/m and a value r_{lb} = 15 s/m, implying $r_{ls} + r_{lb} = 443$ s/m. The above values also compare well with the values in Shuttleworth and Wallace (1985).

Canopy resistance according to Eagleson (2002)

Eagleson (2002) deals with the interleaf resistance by using the concept of interleaf layer resistance. He assumes that the crown consists of a number of horizontal layers, in such a way that the foliage area index of each layer is equal to 1. This conceptual crown is shown in fig. 2.3. So, the number of such "leaf layers" is equal to the foliage area index of the crown, rounded down to the nearest lower whole number. It is further assumed that the lowest leaf layer is inactive and that layers exist between the leaf layers, the so-called interleaf layers. The thickness of the interleaf layers is calculated as the crown height divided by the number of interleaf zones. Vapour from such a "leaf layer' has to pass all interleaf layers above the leaf layer before it reaches the atmosphere above the canopy. In each layer, this vapour movement has to overcome a resistance; the interleaf atmospheric resistance written as r_i.

A value of r_i can be calculated by using again the analogy with Ohm's law, like in the previous section on r_a:

$$R = \frac{V}{i}$$

By analogy we assume that

R = the interleaf layer resistance r_i of a leaf layer [s m^{-1}],

V = the difference between momentum concentration ρu at the top of the layer and momentum concentration ρu at the bottom of the layer [kg m^{-2} s^{-1}],

i = the shear stress τ in the layer [kg m^{-1} s^{-2}].

Substituting these quantities in Ohm's law gives:

$$(r_i)_{layer} = \frac{\rho\, u_{layertop} - \rho\, u_{layerbottom}}{\tau}$$

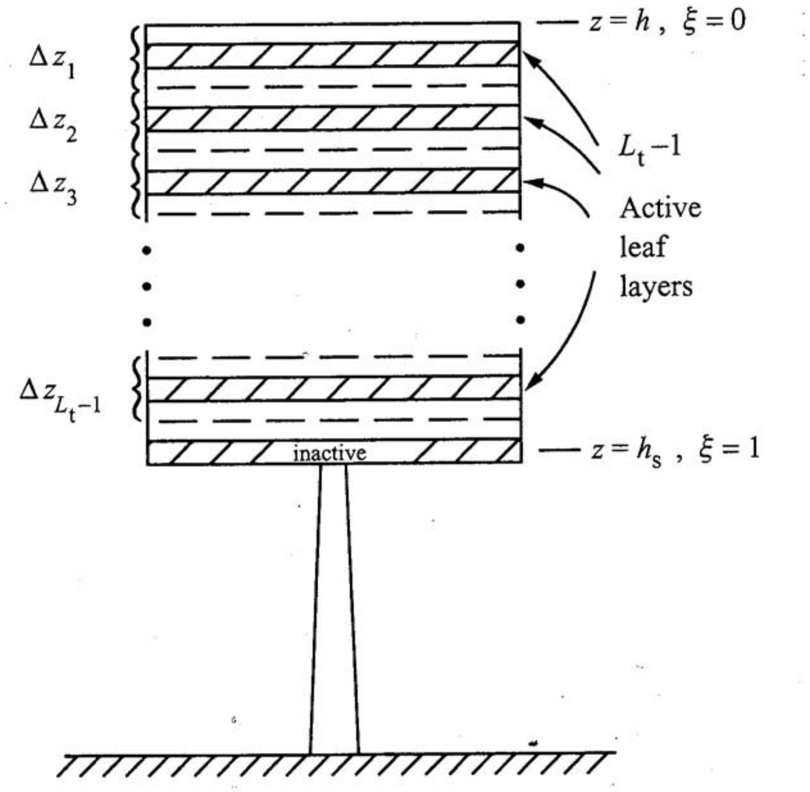

Fig. 2.3. Conceptual model of crown

(Eagleson, 2002).

Values of $u_{layertop}$ and $u_{layerbottom}$ can be found from the exponential wind profile within the crown. (See section 2.1.3. on wind profile). These wind velocity values depend on:

m = exponent relating shear stress on foliage to horizontal wind velocity and having the nominal value 0.5 for the foliage elements of trees [-],

n = number of sides of each foliage element producing surface resistance to wind and having the nominal value 2 for the foliage elements of trees [-],

β = momentum extinction coefficient = cosine of angle leaf surface makes with horizontal [-].

L_t = foliage area index = upper-sided area of all foliage elements per unit of basal area [-].

A value for τ can be found from the law of viscosity in turbulent flow:

$$\tau = \rho K_m \frac{du}{dz}$$

in which

K_m = the so-called eddy viscosity [m^2 s^{-1}]. K_m is calculated from the wind velocity at the canopy top and from m, n, β,

du = $u_{layertop}$ minus $u_{layerbottom}$ [m s^{-1}],

dz = layer thickness [m].

The r_i values of the individual layers are different for each layer. This complicates the calculation of a canopy resistance from the individual, layer specific, r_i values. Eagleson presents a very rough averaging procedure to arrive at an r_i value that may be used for each layer:

$$r_i = \left(\frac{1}{ku_*}\right)\frac{\frac{1-m}{m}(\gamma L_t)^2}{(L_t - 1)[1-\exp(-\frac{1-m}{m}\gamma L_t)]}$$

in which

u_* = shear velocity [m s^{-1}],

$\gamma = mn\beta$ [-].

Because the individual r_i values are identical, they may be combined in a "series-parallel model" in order to find the resistance of the whole canopy, r_c:

$$\frac{1}{r_c} \approx \frac{1}{r_{ls} + r_{lb} + r_i} + \frac{1}{r_{ls} + r_{lb} + 2r_i} + \cdots + \frac{1}{r_{ls} + r_{lb} + (L_t - 1)r_i}$$

Fig. 2.4 shows the canopy modelled by the leaf layers and the series-parallel circuit of the interleaf layer resistances r_i and leaf stomatal resistances r_{ls} (written as r_{lls} in the figure). In the figure, the leaf boundary layer resistances are neglected.

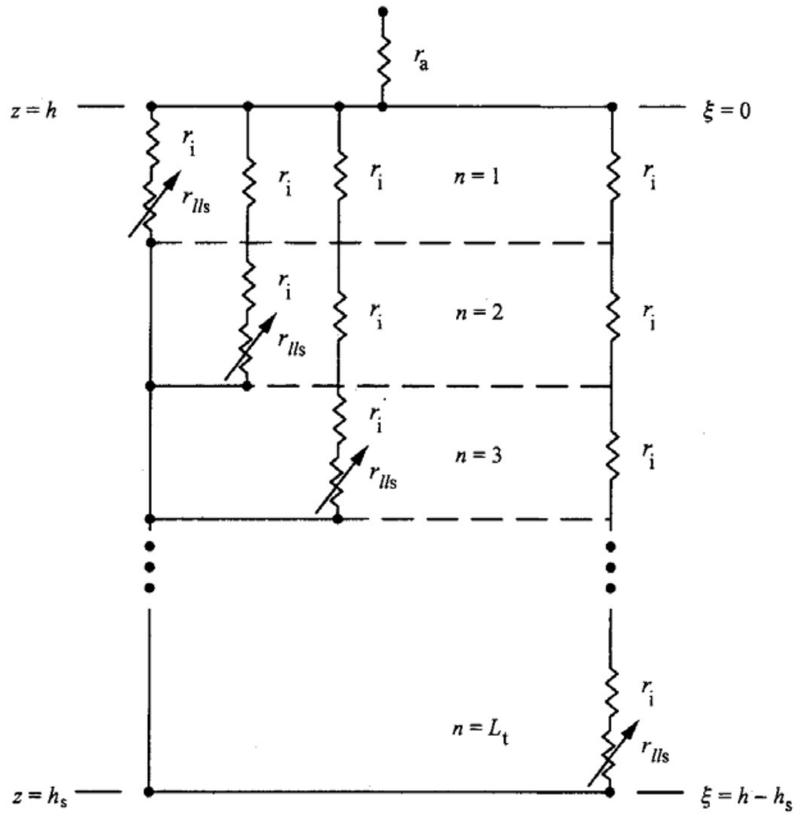

Fig. 2.4. Resistive model of "big leaf" canopy

(Eagleson, 2002).

Concluding remarks

It may be concluded from the above that canopy resistance is a complicated quantity, which is still not fully understood. This especially holds true for tall canopies.

2.3. Selected transpiration models

2.3.1. Makkink's radiation model

A very simple radiation model is the model assuming isothermal conditions. Under these conditions, vertical transport of sensible heat is zero, because there is no vertical gradient of temperature. Then, net radiation must be equal to latent heat:

$LE = R_N$

Makkink (Makkink, 1957, 1962; de Bruin, 1987) recognized that temperature often deviates from the isothermal condition, but not much, and that all measuring values that are needed to calculate R_N are often not available. He proposed the form

$$E_{refM} = \frac{\Delta}{\Delta + \gamma_0}\left(c_1 \frac{R_G}{L} + c_2 \right)$$

E_{refM} = potential evapotranspiration of a surface with a closed dry grass canopy with height 8-15 cm and well supplied with water [mm day^{-1}] (Massop et al., 2005),
R_G = global radiation [MJ m^{-2} d^{-1}],
L = latent heat of vaporization [MJ m^{-3}].

The constants c_1 and c_2 are, for European conditions, 0.75 and 0, respectively (NN, 1996a). They have an empirical background.

The model needs only temperature (for the calculation of Δ) and global radiation R_G. The global radiation can be calculated from the latitude, the day of the year, and the ratio of actual duration of bright sunshine during the day and its maximum possible length if the day would be cloudless.

In The Netherlands, the Makkink model is widely used (Huinink, 1998; Kroes et al., 2002; Kroes and Van Dam, 2003; Massop et al., 2005). The Royal Dutch Meteorological Institute KNMI currently uses the model for the daily calculation of potential evapotranspiration values from daily meteorological measurements.

2.3.2. FAO Guidelines for computing evapotranspiration

Introduction

Allen et al. (1998) recommended, in an FAO publication, guidelines for computing crop water requirements. In that publication, central roles are played by a reference surface and crop coefficients. The reference surface is defined as: “A hypothetical reference crop with an assumed crop height of 0.12 m, a fixed surface resistance of 70 s m^{-1} and an albedo of 0.23.” This definition refers to a grass surface under standardized conditions, and is a more quantitative specification of “short, closed, grass that is well supplied with water”. The (crop specific) crop coefficient is defined as the ratio between the crop evapotranspiration under standard conditions and the evapotranspiration of the reference surface. The standard conditions of the crop evapotranspiration refer to crops grown in large fields under excellent agronomic and soil water conditions. The crop coefficient (K_c) may be split into a basal crop coefficient (K_{cb}) and a soil evaporation coefficient (K_e):

$$K_c = K_{cb} + K_e$$

This splitting may especially be needed when time steps in data and calculations are one day. In our data and calculations time steps are longer, allowing us to follow the more simple approach of K_c without splitting.

Crop coefficients

The values of the crop coefficients change with crop growth stage. Four growth stages are distinguished: Initial stage, Crop development stage, Mid-season stage, Late season stage. For perennial plants the initial stage runs from the ‘greenup’ date, i.e., the time when the initiation of new leaves occurs, to approximately 10% ground cover. The crop development stage runs from 10% ground cover to effective full cover. Effective full cover for many crops occurs at the initiation of flowering. For some crops, especially those taller than 0.5 m, the average fraction of the ground surface covered by vegetation (f_c) at the start of full effective cover is about 0.7−0.8. For dense grasses, effective full cover may occur at about 0.10−0.15 m height. For thin stands of grass, grass height may approach 0.3−0.5 m before effective full cover is reached. Another way to estimate for a vegetation the occurrence of effective full cover is when the leaf area index (LAI) reaches three. The mid-season stage runs from effective full cover to the start of maturity. The start of maturity is often indicated by the beginning of the ageing, yellowing or senescence of leaves, leaf drop, or the browning of fruits to the degree that the crop evapotranspiration is reduced relative to the reference evapotranspiration. The mid-season stage is usually the longest stage for perennials. The late season stage runs from the start of maturity to full senescence or leaf drop.

It is often assumed that:

- in the initial stage, K_c has the constant value $K_{c,ini}$ and K_{cb} has the constant value $K_{cb,ini}$,
- in the crop development stage, both K increase linearly with time, from the value of the initial stage to the value of the mid-season stage,
- in the mid-season stage, K_c has the constant value $K_{c,mid}$ and K_{cb} has the constant value $K_{cb,mid}$,
- in the late season stage, both K decrease linearly with time, from the values of the mid-season stage to the end values $K_{c,end}$ and $K_{cb,end}$, respectively.

Allen et al. (1998) presented tables that give, for most crops, values of: $K_{c,ini}$, $K_{c,mid}$, $K_{c,end}$, $K_{cb,ini}$, $K_{cb,mid}$, $K_{cb,end}$, K_e , planting date, length of growing stages, and maximum crop length. These tables do not apply well to trees, trees in lawn, sparse vegetation, and/or small areas surrounded by other vegetation or hardly-evaporating surfaces. But for these vegetation types and conditions, Allen et al. (1998) provided appropriate calculation procedures and methods.

Potential evapotranspiration of reference surface

The evapotranspiration of the hypothetical reference crop can be calculated in an unambiguous way from meteorological data. This calculation applies the Penman-Monteith model (see section Penman-Monteith model) to the reference crop (with an assumed crop height of 0.12 m, a fixed surface resistance of 70 s m^{-1} and an albedo of 0.23). The aerodynamic resistance is calculated according to Allen et al. (1989). See “A widely accepted model for aerodynamic resistance” in section 2.2.3. The calculation result is:

$$ET_0 = \frac{0.408\,\Delta(R_n - G) + \gamma \dfrac{900}{T+273}\, u_2\,(e_s - e_a)}{\Delta + \gamma\,(1 + 0.34 u_2)}$$

with

ET_0 = reference evapotranspiration [mm day^{-1}],

R_n = net radiation at the crop surface [MJ m^{-2} day^{-1}],

G = soil heat flux density [MJ m^{-2} day^{-1}],
T = mean daily air temperature at 2 m height [ºC],
u_2 = wind speed at 2 m height [m s^{-1}],
e_s = saturation vapour presure [kPa],
e_a = actual vapour pressure [kPa],
$e_s - e_a$ = saturation vapour pressure deficit [kPa],
Δ = slope vapour pressure curve [kPa ºC^{-1}],
γ = psychrometric constant [kPa ºC^{-1}].

Allen et al. (1998) called this equation: FAO Penman-Monteith equation. They also gave directives for measuring/determining the above meteorological input data.

The tabulated crop coefficients refer to a limited range of weather conditions, but crop coefficients do show some dependency on climate. Therefore, the tabulated $K_{c,mid}$, $K_{c,end}$, $K_{cb,mid}$ and $K_{cb,end}$ should be summed with the expression

$$\left[0.04(u_2 - 2) - 0.004(RH_{\min} - 45)\right]\left(\frac{h}{3}\right)^{0.3}$$

with

u_2 = mean value for daily wind speed at 2 m height over grass during the particular growth stage [m s^{-1}], for 1 m s^{-1} $\leq u_2 \leq$ 6 m s^{-1}

$RH_{\min}$ = mean value for daily minimum relative humidity during the particular growth stage [%], for 20% $\leq RH_{\min} \leq$ 80%.

h = mean plant height during the particular growth stage [m], for 0.1 m $\leq h \leq$ 10 m.

Note that this correction is not needed if u_2 = 2.0 m s^{-1} and $RH_{\min}$ = 45%.

Allen et al. (1998) presented the correction graphically in their Figure 32. They also presented a relation between $RH_{\min}$ and RH_{mean} in their Table 16. $K_{c,end}$ values are only corrected for tabulated $K_{c,end} \geq 0.45$.

Crop coefficient for the initial stage $K_{c,ini}$

In the initial stage, evaporation from the soil surface is important. The tabulated values of $K_{c,ini}$ should only be used in preliminary or planning studies. More accurate estimates can be obtained by considering: time interval between wetting events; evaporation power of the atmosphere; magnitude of the wetting event. Such estimates can be done using graphs on pages 117 and 118 or the calculation procedure in Annex 7 of (Allen et al., 1998).

Allen et al. (1998, p. 121) noted that: "$K_{c,ini}$ for trees and shrubs should reflect the ground condition prior to leaf emergence or initiation in case of deciduous trees or shrubs, and the ground condition during the dormancy or low active period for evergreen trees and shrubs. The $K_{c,ini}$ depends upon the amount of grass or weed cover, frequency of soil wetting, tree density and mulch density. For a deciduous orchard in frost-free climates, the $K_{c,ini}$ can be as high as 0.8 or 0.9, where grass ground cover exists, and as low as 0.3 or 0.4 when the soil surface is kept bare and wetting is infrequent."

Crop coefficient for the mid-season stage $K_{c,mid}$

Allen et al. (1998, p. 124) noted that: "$K_{c,mid}$ is less affected by wetting frequency than is $K_{c,ini}$, as vegetation during this stage is generally near full ground cover so that the effects of surface evaporation on K_c are smaller. For frequent irrigation of crops (more frequently than every 3 days) and where the tabulated $K_{c,mid}$ is less than 1.0, the value can be replaced by approximately 1.1−1.3 to account for the combined effects of continuously wet soil, evaporation due to interception (sprinkler irrigation) and roughness of the vegetation, especially where the irrigation system moistens an important fraction of the soil surface (fraction > 0.3)."

Crop coefficient for the end of the late season stage $K_{c,end}$

Tabulated $K_{c,end}$ are only corrected for wind speed and relative humidity with the already mentioned correction expression if $K_{c,end} \geq 0.45$. When vegetation is allowed to senesce and dry (as evidenced by $K_{c,end}$ < 0.45), u_2 and $RH_{\min}$ have less effect on $K_{c,end}$ and no adjustment is necessary. Some guidance on adjustment of K_c values for wetting frequency is provided in Chapter 7 of Allen et al.(1998).

<u>Basal crop coefficients</u> $K_{cb,ini}$, $K_{cb,mid}$, $K_{cb,end}$

A basal crop coefficient is defined as the ratio of the crop evapotranspiration over the reference evapotranspiration when the soil surface is dry but transpiration is occurring at a potential rate, i.e., water is not limiting transpiration. Therefore, a basal crop coefficient represents primarily the transpiration component of the crop evapotranspiration. It does include a residual diffusive evaporation component supplied by soil water below the dry surface and by soil water from beneath dense vegetation.

Allen et al. (1998) presented, in their Table 18, the general guidelines that they used to derive K_{cb} Tables from the K_c Tables:

Initial growth stage:

- annual crop – (nearly) bare soil surface $K_{cb,ini} = 0.15$
- perennial crop – (nearly) bare soil surface $K_{cb,ini} = 0.15 – 0.20$
- grasses, brush and trees – killing frost $K_{cb,ini} = 0.30 – 0.40$
- perennial crop – some ground cover or leaf cover
    - infrequently irrigated (olives, palm trees, fruit trees, …) $K_{cb,ini} = K_{c,ini} - 0.1$
    - frequently irrigated (garden-type vegetables, …) $K_{cb,ini} = K_{c,ini} - 0.2$

Mid-season growth stage:

- ground cover more than 80% $K_{cb,mid} = K_{c,mid} - 0.05$
- ground cover less than 80% (vegetables) $K_{cb,mid} = K_{c,mid} - 0.10$

End-of-season growth stage:

- infrequently irrigated or wetted during late season $K_{cb,end} \approx K_{c,end} - 0.05$
- frequently irrigated or wetted during late season $K_{cb,end} = K_{c,end} - 0.1$

As $K_{c,ini} = K_{cb,ini} + K_e$ we may use the fourth ($K_{cb,ini}$ = 0.30 – 0.40) and sixth/seventh ($K_{cb,ini}$ = $K_{c,ini}$ − 0.1) lines of the above Table to estimate $K_{c,ini}$ for sites with trees and lawn in Moscow:

$$K_{c,ini} = K_{cb,ini} + K_e \approx 0.35 + 0.1 = 0.45$$

This value compares well with the graphs on pages 117 and 118, and with the remarks on $K_{c,ini}$ for trees and shrubs on page 121, of Allen et al. (1998).

Soil evaporation coefficient K_e

Because K_e will not play a large role in our data processing and calculations, we only present a short outline of this coefficient. If one intends to derive daily values of K_e a main starting point is the equation:

$$K_e = K_r (K_{c,\max} - K_{cb}) \leq f_{ew} K_{c,\max}$$

$K_{c,\max}$ = maximum value of K_c following rain or irrigation,

K_r = dimensionless evaporation reduction coefficient dependent on the cumulative depth of water depleted (evaporated) from the topsoil. It can be calculated from a daily water balance of the surface soil layer with thickness 0.10 – 0.15 m. K_r is 1 when the soil surface is wet, and 0 when the top layer water content is halfway between oven dry (no water left) and wilting point,

f_{ew} = fraction of the soil that is both exposed and wetted, i.e., the fraction of soil surface from which most evaporation occurs.

Evapotranspiration under water stress and/or salinity stress

Where the growth conditions differ from standard, unstressed, conditions, a correction on the evapotranspiration is required. Soil water shortage and salinity may reduce soil water uptake and limit crop evapotranspiration. A water stress coefficient K_s can be derived from a water balance of the root zone. Effects of salinity can be derived from a growth – salinity relationship for the root zone.

Allen et al. (1998) followed procedures very similar to methods published by other authors.

Evapotranspiration for natural, non-typical and non-pristine vegetations

A "non-pristine" vegetation is defined, in the usage here, as a vegetation having less than perfect growing conditions or stand characteristics (i.e., relatively poorer conditions of density, height, leaf area, fertility, or vitality) as compared to 'pristine'conditions. These definitions of pristine and non-pristine vegetation follow Allen et al. (1998). The procedure to estimate crop coefficients for the initial growth stage for natural, non-typical and non-pristine vegetation is identical to that described earlier. The crop coefficient in this stage is primarily determined by the frequency with which the soil is wetted. The crop coefficient during the mid-season period and to a lesser extent the crop coefficient during the late season period differ from that described in previous parts. As the ground cover for natural and non-pristine vegetation is often reduced, they are often called: sparse vegetation. The crop coefficient of sparse vegetation is affected to a large extent by the frequency of precipitation and/or irrigation and by the amount of leaf area and ground cover.

Mid-season stage

Allen et al. (1998) presented in their Chapter 9 several methods for estimating $K_{c,mid}$ for sparse vegetation. These methods use leaf area index (LAI) or effective ground cover ($f_{c,eff}$). A method using LAI is similar to a procedure used by Ritchie (Allen et al., 1998, p. 184 and p. 186; Ritchie, 1972):

$$K_{c,mid} = K_{c,ini} + \left(K_{c,full} - K_{c,ini}\right)\left(1 - \exp\left(-0.7 LAI\right)\right)$$

The following equation applies well to shrubs and trees:

$$K_{c,mid} = K_{c,ini} + \left(K_{c,full} - K_{c,ini}\right)\left(\min\left(1;\, 2 f_c;\, \left(f_{c,eff}\right)^{\left(\frac{1}{1+h}\right)}\right)\right)$$

$K_{c,full}$ = upper limit on the evaporation and transpiration from any cropped surface,

$K_{c,full} = K_{cb,full} + 0.05$ (see Allen et al., 1998, p. 143),

$K_{cb,full}$ = estimated basal K_{cb} during the mid-season (at peak plant size or height) for vegetation having full ground cover or LAI>3 (see below),

f_c = observed fraction of soil surface covered by vegetation as observed from nadir (overhead),

$f_{c,eff}$ = the effective fraction of soil surface covered or shaded by vegetation. For trees, it can be estimated as $f_{c,eff} = f_c / \sin\eta$ where η = the mean angle of the sun above the horizon during the period of maximum evapotranspiration (generally between 11.00 and 15.00),

h = plant height [m].

$K_{cb,full}$ is estimated as

$$K_{cb,full} = K_{cb,h} + \left[0.04\,(u_2 - 2) - 0.004\,(RH_{\min} - 45)\right]\left(\frac{h}{3}\right)^{0.3}$$

$K_{cb,h}$ = $K_{cb,mid}$ for full cover vegetation (LAI > 3) under subhumid and calm wind conditions ($RH_{\min} = 45\%$ and $u_2 = 2$ m s^{-1}). The value for $K_{cb,h}$ is estimated as 1.0 + 0.1h for $h \leq 2$ m and as 1.20 for h > 2 m. The value 1.2 represents a general upper limit on $K_{cb,mid}$ for tall vegetation having full ground cover and LAI > 3 under the sub-humid and calm wind conditions),

u_2 = mean value for wind speed at 2 m height during the mid-season [m s^{-1}],

$RH_{\min}$ = mean value for minimum daily relative humidity during the mid-season [%],

h = mean maximum plant height [m].

The $K_{c,mid}$ as calculated with the equation at the beginning of this paragraph on “Mid-season stage” may need to be multiplied by a resistance correction factor F_r if the leaf resistance is significantly greater than that of most agricultural crops where leaf resistance r_l is commonly about 100 s m^{-1}.

$$F_r \approx \frac{\Delta + \gamma(1 + 0.34 u_2)}{\Delta + \gamma\left(1 + 0.34 u_2 \frac{r_l}{100}\right)}$$

where r_l = mean leaf resistance for the vegetation in question [s m^{-1}].

Late season stage

During the late season stage K_c of "non-pristine" shrubs and trees may be estimated using similar procedures as above for the mid-season stage. But no suitable guidelines for estimating $K_{c,end}$ of a trees-grass combination were found in Allen et al. (1998). Therefore, we assume that $K_{c,end}$ of a trees-grass combination is similar to that of the fruit trees "apples, cherries, pears" after leaf drop. Note 18 of Table 12 of Allen et al. (1998) states that $K_{c,end}$ of these fruit trees after leaf drop is about 0.20 for bare, dry soil or dead ground cover and about 0.50-0.80 for actively growing ground cover. We already estimated that $K_{c,ini}$ = 0.45. This may justify that we assume that

$$K_{c,ini} = K_{c,end} = 0.45$$

for the tree-grass combinations in Moscow.

Small areas of vegetation

The value for K_c for small stands depends on the type and condition of other vegetation surrounding the small stand. In the majority of cases for natural vegetation or for "non-pristine" agricultural vegetation, the value of K_c must adhere to upper limits for K_c of approximately 1.20 –1.40, when the area of the vegetation is larger than about 2 000 m^2. This is required as ET from large areas of vegetation is governed by one-dimensional energy exchange principles and by the principle of conservation of energy. ET from small stands (< 2 000 m^2) will adhere to these same principles and limits only where the vegetation height, leaf area, and soil water availability are similar to that of the surrounding vegetation. Under the clothesline effect or under the oasis effect the peak K_c values may exceed the 1.2 –1.40

limit. An upper limit of 2.5 is usually placed on K_c to represent an upper limit on the stomata capacity of the vegetation to supply water vapour to the air stream under the clothesline or oasis conditions. For vegetation with a great leaf resistance the upper limit should be multiplied by the resistance correction factor F_r.

Allen et al. (1998, pp. 200-203) present example curves and an equation allowing us to estimate clothesline and oasis effects on small areas of vegetation. The equation suggests that we may estimate K_c of a small area (tall wind breaks, such as single rows of trees) as

$$K_c = \min\left(1.2 + \frac{F_r h_{canopy}}{width}; 2.5\right)$$

h_{canopy} = mean vertical height of canopy area [m],

width = width (horizontal thickness) of the windbreak [m].

ET estimates from large areas of vegetation or from small areas of vegetation that are surrounded by mixtures of other vegetation having similar roughness and moisture conditions should almost always be less than or equal to 1.4 ET_0, even under arid conditions.

2.3.3. Application of the FAO guidelines to tree-lawn combinations in Moscow

We applied the FAO guidelines to trees-lawn combinations in the following way:

1) Determination of the growth stage of *Tila cordata* of each of the six distinguished periods. According to the FAO guidelines they were classified as initial period, development period, three mid-season periods, and late season period, successively.

2) Calculation of the potential evapotranspiration of the grass reference ET_0 for each of the six periods.

3) Calculation of "overall" values $f_{c,combination}$ for each site and each mid-season period using the values of the fraction of ground cover f_c for trees alone ($f_{1,t}$) and grass alone ($f_2 = f_{1,g}$) for each site and mid-season period. These values were obtained from digital photographs

through image analysis for each site and period.

Index 1 refers to area under crowns; index 2 refers to area outside crowns.

Index *t* refers to tree crowns; index *g* refers to lawn (grass).

The calculation of "overall" values $f_{c,combination}$ for each site and each mid-season period is made with the equation

$$f_{c,combination} = \frac{\left[\left(f_1 \cdot \sum S_{crown}\right) + \left(f_2 \cdot (S_{area} - \sum S_{crown})\right)\right]}{S_{area}}$$

ΣS_{crown} = total area of crown projections [m^2],

S_{area} = total area of object [m^2],

f_1 = total fraction of ground under crowns that is covered by trees and/or grass [-],

f_2 = fraction of lawn outside the tree crown projections that is covered by the grass canopy (1-fraction of "bare soil") [-].

The quantity f_1 is calculated according to

$f_1 = f_{1,t} + (1- f_{1,t}) \cdot f_{1,g}$

$f_{1,t}$ = fraction of lawn (grass + "bare soil") under the tree crown projections that is covered by the tree canopy [-],

$1- f_{1,t}$ = fraction of lawn under the tree crown projections that is not covered by tree canopy (fraction of "sky") [-],

$f_{1,g}$ = fraction of lawn covered by grass canopy, in spots within the tree crown projections that are not covered by tree canopy [-].

The quantity $f_2 = f_{1,g}$.

4) Calculation of "overall" values of $LAI_{combination}$ for each site and each mid-season period according to

$$LAI_{combination} = -\frac{\ln\left(1 - f_{c,combination}\right)}{0.5},$$

$(1-f_{c,combination})$ = fraction of the ground of the object, that is not covered by tree and/or grass leaves. The above equation is obtained by inversion of a relation between fraction of ground cover and leaf area index (Beer's extinction law for spherically oriented leaves and vertical radiation beams; Bakker, 1992; Bakker et al., 1995; Oker-Blom, 1988).

5) Calculation of $K_{c,mid,combination}$ values for each site and mid-season period from the LAI values using the Ritchie type equation (Allen et al., 1998, p. 186)

$$K_{c,mid} = K_{c,ini} + \left(K_{c,full} - K_{c,ini}\right)\left(1 - \exp(-0.7LAI)\right)$$

For this we used that equation in the following form (the equation can be applied to the trees vegetation as well as to the combination vegetation (trees and grass)):

$$K_{c,mid,combination} = K_{c,ini} + \left(K_{c,full} - K_{c,ini}\right)\left(1 - \exp(-0.7LAI_{combination})\right)$$

6) Calculation, from the obtained $K_{c,mid,combination}$ values and the $K_{c,ini}$ (0.45) and $K_{c,end}$ (0.45) values, and from the grass reference, the potential evapotranspiration of each site and period. Here, we calculated $K_{c,development}$ as the mean of $K_{c,ini}$ and $K_{c,mid}$ for the first mid-season period.

7) Estimation of soil water and salinity stress of the sites.

8) Calculation, from the potential evapotranspiration and water- and salinity stress, the actual evapotranspiration for each site and period.

9) Making graphs of the courses of potential and actual evapotranspiration of each site during the total growing period.

Estimation accuracy of the selected FAO methodology

The authors of the FAO methodology aimed at providing a method that is consistent with actual crop water use data worldwide. The methodology is a consistent and transparent basis for a globally valid standard for crop water requirement calculations. The authors (Allen et al., 1998) write:

"To evaluate the performance of these and other estimation procedures under different climatological conditions, a major study was undertaken under the auspices of the Committee on Irrigation Water Requirements of the American Society of Civil Engineers (ASCE). The ASCE study analysed the performance of 20 different methods, using detailed procedures to assess the validity of the methods compared to a set of carefully screened lysimeter data from 11 locations with variable climatic conditions (Jensen et al., 1990). The study proved very revealing and showed the widely varying performance of the methods under different climatic conditions. In a parallel study commissioned by the European Community, a consortium of European research institutes evaluated the performance of various evapotranspiration methods using data from different lysimeter studies in Europe…..

The relatively accurate and consistent performance of the adopted FAO methodology in both arid and humid climates has been indicated in both the ASCE and European studies…

The methodology is recommended as the sole standard method. It is a method with strong likelyhood of correctly predicting evapotranspiration in a wide range of locations and climates."

The selected FAO methodology consists of two parts: use of the FAO-Penman-Monteith equation for calculating reference evapotranspiration; calculation of the crop factor of non-pristine, sparse, tall, vegetation.

Reference evapotranspiration calculation

Jensen et al. (1990) evaluated the adopted FAO-Penman-Monteith reference calculation using lysimeter data sets from 6 arid and 5 humid lysimeter sites all over the world. Table 2.1 compares characteristics of these sites with weather information from Moscow. Table 2.2 indicates the range of estimation accuracies for all locations. It may be concluded that the reference calculation method has a strong likelihood of correctly estimating reference evapotranspiration in Moscow.

Crop factor calculation

The crop factors of regular agricultural crops have been determined by lysimeter experiments. These are empirical values and can be found in several manuals. Lysimeter values are scarce for non-pristine, sparse, vegetation. But for this type of vegetation, lysimeter research provided an empirical relationship between crop factor and LAI (Ritchie, 1972; Ritchie and Johnson, 1990). This relationship is included in the FAO methodology.

Crop factors show some dependency on wind speed and relative humidity. Generally, crop factors increase as wind speed increases and minimum daily relative humidity decreases. This is primarily due to differences in roughness between taller plants and clipped grass (NN, 1996b). The dependency increases with vegetation height. Several manuals present graphs and/or equations for the determination of correction factors for this. The factors follow the

Table 2.1. Comparison of Moscow climate with lysimeter sites at other locations

Characteristics	Moscow[2] June 15 – July 16, 2004	All[1] lysimeter locations and periods[3]
Latitude, ^{o}	56	0 – 56
Mean air temperature, ^oC	17.2	6 – 32
Wind speed, m s^{-1}	0.95	0.8 – 4.2
Net radiation, MJ m^{-2} d^{-1}	9.80	3.7 – 8.5

[1] Included in the study of Jensen et al. (1990).
[2] According to Chaper 4 of this report.
[3] May, July, September, and November, January, March for northern and southern latitudes, respectively.

Table 2.2. Estimation accuracy of the FAO-Penman-Monteith equation (Jensen et al., 1990) for estimating reference evapotranspiration

Estimated quantity of reference evapotranspiration	11 lysimeter locations
Average peak monthly estimates expressed as % of lysimeter values	82 – 107
Seasonal estimates expressed as % of lysimeter values	90 – 106
Standard errors of estimate of estimates versus lysimeter values, in mm d^{-1}, of monthly values over entire seasons of record	0.11 – 0.65

general trends in lysimeter results at different wind speeds, different values of minimum daily relative humidity and different vegetation heights. The correction is included in the FAO methodology.

2.4. CONCLUSION

Evapotranspiration is a very complex process. The application of mechanistic models introduces many difficulties and uncertainties. Section 2.2 showed that this especially holds true for the aerodynamic resistance r_a and the canopy resistance r_c of sparse, tall, vegetation. We made example calculations with a number of mechanistic models. The outcome of these calculations appeared often to be unrealistic. Therefore, the further part of the thesis uses the empirical-analytical FAO guidelines for computing evapotranspiration of “non-pristine”, sparse, tall vegetation. The method according to the FAO guidelines uses, as a first step, a mechanistic model for the calculation of the potential evpotranspiration of a reference crop (short, closed, grass). This calculation also needs values of r_a and r_c , but these values are accurate in the case of short, closed, grass. In the second step, the difference between the potential evapotranspiration of the crop under consideration and the potential evapotranspiration of the grass reference is determined on the basis of empirical information that has been collected from a vast amount of lysimeter (or lysimeter-like) experiments. The reference evapotranspiration is not only computed according to the FAO guidelines but also according to Makkink (1957, 1962).

CHAPTER 3. RESEARCH SITES AND DATA COLLECTION

3.1. Selected sites in Moscow

3.1.1. Locations

The territory of Moscow city is 1081 km^2. Therefore, climatic, hydrological and soil conditions of various parts of the city are different. In order to reduce differences between conditions only one part of the city was chosen: the north-east.

Differences in city conditions are also connected with anthropogenic factors: intensity of air pollution and degradation of soil under the influence of industry and transport; housing density; population size. In the central part of the city adverse ecological conditions are observed (poor aeration, increased concentration of pollutants, etc.). The best ecological conditions are in the suburbs of the city. The middle part of the city has average conditions (NN, 2004).

Therefore, for our studies, sites were selected in the central and middle parts of the city and at the outerparts: Saharov prospect, Sokolniki (Strominka street) and Habarovskaya street (Figs. 3.1. and 3.2.).

Objects of studies were Linden trees (*Tilia cordata*) and lawn (combination of trees with lawn), located along main streets on the solar side. This species of trees is most frequent in Moscow (19.5% of all city tree vegetation). In a first step, the state of a large number of trees in each ecological zone was assessed on the base of visual estimation. The assessment classified these trees using the following tree state categories: 1: trees with less than 25% of leaves wilting; 2: trees with 25–50% of leaves wilting; 3: trees with 50–75% of leaves wilting; 4: trees with over 75% of leaves wilting (see section 1.6.). In the second step, trees, all of similar age, were selected in such a way that the distribution of the states of the selected trees was representative for the distribution of tree states. In summary:

In total, the state of 139 trees was visually assessed;

from them, 40 trees were selected;

Saharov pr. – 15 trees (coded 2–4; 6–10 and 1–7 (I–III);

Sokolniki (Strominka st.) – 14 trees (coded 1*–10* and 1–4);

Habarovskaya st. – 11 trees (coded 1–11).

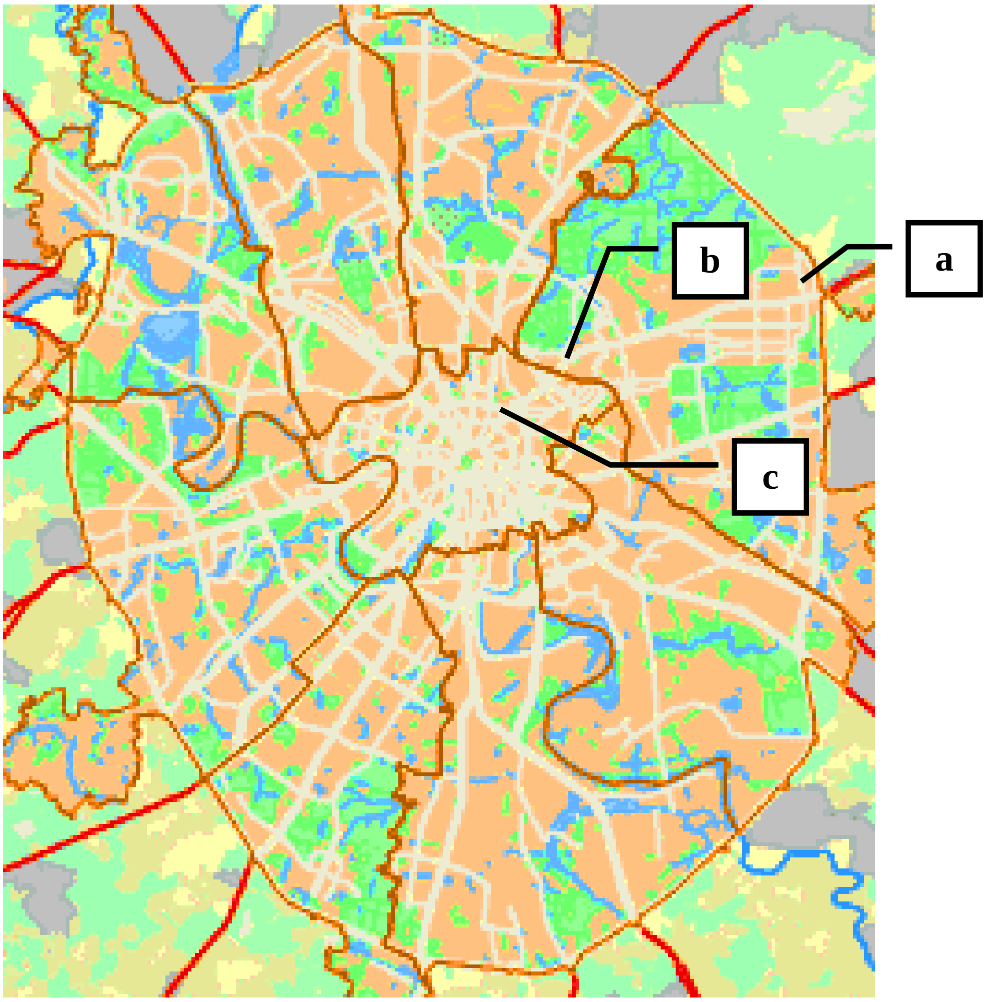

Fig. 3.1. Location of the sites in the territory of Moscow (overview):
a – Habarovskaya st; b – Sokolniki (Strominka st.); c – Saharov pr.

3.1.2. Soil profiles of the study sites

The results of a soil survey that was carried out on the objects are given in Table 3.1. The profiles of urban soil strongly differ from agricultural and natural soils (humus-podzol) (Fig. 3.3).

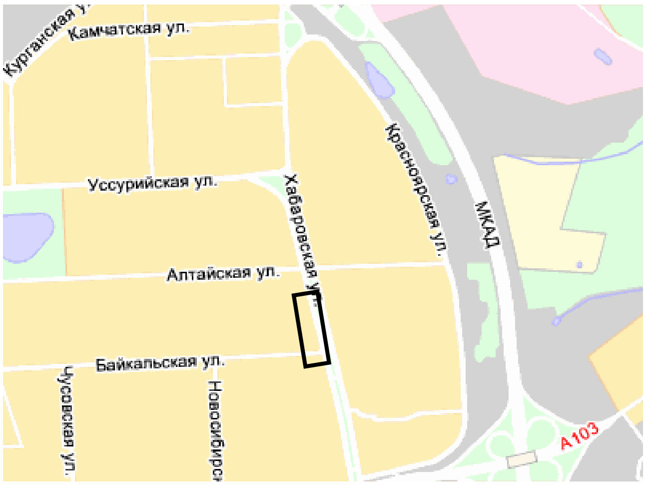

a

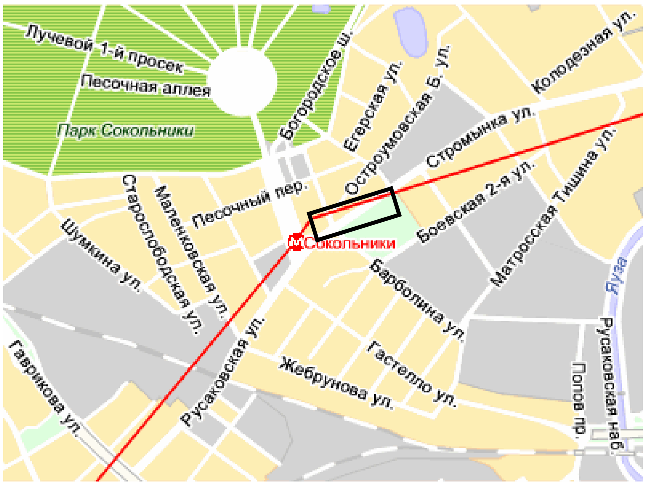

b

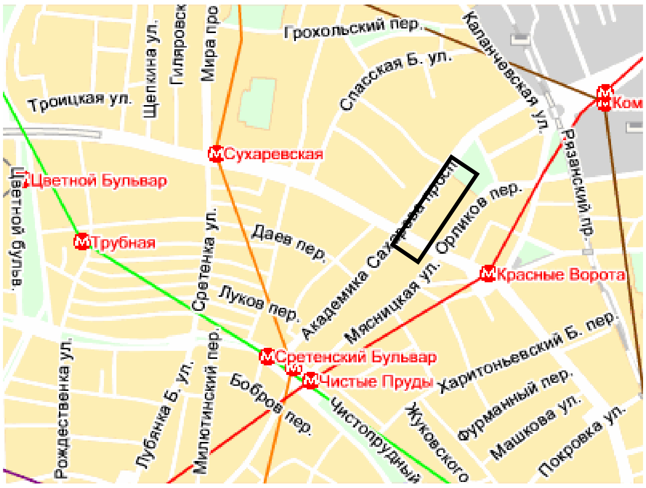

c

Fig. 2.2. Location of the sites (enlarged):

a – Habarovskaya st; b – Sokolniki (Strominka st.); c – Saharov pr.

Table 3.1. Description of three urban soil profiles, one agricultural soil profile, and one natural soil*

Object	Index of layer	Depth of layer, cm	Some characteristics
Habarovskaya st.	Ud_1	0–30	urban mix from peat, sand and top (humus) layers of natural soil; colour – dark-gray; texture – sandy clay loam with high organic matter content (silty clay loam with high dust content), much dust; not compact; soil aggregates with predominant size < 1 mm and content not more than 10%.
	Ud_2	30–60	urban mix from peat, sand and top (humus) layers of natural soil, but with less organic matter content than Ud_1; colour – gray; texture – silty clay loam with high dust content, more dust than in Ud_1; not compact; soil aggregates with predominant size < 1 mm and content not more than 5–10%.
	CU_{1g}	60–80	mix from Ud_2, layer B of natural soil (subsoil) and moraine; colour – mix from gray and red-brown (foxy); texture – clay loam with dust from subsoil; compact; gleyic layer.
	CU_{2g}	80–100	mix from layer B of natural soil (subsoil) and moraine; colour – red-brown (foxy); texture – clay loam; compacted; gleyic layer.
Sokolniki (Strominka st.)	Ud_1	0–20	urban mix from peat and sand; colour – very dark–gray (black); texture – sandy clay loam with high organic matter content, much dust; not compact; size of predominant soil aggregates not more than 0.25 mm; very bad structure.
	Ud_2	20–40	urban mix from peat, sand and top (humus) layers of natural soil; colour – dark-gray; texture – silty clay loam with high dust content; not compact; soil aggregates with predominant size not more than 0.25 mm; unstructured layer.
	CU_1	40–60	mix from Ud_2 and layer B of natural soil (subsoil); colour – mix from light brown and gray; texture – silty clay loam with dust, but almost without organic matter; not so compact.
	CU_2	60–80	mix from CU_1 and moraine; colour – mix from brown and red-brown (foxy); texture – clay loam with dust and fine sand; compact.

	CU_{3g}	80–100	colour – red-brown (foxy); texture – clay loam with sand; very compact; gleyic layer.
Saharova pr.	Ud_1	0–20	urban mix from peat, sand and top (humus) layers of natural soil; colour – dark-gray; texture – silty clay loam with high dust content and high organic matter content; not compact; soil aggregates with predominant size < 0.25 mm and content not more than 10%.
	Ud_2	20–100	urban mix from peat, sand and top (humus) layers of natural soil; colour – gray; texture – silty clay loam with high dust content but with less organic matter content than Ud_1; not compact; soil aggregates with predominant size < 1–3 mm and content not more than 10–20%; contains gravel and small parts of brick (anthropogenic, construction, influence).

Agricultural soil	A_{plough}	0–24	Plough layer; colour – gray; silty clay loam with high dust content; not compact.
	A_2B	24–52	colour – mix from light brown and whitish; texture – silty clay loam; compact.
	B_{1g}	52–66	colour – red-brown (foxy); texture – clay loam; compact; gleyic layer.
	B_2	66–94	colour – brown; texture – clay loam; compact.

Natural soil (humus-podzol)	A_1	0–13	Humus layer; colour – gray; silty clay loam with high dust content; not compact.
	A_2B_g	13–46	colour – mix from light brown and whitish; texture – silty clay loam; compact; gleyic layer.
	B_{1g}	46–73	colour – light brown; texture – clay loam; compact; gleyic layer.
	B_2	> 73	colour – brown; texture – clay loam; compact.

* The indices U, Ud, and CU refer to an urban soil classification system that has been developed by M.N. Stroganova at the Moscow State University:

U = urban layer.

Ud = urban layer with much organic matter (d from “djoem”), often originated from grass roots.

CU = mix from natural soil (B and/or C) with urban soil.

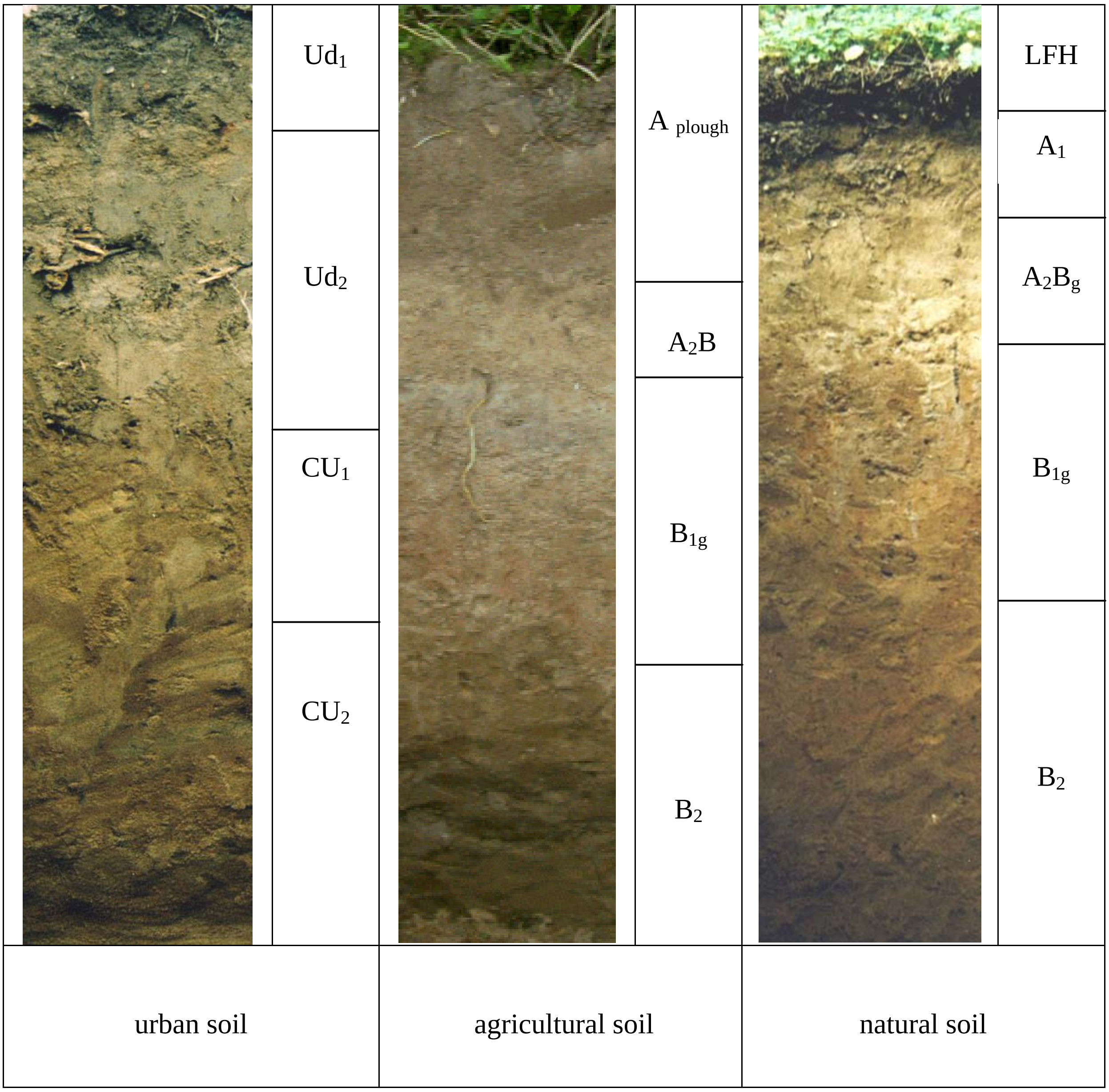

Fig. 3.3. Profiles of different types of soil

3.2. Materials and methods

3.2.1. Soil measurements

Soil in the root zone of each tree of each object was sampled with an auger and with 100 cc metal cylinders (Fig. 3.4a). Samples were taken from each 10 cm layer down to a depth of 1 m. The studies of urban soil were for a depth of 1 m, because for this depth on all territories of

Moscow city actions are carried out for monitoring, improvement and restoration of properties of soil favourable for vegetation (according to the Law of Moscow city about urban soil).

Sampling at each tree was carried out fivefold. The soil in the cylinders was taken to the laboratory in order to estimate texture and organic matter content, and to make a morphological description of the layers. At the sites, immediately after collecting the soil, a special so-called W.E.T. sensor (Eijkelkamp, Giesbeek, The Netherlands) was used to measure volumetric water content, soil temperature, and electric conductivity (Fig. 3.4b).

a b

Fig. 3.4. The used equipment:

a – Kit with soil sampling cylinders; b – W.E.T. sensor (Eijkelkamp)

3.2.2. Vegetation measurements

Measurements were taken from each tree and corresponding lawn area of each object, in order to obtain values of crown projection areas of trees, tree fractions of ground cover, tree Leaf Area Index, grass fractions of ground cover, and grass Leaf Area Index. Fraction of ground cover and LAI of tree crowns and lawn areas were estimated through image processing of digital photos that were taken in an upward direction beneath the tree crowns and in a downward direction towards lawn areas. The method is explained in detail in section 3.2.3. Here we describe some general considerations on the method to be chosen.

Several methods for measuring canopy structure exist (Norman and Campbell, 1989; Lindsey and Bassuk, 1992; Hardin and Jensen, 2007). Traditional methods involve: destructive harvesting of leaves within a vertical column passing through the canopy; collection of leaf litter. We required a method which was non-destructive, suitable for high (tree) as well as for low (grass) canopies, insensitive to quickly changing weather conditions, objective, very quick, and available.

Gap fraction analysis is a powerful non-destructive field method. The analysis assumes a relationship between LAI and gap fraction. One class of gap fraction methods further assumes a relationship between gap fraction and light attenuation with increasing depth in vegetative canopies. A second class of gap fraction methods is based on the measurement of gap fractions from images of the canopy. This measurement may be done by simple counting techniques, by special counting devices, using a planimeter, or by digital image analysis. The selected method belongs to the last category. It includes a two-steps procedure to optimize accuracy of gap fraction estimation. In the first step, processed images are visually compared with the original image. Such processed image has the property that its resemblance with the original image can be easily inspected and optimized by eye. In the second step, the gap fraction of the processed and optimized image is determined by computer. Physical backgrounds of digital image processing are given in Pratt (2007). The method is non-destructive, suitable for high (tree) as well as for low (grass) canopies, insensitive to quickly changing weather conditions, objective, and very quick. It could be made available by courtesy of J. Meuleman (Wageningen University and Research Centre).

In order to determine LAI of a tree four quadrants of the tree crown were photographed. LAI of each quadrant was determined from the four quadrant images. The four values of the quadrant LAI were averaged in order to obtain the tree LAI. Due to heterogeneity of the tree crown the LAI values of each of the four quadrants will not be the same. The standard deviation of these four values is a measure of tree crown heterogeneity. If overlap of the quadrant images is negligible, and the determination of quadrant LAI is accurate, the procedure provides an accurate tree LAI value. So, the standard deviation of the four values of quadrant LAI is a measure of tree crown heterogeneity rather than a measure of accuracy of the tree LAI determination. Similarly, standard deviation of LAI values of different lawn areas of a site is a measure of lawn heterogeneity of the site rather than a measure of accuracy of the lawn LAI determination.

For comparison and transformation of information about tree state categories, obtained on the base of visual estimation, we can use the correlations with values of leaf area index LAI given in Table 3.2. The LAI values in this table have been calculated assuming that the gap fraction D of categories 25%, 50%, 75% wilted leaves is 0.25, 0.50, and 0.75, respectively, and by applying equation:

$$LAI = - 2* \ln D$$

A common value of LAI of trees in good condition is, e.g., six (corresponding to category zero, with D = 0.05, in the Russian classification). Comparing this with the table, we see that visual estimation is not so “sensitive” in the LAI range of 2.8 – 6.

Table 3.2. Tree state categories and values of LAI

№ of category	Tree state categories (visual estimation)	Values of LAI
1	Trees with less than 25% wilted leaves	> 2.8
2	Trees with 25% – 50% wilted leaves	2.8–1.4
3	Trees with 50% – 75% wilted leaves	1.3–0.6
4	Trees with over 75% wilted leaves	< 0.6

3.2.3. Estimation of canopy parameters through image processing

A number of parameters of the tree canopies and the lawn canopies were estimated by taking photos with a digital camera and processing the photos with a special computer program. The photos were taken in an upward direction beneath the tree crowns and in a downward direction towards lawn areas. Photos were taken at six points of time during the growing season. At each of these points of time each tree crown was photographed from four positions underneath the crown. After image processing, results were averaged per tree. The digital camera provided JPEG images of 1600 × 1200 pixels. Before applying the image analysis program all digital photos had to be transferred from format JPEG to BMP. The image analysis program was developed and written in C++ by J. Meuleman, Wageningen University, Wageningen, The Netherlands. The application of the program involved regular comparisons between originals and processed versions, which appeared to be feasible with a 55 cm colour display monitor.

The program results are the fraction of ground cover by the tree crown, the visible fraction of leaf area of the tree crown, the visible fraction of stem and branch area of the tree crown, the fraction of ground cover by the lawn, the visible fraction of the canopy of the lawn. The program has the possibility to select or exclude parts of the images, by defining an envelope around parts through a mouse-clicking procedure. The accuracy of the determination of the fractions of ground cover, which can be judged visually on the screen, appears to be very high. It is this fraction that is used to calculate a value of LAI. This calculation is based on an inverse form of Beer's law.

Theoretical background. Applied to plant canopies, Beer's law states that the relative attenuation rate of the direct component of solar radiation is proportional to the amount of foliage (leaves) along the path of the solar beam:

$$d\,I_s / I_s = -\,k_s * d\,(LAI_{path})$$

I_s = direct solar radiation along the path of the solar beam in the canopy [J s^{-1}],
LAI_{path} = LAI along the path (fractional surface area of leaves projected on a plane perpendicular to the path) [-],
k_s = extinction coefficient = mean projection of a unit foliage area on a plane perpendicular to the solar beam. For spherically oriented leaves (no preferred direction of the leaf normal),
k_s = 0.5 [-].

Integration of the above equation gives:

$$I_s = I_{so}\,exp\,(-\,k_s * LAI_{path})$$

I_{so} = direct solar radiation of the beam just above the canopy [J s^{-1}],
I_s = direct solar radiation of the beam just under the tree crown [J s^{-1}],
LAI_{path} = LAI_{path} along the total path length of the beam through the canopy [-].

This equation can be rewritten as:

$$LAI_{path} = -\,(1/k_s) * ln\,(I_s / I_{so})$$

This equation may be applied to a (hypothetical) vertical beam. Then:
$LAI_{path} = LAI,$

I_s / I_{so} = fractional area of sky that can be seen in the direction of the beam (vertical).

It means that for $k_s = 0.5$:

$LAI = - 2 * \ln D$

D = fraction of sky that can be seen on a photo that is taken from beneath a tree crown in the vertical direction (or fraction of bare soil in the case of lawn photos) [-].

The image processing procedure provides accurate values of *D*. From the accurate *D*, a value of LAI is calculated according to the above equation. This calculation may result in more or less accurate LAI values. The accuracy of the calculated LAI is less if the canopy parts are strongly clustered (Welles and Norman, 1991). Evapotranspiration is not very sensitive to LAI.

Algorithm for the digital image analysis. The computer program for analysing photos that are taken vertically upwards through a tree crown has the following structure and algorithm. One complete image consists of 1200x1600 pixels each having a 32 bits address. These 32 bits contain the intensities of three colour channels:

- 8 bits being the intensity of the red channel (the r-value),
- 8 bits being the intensity of the green channel (the g-value),
- 8 bits for the intensity of the blue channel (the b-value),
- 8 bits unused.

The range of each of the r, g, b values is 0–255. From all measured r, g, b values r-, g-, and b-histograms are made. An r-histogram of an image is a function that gives the frequency of occurrence of each r-level in the image (this level ranges from 0 to 255). The value of the histogram at a particular r-level is the fraction of pixels in the image with that r-level. In the same way, the g- and b-histograms are defined. Generally, the tree images have histograms with rising right parts. These rising right parts represent “sky”. The intensities where these rising right parts start are identified by mouse clicking in the histogram, above the curve-part where rising starts. The intensities at which clicking in each of the three histograms occurred are recorded and named threshold_blue, threshold_green, and threshold_red. Intensity values larger than the respective thresholds likely belong to pixels representing “sky”. The threshold values are displayed in the upper part of the histogram window (for instance: r = 213 g = 221 b = 215). In the next step the program transforms the colour of each pixel into sole blue 255 or sole green 255 or sole red 255 on the basis of the following criteria:

- If all three threshold values are exceeded, the pixel will be made blue. Otherwise:
- If the intensity of the green or the intensity of the red is smaller than 2, the program will transform the colour of the pixel into red. It means that the signal levels are too small to take a decision. In most cases this happens on parts of the trunk or branches of a tree. Otherwise:
- If (green intensity + 1) is larger than 1.25 times (blue intensity + 1), the pixel will be transformed into green. The 1-additions only have computational reasons.
- The remaining pixels represent trunk and branches.

Subsequently, the new image is displayed together with the original image, which allows a visual inspection of the “goodness of classification”. If the correspondence is not satisfactory, the threshold values may be changed in order to improve correspondence. This trial and error procedure may be repeated until the correspondence is sufficient. Finally, the program computes the number of blue, green and red pixels as percentages of all pixels of the image.

Blue = sky

Green = leaves

Red = stem (trunk and branches)

For the lawn, a slightly modified program is used:

- All thresholds are set equal to 255, eliminating “sky”.
- If the intensity of the green or the intensity of the red is smaller than 2, the program will transform the colour of the pixel into white. Otherwise:
- If (green intensity + 1) is larger than 1.25 times (blue intensity + 1), the pixel will be transformed into green. The 1-additions only have computational reasons.
- Otherwise, the pixel will be made red.

Green = leaves

Red = bare soil

The “select” option in the program allows selecting areas in the image that can be let out of consideration. This option is used to exclude the trunk to prevent the trunk from influencing the image processing results.

Step 2 of both algorithms is not really important. It solves situations where no decision can be made concerning the signal levels. By manual inspection, during the development of the program, these pixels were assigned to the most likely category (“trunk and branches” in the case of crowns; not-considered part in the case of lawn).

Illustration of program application. The remaining part of this section illustrates the digital image processing. Point 1 is a photo of object Saharov pr., alley of trees 1−7 (I−III) at a certain point of time. Point 2 presents the trees at the subsites I, II, and III. Point 3 presents the digital photos taken from 4 positions underneath the crown of one of the trees. Point 4 is a digital photo from a lawn area belonging to a tree. Point 5 gives technical data of the digital camera. Point 6 illustrates buttons and information on the screen, together with some screen pictures. These pictures play a role in the interaction of the operator with the program.

1. Object

Saharov prospect

2. Trees

Trees 1–3 (I)

Trees 4–5 (II)

Trees 6–7 (III)

3. Digital photos of 4 sides of tree crown (JPEG Image, 1600 × 1200 pixels)

a

b

c

d

4. Lawn under tree

5. Equipment – Digital camera “Nikon Cool Pix 5700”

Nikon Cool Pix 5700

Camera controls	Top, Rear, Lens barrel
LCD monitor	1.5" 110,000 pixel, flip-out & twist
LCD 'soft buttons'	No
Status LCD	Top of camera, illuminated
Lens	35 - 280 mm equiv. (8×), F2.8 - F4.2
Lens accessories	0.8x wide angle, 1.5× tele, thread adapter, hood
Macro range	3 cm – Infinity
Max shutter	1/4000 sec 1.3 stops from max aperture
RAW format	Yes (Nikon NEF)
JPEG type	EXIF 2.2 (ExifPrint)
Continuous	Continuous H, Continuous L, Multi-Shot 16, Ultra High-Speed Continuous
Flash	Electronic automatic pop-up
Flash range	Approx. 4.0 m (13.1 ft) @ Wide
Viewfinder	180,000 pixel electronic viewfinder
Weight (inc batt.)	512 g
Dimensions	108 x 76 x 102mm

6. Some buttons, windows and screen pictures of the special program for estimation of Leaf Area Index (LAI) of tree and of lawn. Before using this program all digital photos must be transferred from format JPEG to BMP.

<u>Tree</u>

Read BMP-image
Make Histogram
Sky
Envelope

Results Complete Image
Sky = ??? %
Leaves = ??? %
Stem = ??? %

Results Within Envelope
Sky = ??? %
Leaves = ??? %
Stem = ??? %
LAI = ???

<u>Gazon (lawn)</u>

Read BMP-image
Make Histogram
Bare Soil
Remove Stem, etc.
Calculate minus stem

Results Complete Image
Excluded = 0.00 %
Leaves = ??? %
Bare Soil = ??? %

Results Within Envelope
Excluded = ??? %
Leaves = ??? %
Bare Soil = ??? %
LAI = ???

Tree

BMP-image

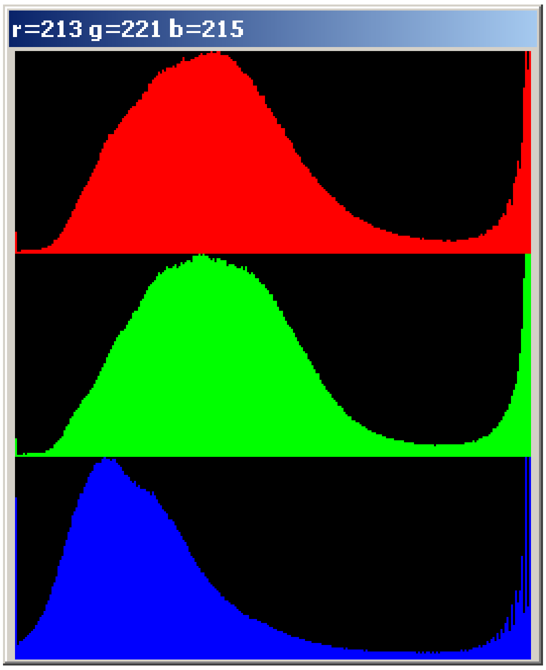

Histogram

RGB-image

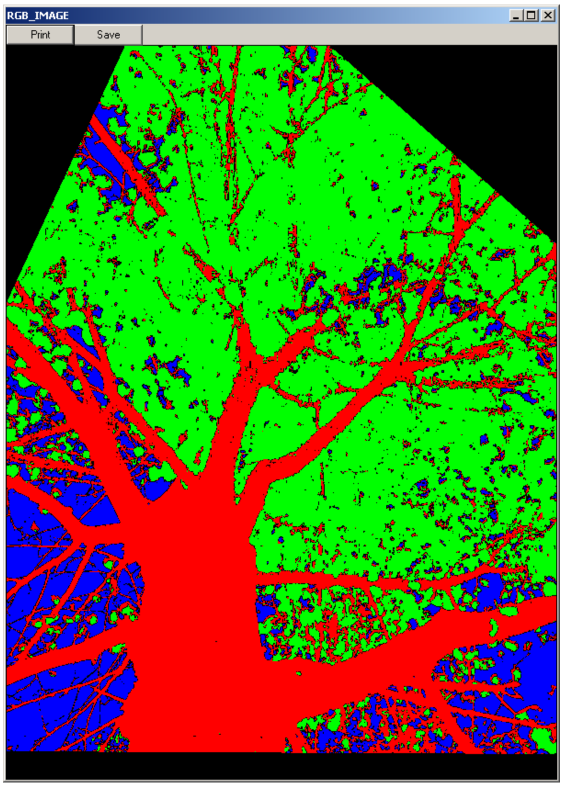

RGB-image (Within Envelope)

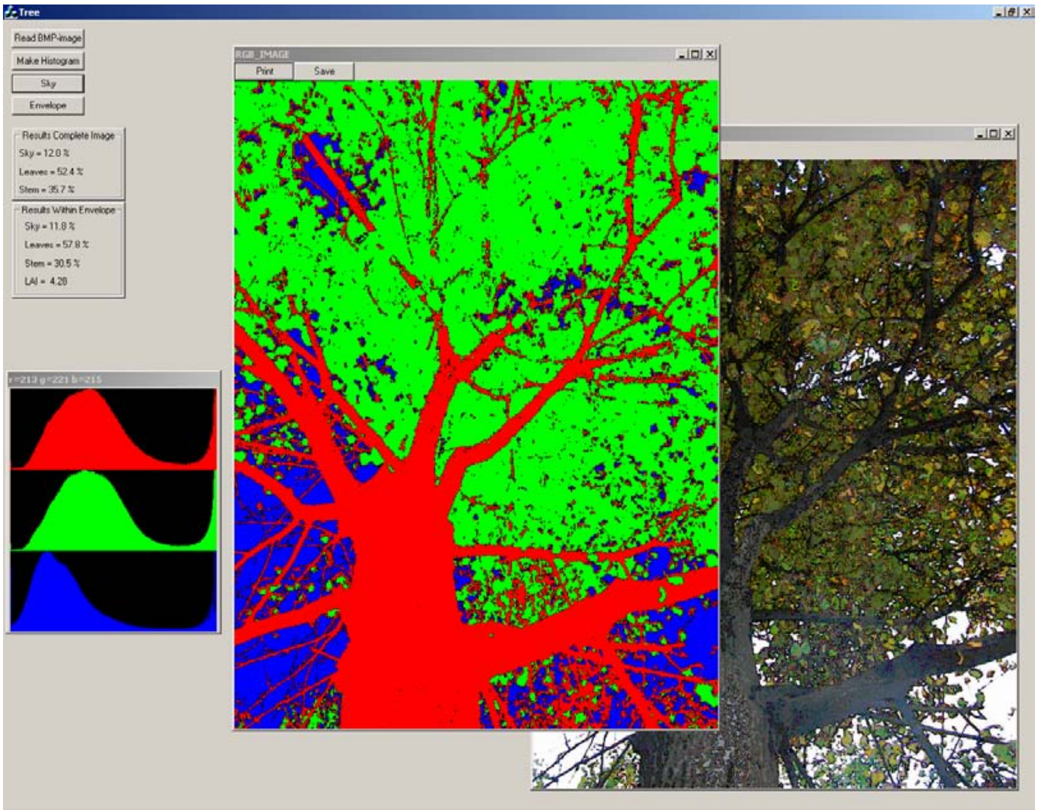

Results Complete Image

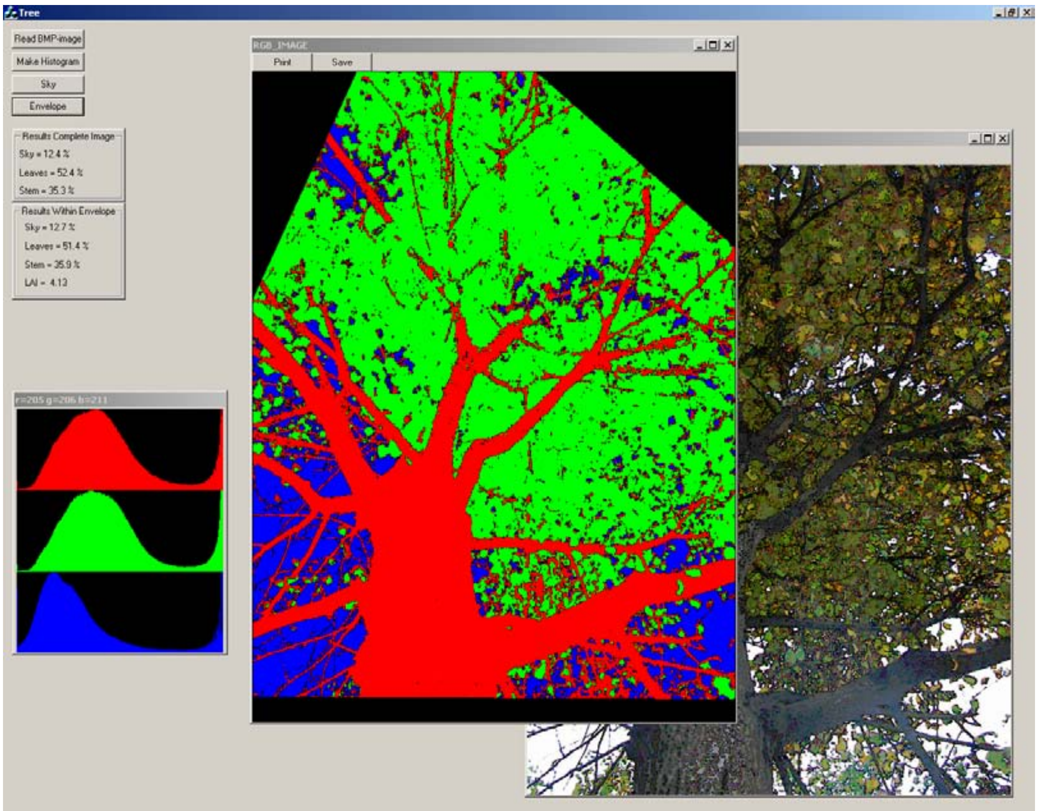

Results Within Envelope

Gazon (lawn)

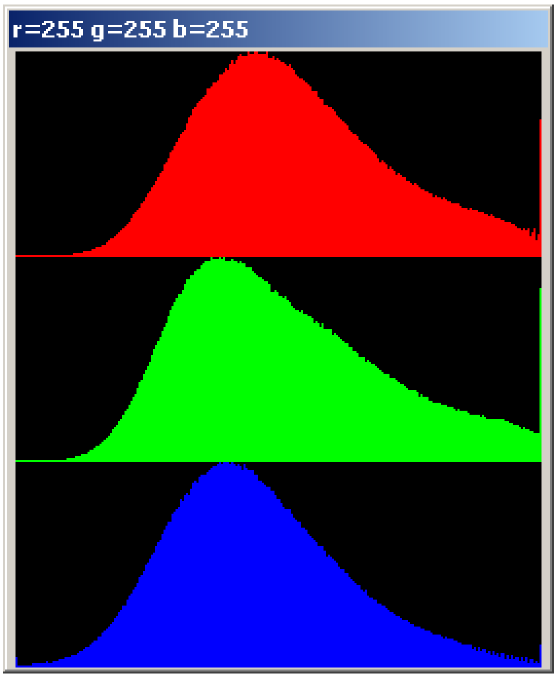

BMP-image

Histogram

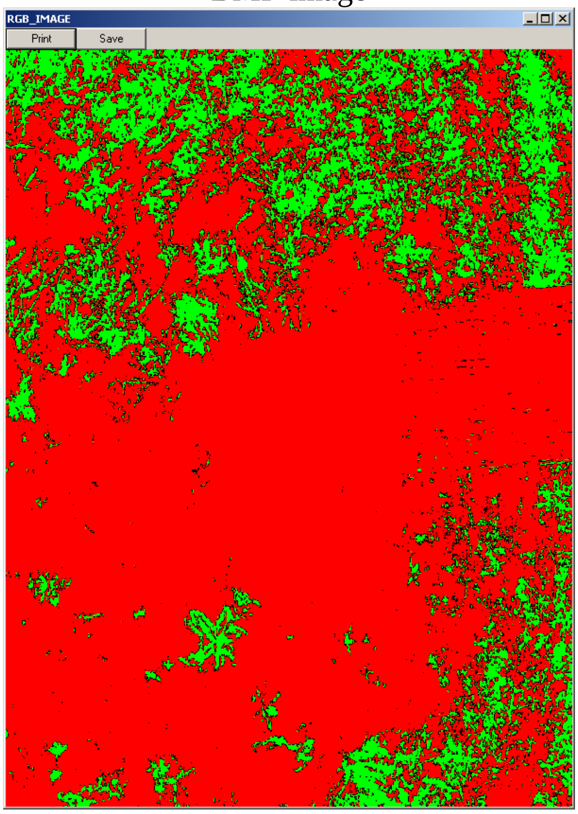

RGB-image

Remove Stem

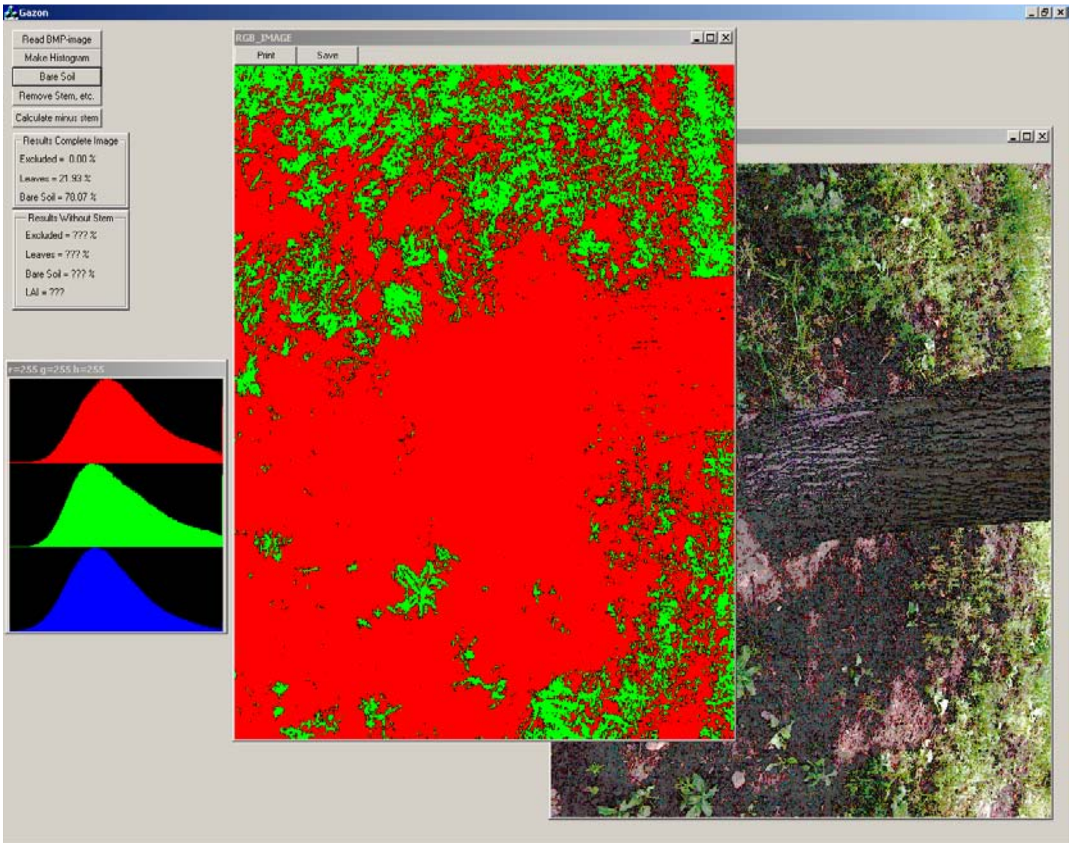

Results Complete Image

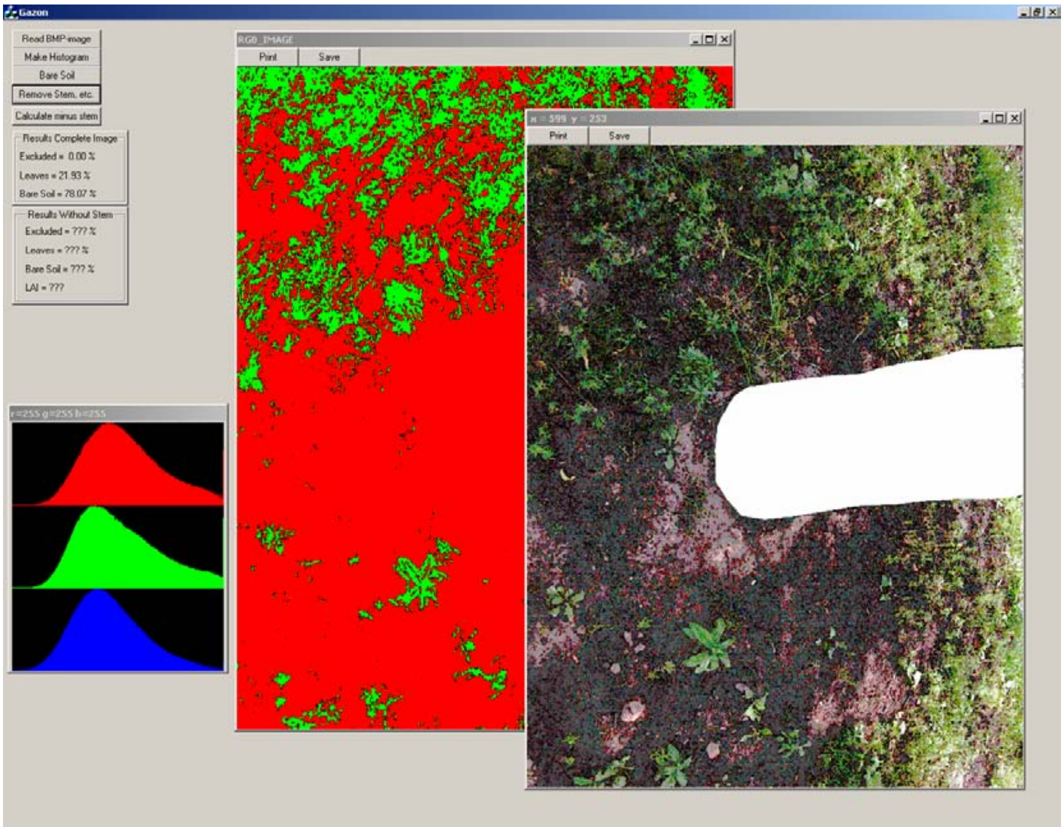

Results After Remove Stem

3.2.4. Meteorological data

The Meteorological Institute of Moscow provided meteorological data which were measuring values averaged over the meteorological stations of Moscow, for the considered period:

- diurnal rainfall,
- diurnal maximum and minimum temperatures,
- diurnal maximum and minimum relative air humidities,
- diurnal maximum and minimum cloudiness values,
- diurnal maximum and minimum wind speeds.

We converted these data into needed parameters, averaged over distinguished periods. Values for clear-sky solar (clear-sky short-wave) radiation were derived from latitude and time of the year. Values for net outgoing long-wave radiation were derived from mean air temperature, air humidity and cloudiness. These derivations followed Van Keulen and Wolf (1986).

3.2.5. Deviation calculations

In this thesis, means $\bar{x}$ and deviations $s_{\bar{x}}$ from means are calculated according to

$$\bar{x} = \frac{(X_1 + X_2 + \dots X_n)}{N}$$

$$s = \sqrt{\left[(X_1 - \bar{x})^2 + (X_2 - \bar{x})^2 + \dots (X_n - \bar{x})^2 \right] / N}$$

$$s_{\bar{x}} = s / \sqrt{N}$$

$$\bar{x} \pm s_{\bar{x}}$$

X_i and N are individual measuring data and number of measurements, respectively.

CHAPTER 4. MODELING AND CALCULATION OF POTENTIAL EVAPOTRANSPIRATION FROM MEASURING DATA

4.1. Calculation of reference evapotranspiration

The growth stages of Linden (*Tilia cordata*) in Moscow and suitable evapotranspiration periods were determined according to the FAO guidelines. See Table 4.1.

Table 4.1. Selected evapotranspiration periods and growth stages of linden (*Tilia cordata*) in Moscow

Periods	Stages
15.04.04−15.05.04	Initial
16.05.04−14.06.04	Development
15.06.04−16.07.04	Mid-season
17.07.04−16.08.04	
17.08.04−14.09.04	
15.09.04−15.10.04	Late season

Reference evapotranspiration was calculated for each period according to the FAO guidelines (section 2.3.3.) and according to Makkink's radiation model (section 2.3.1.).

Calculation of the evapotranspiration of the grass reference for each period

1. *Needed data that were derived from Moscow meteorological data, and location*

T_{max} = monthly average daily maximum air temperature at 2 m above ground surface [^{0}C],
T_{min} = monthly average daily minimum air temperature at 2 m above ground surface [^{0}C],
u_2 = monthly average wind speed at 2 m above ground surface [m s^{-1}],
RH_{max} = monthly average daily maximum relative humidity [%],
RH_{min} = monthly average daily minimum relative humidity [%],
n = actual duration of sunshine in a day [hour],

Altitude = 150 [m],

Latitude = 56^0 N.

2. Quantities that are required by the FAO reference model for each period

T_{mean} = daily mean air temperature [^{0}C],

Δ = slope of saturation vapour pressure curve [kPa $^0C^{-1}$],

γ = psychrometric constant [kPa $^0C^{-1}$],

$e^0\ (T_{max})$ = saturation vapour pressure at maximum air temperature [kPa],

$e^0\ (T_{min})$ = saturation vapour pressure at minimum air temperature [kPa],

e_s = saturation vapour pressure for a given time period [kPa],

e_a = actual vapour pressure [kPa],

$e_s - e_a$ = saturation vapour pressure deficit [kPa],

R_a = extraterrestrial radiation [MJ m^{-2} day^{-1}]

(solar radiation received at the top of the Earth's atmosphere on a horizontal surface),

N = maximum possible sunshine duration in a day, daylight hours [hour],

n/N = relative sunshine duration [dimensionless],

R_s = solar or shortwave radiation [MJ m^{-2} day^{-1}]

(amount of radiation reaching a horizontal plane, after some of the radiation is scattered or absorbed by the atmospheric gases, clouds and dust),

R_{so} = clear-sky solar or clear-sky shortwave radiation [MJ m^{-2} day^{-1}]

(solar radiation that would reach the same surface during the same period but under cloudless conditions),

R_s / R_{so} = relative solar or relative shortwave radiation [dimensionless],

R_{ns} = net solar or shortwave radiation [MJ m^{-2} day^{-1}]

(fraction of the solar radiation R_s that is not reflected from the surface),

σ = Stefan-Boltzmann constant [$4.903 \cdot 10^{-9}$ MJ K^{-4} m^{-2} d^{-1}],

R_{nl} = net longwave radiation [MJ m^{-2} day^{-1}]

(difference between outgoing and incoming longwave radiation),

R_n = net radiation [MJ m^{-2} day^{-1}]

(difference between incoming and outgoing radiation of both short and long wavelengths),

G = soil heat flux [MJ m^{-2} day^{-1}]

(energy that is utilized in heating the soil; *G* is positive when the soil is warming and negative when the soil is cooling)

ET_o = reference evapotranspiration [mm day^{-1}] (grass reference evapotranspiration).

3. Transformation of the Moscow data into the required data

Table 4.2. Values of different climatic parameters and estimation of reference evapotranspiration, for each period

Parameters	Values of parameters for each period					
	15.04.04–15.05.04	16.05.04–14.06.04	15.06.04–16.07.04	17.07.04–16.08.04	17.08.04–14.09.04	15.09.04–15.10.04
T_{max}, ^{0}C	12.9	15.7	20.4	22.4	20.2	11.8
T_{min}, ^{0}C	4.8	8.7	14.0	15.4	13.1	7.2
u_2, m/s	1.27	1.28	0.95	0.65	0.98	1.06
RH_{max}, %	85.6	85.7	91.0	94.2	92.8	91.5
RH_{min}, %	52.5	59.8	65.6	66.2	65.7	72.2
n, h	4.7	4.0	4.3	4.0	4.6	2.6
Altitude, m	150	150	150	150	150	150
Latitude, °	56	56	56	56	56	56
T_{mean}, °C	8.9	12.2	17.2	18.9	16.7	9.5
Δ, kPa/°C	0.078	0.092	0.123	0.137	0.123	0.082
γ, kPa/°C	0.066	0.066	0.066	0.066	0.066	0.066
e^0 (T_{max}), kPa	1.50	1.82	2.34	2.64	2.34	1.40
e^0 (T_{min}), kPa	0.87	1.15	1.60	1.71	1.50	1.00
e_s, kPa	1.19	1.48	1.97	2.18	1.92	1.20
e_a(average), kPa	0.77	1.04	1.49	1.68	1.46	0.97
(e_s–e_a), kPa	0.42	0.44	0.48	0.50	0.46	0.23
R_a, MJ m^{-2} d^{-1}	33.3	39.4	40.5	36.1	27.7	18
N, h	15.0	16.7	17.1	15.9	13.6	11.3
n/N	0.31	0.24	0.25	0.25	0.34	0.23
R_s, MJ m^{-2} d^{-1}	13.49	14.58	15.19	13.54	11.63	6.57
R_{so}, MJ m^{-2} d^{-1}	25.08	29.67	30.50	27.18	20.86	13.55
R_s/R_{so}	0.54	0.49	0.50	0.50	0.56	0.49
R_{ns}, MJ m^{-2} d^{-1}	10.39	11.23	11.69	10.42	8.96	5.06
σ, MJ K^{-4} m^{-2} d^{-1}	$4.903 \cdot 10^{-9}$	$4.903 \cdot 10^{-9}$	$4.903 \cdot 10^{-9}$	$4.903 \cdot 10^{-9}$	$4.903 \cdot 10^{-9}$	$4.903 \cdot 10^{-9}$
R_{nl}, MJ m^{-2} d^{-1}	2.55	2.02	1.89	1.82	2.38	1.93
R_n, MJ m^{-2} d^{-1}	7.84	9.20	9.80	8.61	6.58	3.13
G, MJ m^{-2} d^{-1}	0.71	0.47	0.70	0.24	-0.32	-1.00
FAO model:						
ET_0, mm d^{-1}	1.97	2.39	2.61	2.45	2.07	1.11
Makkink's model:						
ET_0, mm d^{-1} (c_1 = 0.75)	2.24	2.60	3.03	2.80	2.32	1.11
ET_0, mm d^{-1} (c_1 = 0.65)	1.94	2.25	2.62	2.42	2.01	0.97

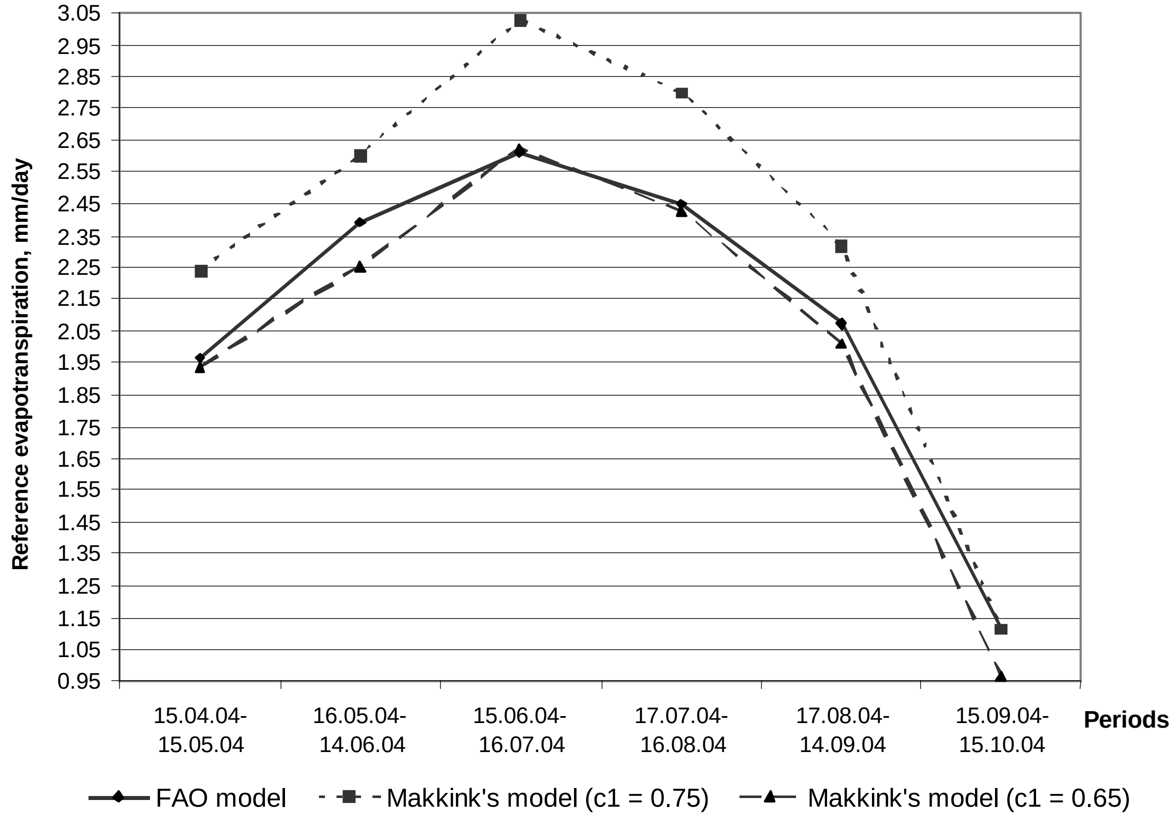

Fig. 4.1. Reference evapotranspiration for all periods

4.2. Estimation of Leaf Area Index of trees and lawn

Application of the special program for the estimation of Leaf Area Index (LAI) of a tree or lawn (see section 3.2.) provided these values for all objects and periods (Tables 4.3–4.6) and (Figs 4.2–4.12). The photos show each object in each period.

Table 4.3. LAI of trees and lawn in the successive periods (Habarovskaya st.)

Object	Values of Leaf Area Index of trees and lawn for each period					
	15.04.04–15.05.04	16.05.04–14.06.04	15.06.04–16.07.04	17.07.04–16.08.04	17.08.04–14.09.04	15.09.04–15.10.04
Habarovskaya st. *Trees*						
1	0.79 ± 0.24	2.49 ± 0.52	3.27 ± 0.33	3.24 ± 0.37	2.82 ± 0.68	1.59 ± 0.18
2	1.65 ± 0.19	2.01 ± 0.29	2.74 ± 0.42	3.73 ± 0.49	3.45 ± 0.50	3.22 ± 0.62
3	2.27 ± 0.31	3.67 ± 0.77	4.77 ± 0.66	5.08 ± 0.74	5.06 ± 0.72	3.75 ± 0.39
4	1.91 ± 0.03	2.67 ± 0.29	3.50 ± 0.31	4.10 ± 0.25	3.12 ± 0.49	1.86 ± 0.22
5	1.83 ± 0.09	2.45 ± 0.62	3.35 ± 0.80	5.17 ± 0.60	3.90 ± 0.83	2.00 ± 0.29
6	0.67 ± 0.07	1.13 ± 0.23	1.57 ± 0.36	1.92 ± 0.27	1.59 ± 0.11	0.63 ± 0.07
7	2.23 ± 0.17	3.22 ± 0.39	4.10 ± 0.24	4.49 ± 0.34	3.34 ± 0.42	1.07 ± 0.05
8	1.85 ± 0.26	2.81 ± 0.25	3.90 ± 0.36	4.63 ± 0.47	2.59 ± 0.42	1.20 ± 0.07
9	1.98 ± 0.04	2.36 ± 0.28	2.96 ± 0.61	3.88 ± 0.60	2.26 ± 0.45	1.09 ± 0.15
10	2.67 ± 0.06	3.12 ± 0.25	3.78 ± 0.49	4.69 ± 0.33	3.80 ± 0.43	2.13 ± 0.33
11	2.63 ± 0.27	2.75 ± 0.33	3.00 ± 0.41	3.48 ± 0.45	2.33 ± 0.42	1.19 ± 0.14
Lawn						
1	1.18	1.64	1.95	1.90	0.83	1.55
2	1.06	1.02	0.96	2.51	2.17	1.24
3	0.78	0.75	0.69	0.25	1.28	0.92
4	0.56	0.51	0.42	0.18	1.08	0.88
5	0.68	0.69	0.73	0.65	1.08	0.94
6	0.45	1.23	1.54	1.51	1.21	1.75
7	0.34	0.33	0.33	0.64	0.91	0.26
8	0.09	0.12	0.15	0.08	1.18	0.37
9	0.18	0.29	0.37	0.34	1.34	0.42
10	0.36	0.78	0.87	0.44	0.61	0.63
11	0.29	0.81	0.89	0.48	0.48	0.53
Average LAI grass	0.54 ± 0.28	0.74 ± 0.32	0.81 ± 0.39	0.82 ± 0.63	1.11 ± 0.30	0.86 ± 0.38

Table 4.4. LAI of trees and lawn in the successive periods (Saharov pr.)

Object	Values of Leaf Area Index of trees and lawn for each period					
	15.04.04–15.05.04	16.05.04–14.06.04	15.06.04–16.07.04	17.07.04–16.08.04	17.08.04–14.09.04	15.09.04–15.10.04
Saharov pr. *Trees*						
2	4.08 ± 0.27	5.34 ± 0.34	5.97 ± 0.39	6.36 ± 0.39	6.16 ± 0.38	4.93 ± 0.24
3	4.39 ± 0.33	6.09 ± 0.25	6.81 ± 0.22	7.12 ± 0.35	6.48 ± 0.68	5.66 ± 0.41
4	6.04 ± 0.83	7.94 ± 1.23	8.69 ± 1.44	8.12 ± 1.26	6.71 ± 0.91	6.18 ± 1.03
6	3.82 ± 0.21	5.12 ± 0.20	5.73 ± 0.38	6.57 ± 0.64	6.28 ± 0.51	4.60 ± 0.25
7	3.39 ± 0.34	4.67 ± 0.35	5.13 ± 0.28	5.01 ± 0.38	4.37 ± 0.73	3.23 ± 0.35
8	3.47 ± 0.44	4.58 ± 0.49	4.99 ± 0.45	5.05 ± 0.30	4.70 ± 0.28	4.26 ± 0.19
9	5.12 ± 0.46	5.62 ± 0.38	5.81 ± 0.32	5.60 ± 0.37	4.79 ± 0.25	1.46 ± 0.16
10	4.46 ± 0.29	5.37 ± 0.47	5.70 ± 0.53	5.93 ± 0.41	5.61 ± 0.48	4.76 ± 0.43
1 (I)	2.90 ± 0.04	4.61 ± 0.15	5.29 ± 0.27	5.65 ± 0.55	5.37 ± 0.43	3.95 ± 0.07
2 (I)	3.61 ± 0.18	4.05 ± 0.17	4.24 ± 0.19	4.07 ± 0.29	3.64 ± 0.51	2.41 ± 0.15
3 (I)	3.15 ± 0.16	4.05 ± 0.29	4.42 ± 0.37	4.08 ± 0.44	3.60 ± 0.44	3.24 ± 0.52
4 (II)	2.58 ± 0.25	3.29 ± 0.42	3.69 ± 0.50	3.24 ± 0.49	2.49 ± 0.55	1.80 ± 0.32
5 (II)	4.19 ± 0.47	4.85 ± 0.42	5.22 ± 0.43	4.94 ± 0.65	4.32 ± 0.99	2.36 ± 0.43
6 (III)	3.46 ± 0.16	4.01 ± 0.15	4.81 ± 0.26	4.64 ± 0.28	4.13 ± 0.38	2.76 ± 0.22
7 (III)	1.92 ± 0.24	2.30 ± 0.27	2.55 ± 0.28	2.39 ± 0.27	2.06 ± 0.25	0.93 ± 0.16
Lawn						
2	2.25	1.54	0.69	1.13	1.43	0.77
3	1.47	1.46	1.43	1.34	1.26	0.69
4	1.40	1.22	1.13	1.67	1.84	0.37
6	0.72	1.73	2.36	2.54	2.60	1.85
7	0.77	0.68	0.59	0.61	0.65	0.85
8	0.62	0.67	0.74	0.52	0.58	0.60
9	1.19	1.00	0.92	0.88	0.84	0.29
10	0.40	1.24	2.09	1.69	0.77	1.05
Average LAI grass	1.10 ± 0.48	1.19 ± 0.31	1.24 ± 0.54	1.30 ± 0.51	1.25 ± 0.54	0.81 ± 0.33
1 (I)	0.25	0.21	0.14	0.11	0.12	0.09
2 (I)	0.26	0.22	0.16	0.15	0.12	0.26
3 (I)	1.15	1.34	1.40	1.95	2.13	0.94
4 (II)	1.51	0.89	0.43	0.93	1.21	0.61
5 (II)	1.94	1.51	1.49	1.14	0.77	0.83
6 (III)	1.23	0.75	0.58	1.53	2.08	0.53
7 (III)	1.84	2.19	3.03	2.18	1.78	1.89
Average LAI grass	1.17 ± 0.53	1.02 ± 0.57	1.03 ± 0.81	1.14 ± 0.64	1.17 ± 0.72	0.74 ± 0.42

Table 4.5. LAI of trees and lawn in the successive periods (Sokolniki (Strominka st.))

Object	Values of Leaf Area Index of trees and lawn for each period					
	15.04.04–15.05.04	16.05.04–14.06.04	15.06.04–16.07.04	17.07.04–16.08.04	17.08.04–14.09.04	15.09.04–15.10.04
Sokolniki (Strominka st.) *Trees*						
1*	5.43 ± 0.77	6.10 ± 0.90	6.55 ± 1.11	6.30 ± 0.93	5.76 ± 0.79	4.33 ± 0.54
2*	4.77 ± 0.54	5.62 ± 0.97	6.14 ± 1.17	6.08 ± 0.77	5.93 ± 0.71	4.40 ± 0.25
3*	4.37 ± 0.38	4.70 ± 0.46	5.19 ± 0.55	5.29 ± 0.52	5.13 ± 0.55	4.31 ± 0.18
4*	5.68 ± 0.47	6.22 ± 0.51	6.71 ± 0.30	6.76 ± 0.31	6.70 ± 0.27	5.16 ± 0.12
5*	5.07 ± 0.68	6.64 ± 0.81	7.48 ± 1.06	7.57 ± 1.26	6.32 ± 0.95	5.48 ± 0.51
6*	3.51 ± 0.40	3.79 ± 0.35	4.09 ± 0.20	4.11 ± 0.20	3.92 ± 0.32	3.29 ± 0.42
7*	4.89 ± 0.70	5.88 ± 1.84	6.51 ± 2.22	6.36 ± 2.14	5.48 ± 2.12	4.31 ± 0.90
8*	3.74 ± 0.48	4.58 ± 0.57	4.87 ± 0.59	4.81 ± 0.71	4.48 ± 0.84	3.77 ± 0.30
9*	4.10 ± 0.15	4.64 ± 0.24	5.09 ± 0.31	5.17 ± 0.29	4.95 ± 0.34	4.55 ± 0.21
10*	5.44 ± 0.67	5.88 ± 0.76	6.28 ± 0.64	6.28 ± 0.64	6.10 ± 0.60	5.84 ± 0.66
1	5.32 ± 0.53	7.39 ± 0.73	8.96 ± 0.72	8.12 ± 1.04	6.63 ± 0.40	6.08 ± 0.37
2	5.44 ± 0.30	6.72 ± 0.60	7.48 ± 0.61	6.94 ± 0.55	6.32 ± 0.56	2.60 ± 0.21
3	5.27 ± 0.55	5.94 ± 0.29	6.29 ± 0.29	5.90 ± 0.55	5.66 ± 0.49	4.86 ± 0.32
4	4.34 ± 0.92	5.01 ± 0.95	5.42 ± 1.04	4.91 ± 0.76	4.23 ± 0.55	2.64 ± 0.38
Lawn						
1*	0.49	0.52	0.61	1.62	0.63	0.88
2*	0.58	0.63	0.69	0.54	0.56	0.96
3*	1.20	0.92	0.78	0.28	0.71	1.52
4*	2.06	1.83	1.27	0.55	1.28	1.15
5*	1.56	1.44	1.02	0.37	0.83	1.17
6*	1.60	1.12	0.96	0.65	1.78	1.04
7*	1.23	1.09	0.89	0.66	1.63	0.71
8*	1.65	1.43	1.23	1.42	1.50	1.25
9*	1.27	1.35	1.66	2.51	1.87	1.46
10*	1.50	1.26	1.01	1.41	0.73	1.23
Average LAI grass	1.31 ± 0.36	1.16 ± 0.30	1.01 ± 0.23	1.00 ± 0.59	1.15 ± 0.46	1.14 ± 0.19
1	5.26	2.75	0.95	1.91	1.27	0.96
2	4.99	2.14	0.80	1.92	0.25	0.79
3	4.45	1.96	1.07	2.79	0.35	0.68
4	4.54	2.03	1.17	3.74	0.32	0.80
Average LAI grass	4.81 ± 0.32	2.22 ± 0.27	1.00 ± 0.12	2.59 ± 0.69	0.55 ± 0.36	0.81 ± 0.08

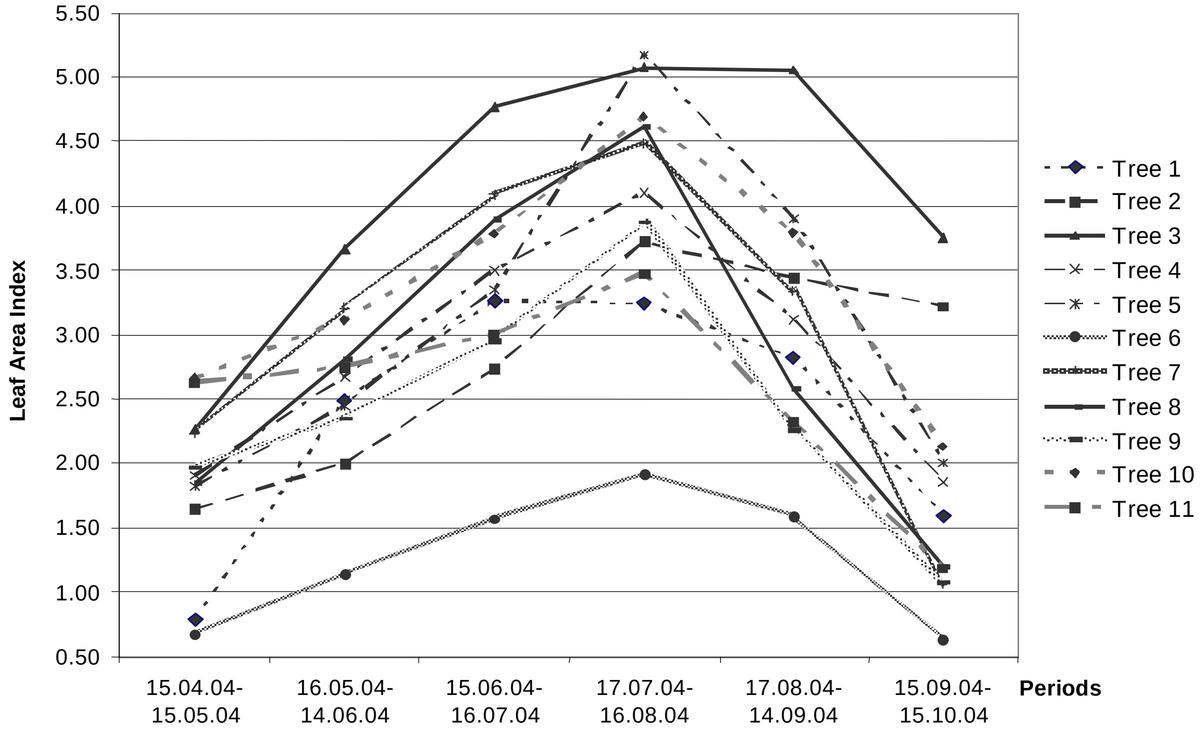

Fig. 4.2. LAI of trees in the successive periods (Habarovskaya st.)

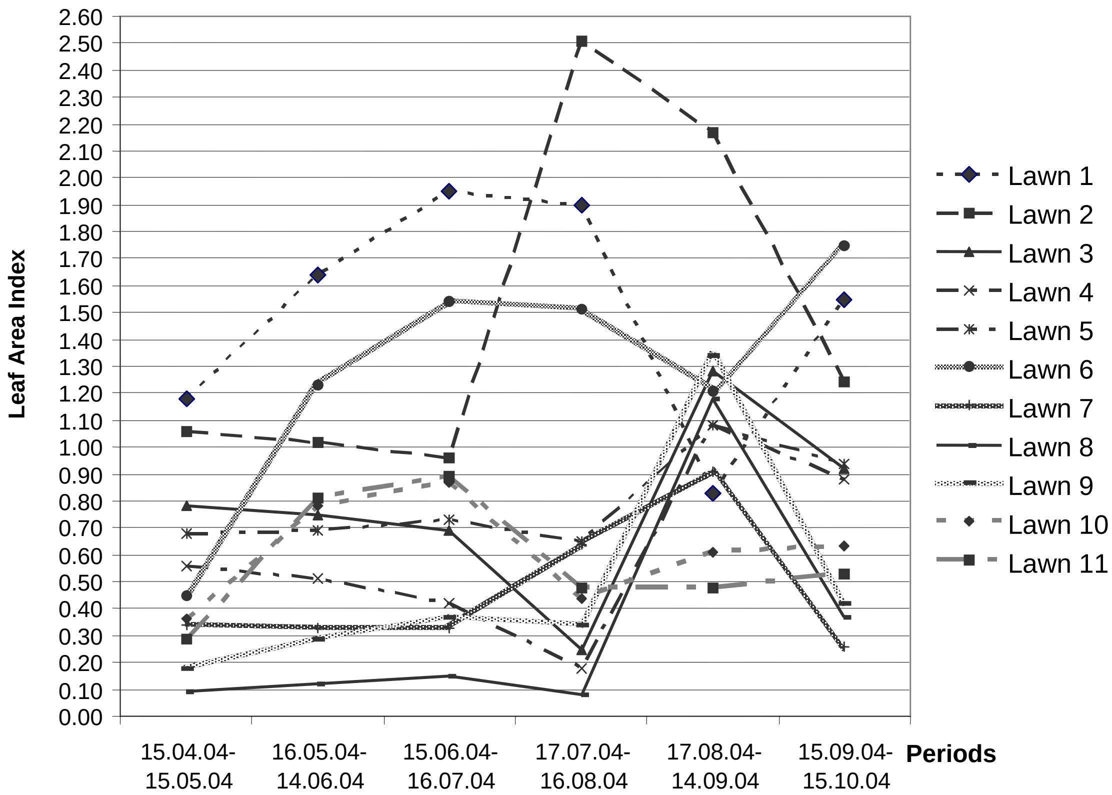

Fig. 4.3. LAI of lawn in the successive periods (Habarovskaya st.)

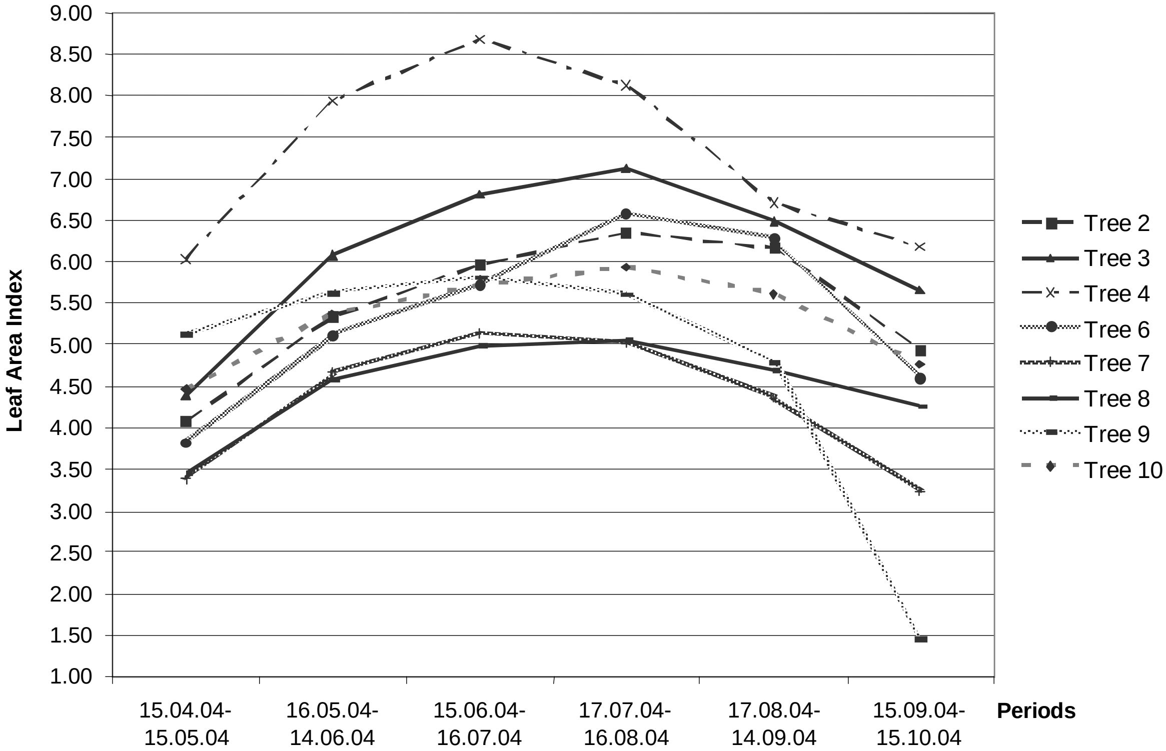

Fig. 4.4. LAI of trees in the successive periods (Saharov pr.)

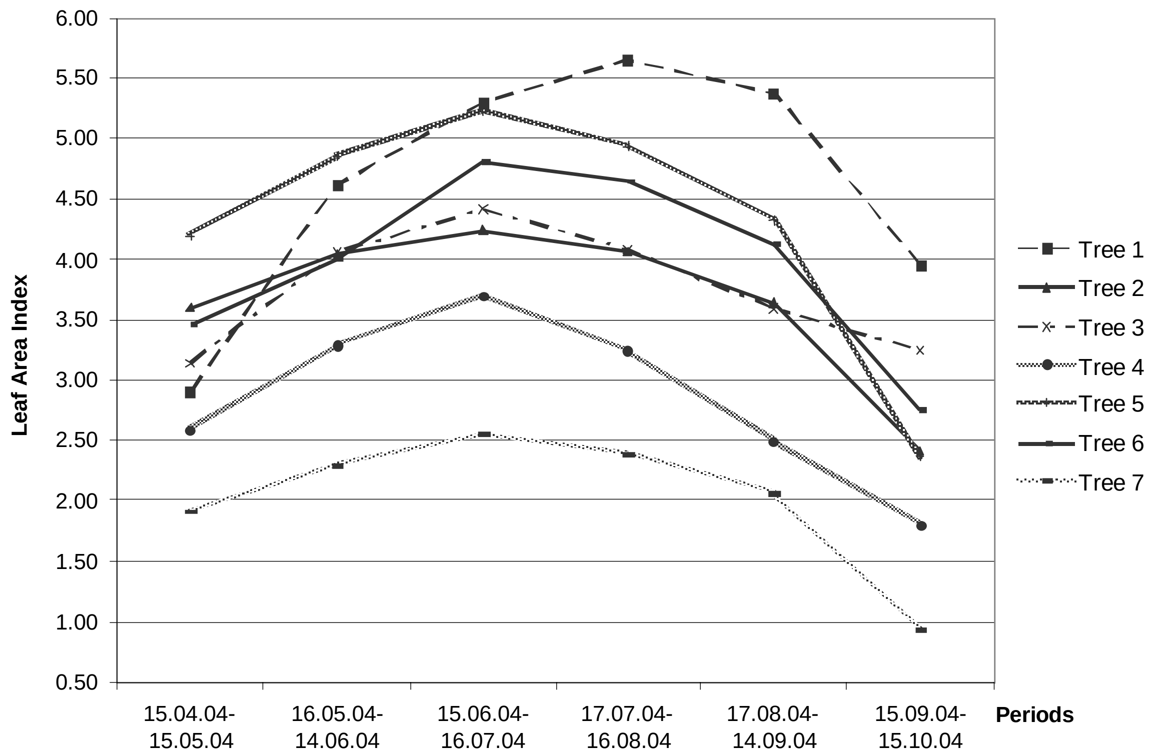

Fig. 4.5. LAI of trees in the successive periods (Saharov pr.)

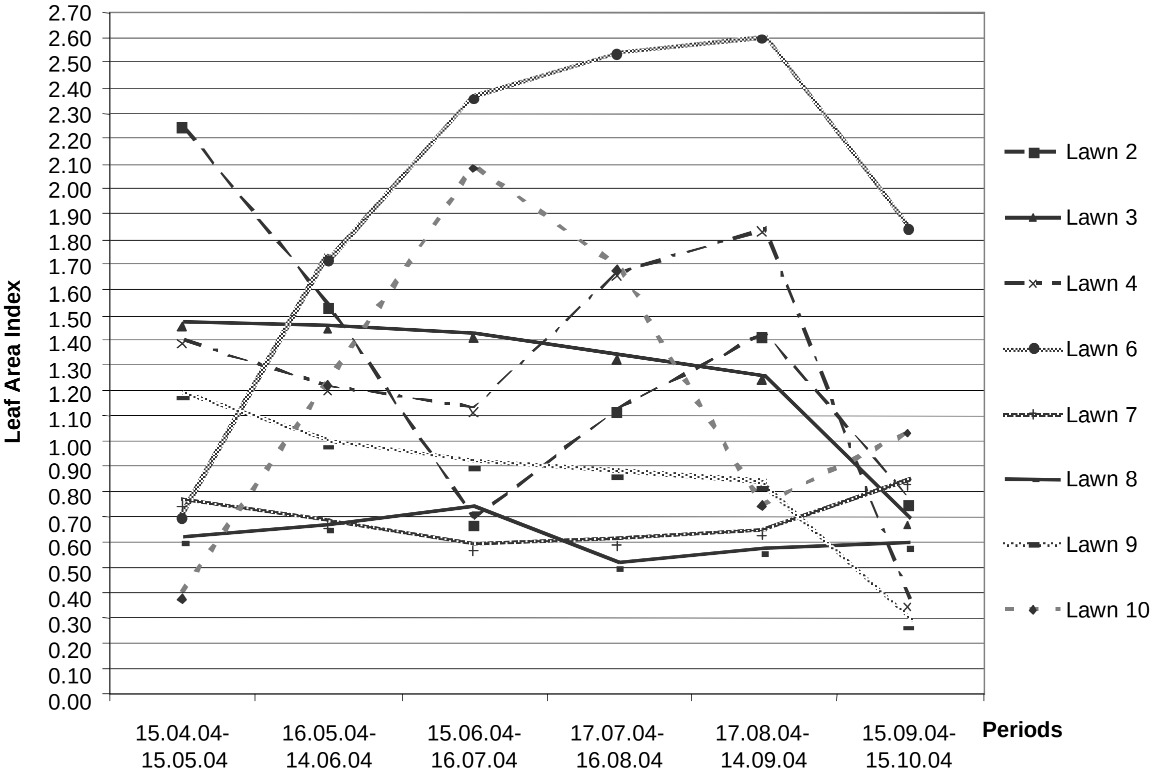

Fig. 4.6. LAI of lawn in the successive periods (Saharov pr.)

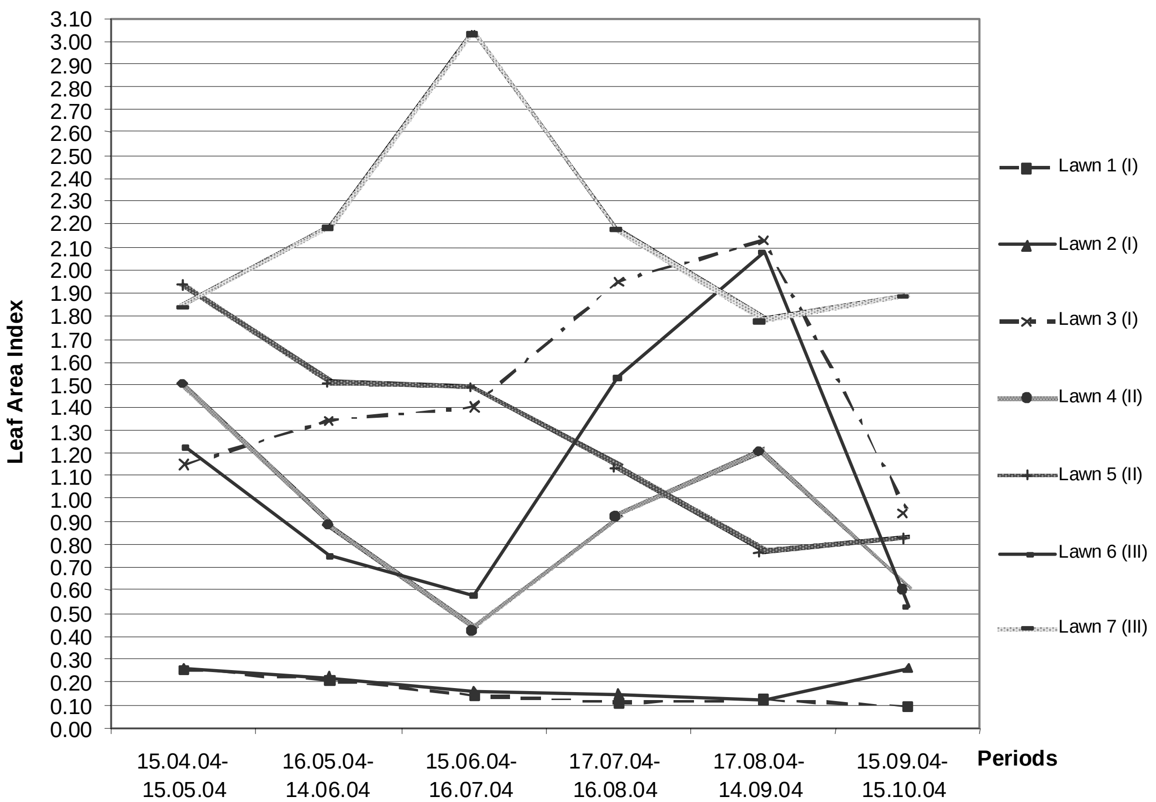

Fig. 4.7. LAI of lawn in the successive periods (Saharov pr.)

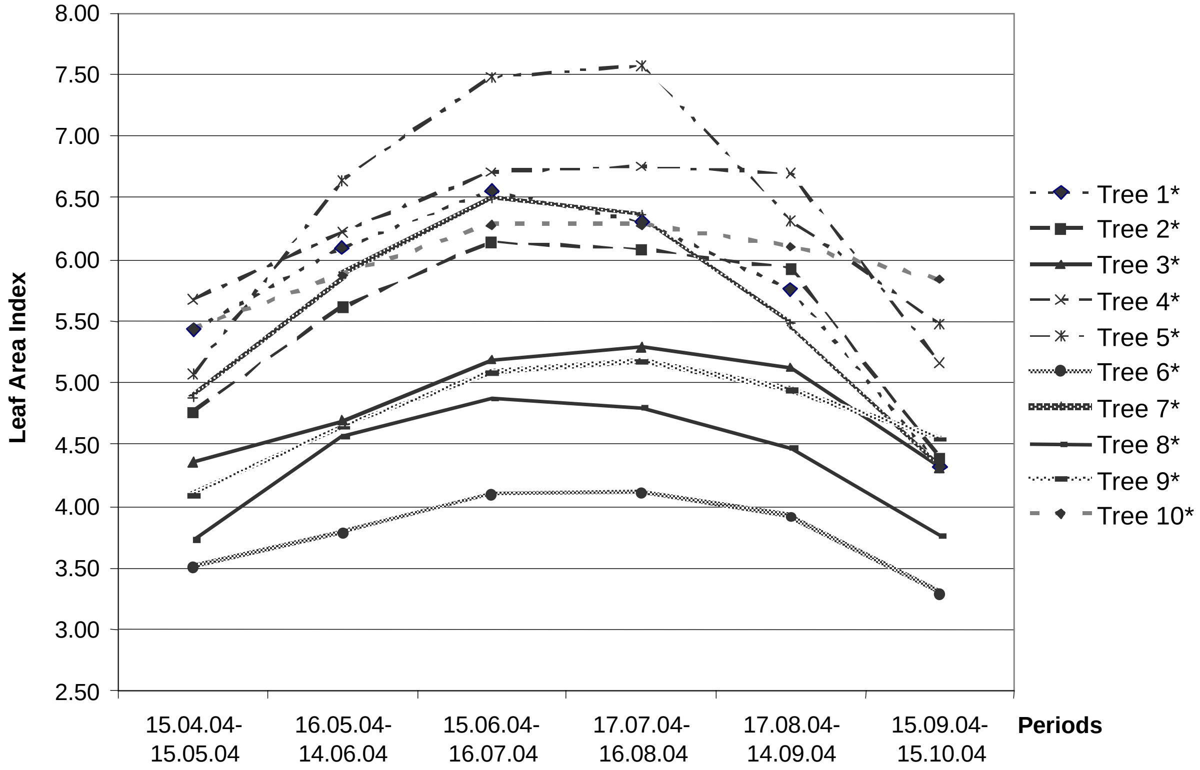

Fig. 4.8. LAI of trees in the successive periods (Sokolniki (Strominka st.))

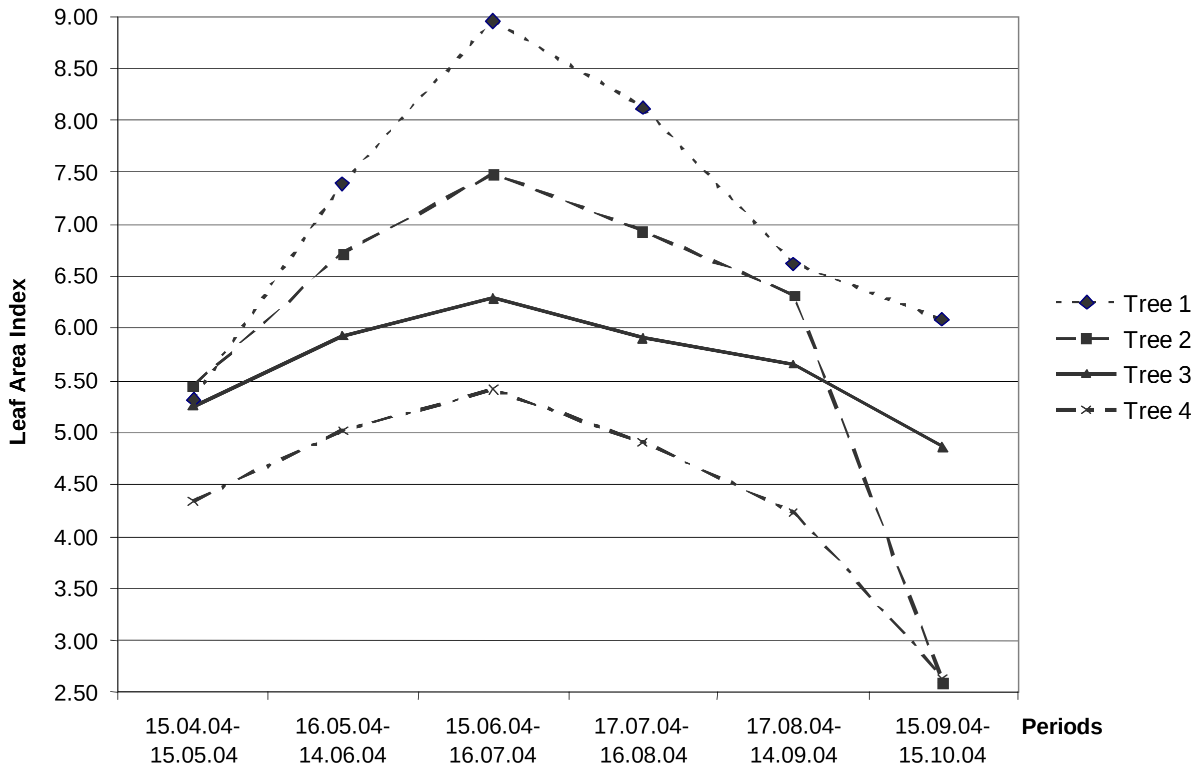

Fig. 4.9. LAI of trees in the successive periods (Sokolniki (Strominka st.))

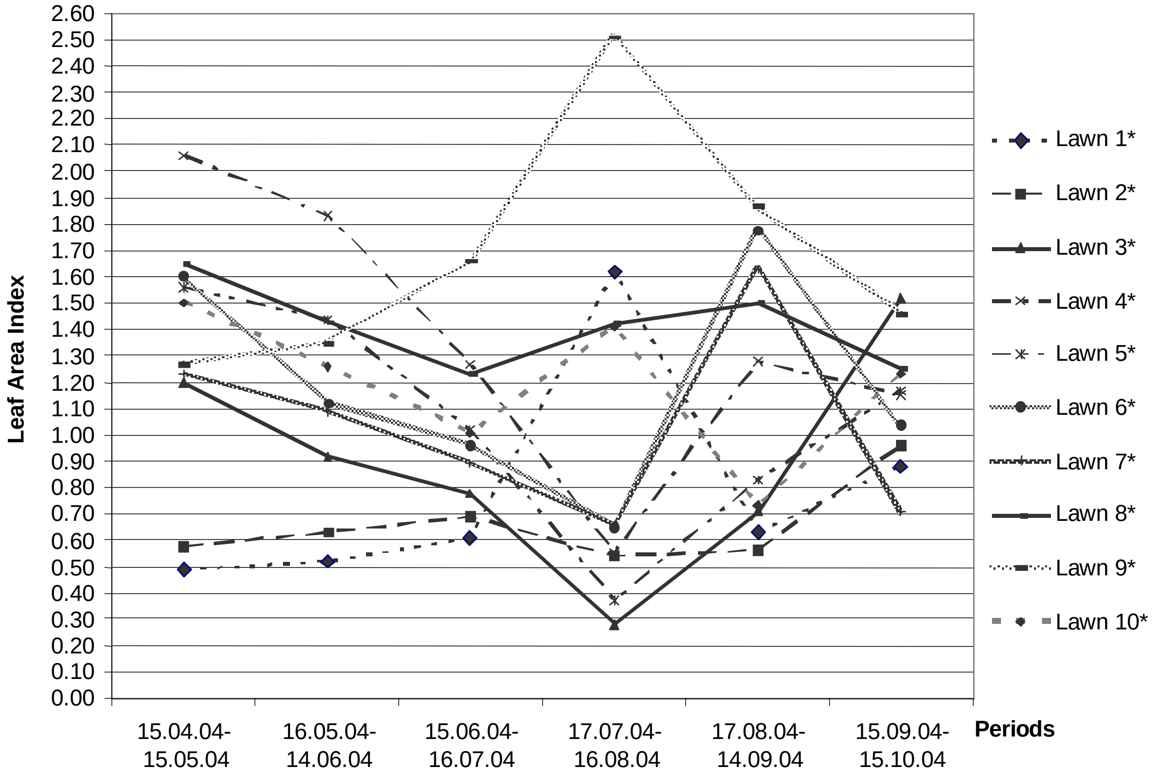

Fig. 4.10. LAI of lawn in the successive periods (<u>Sokolniki (Strominka st.)</u>)

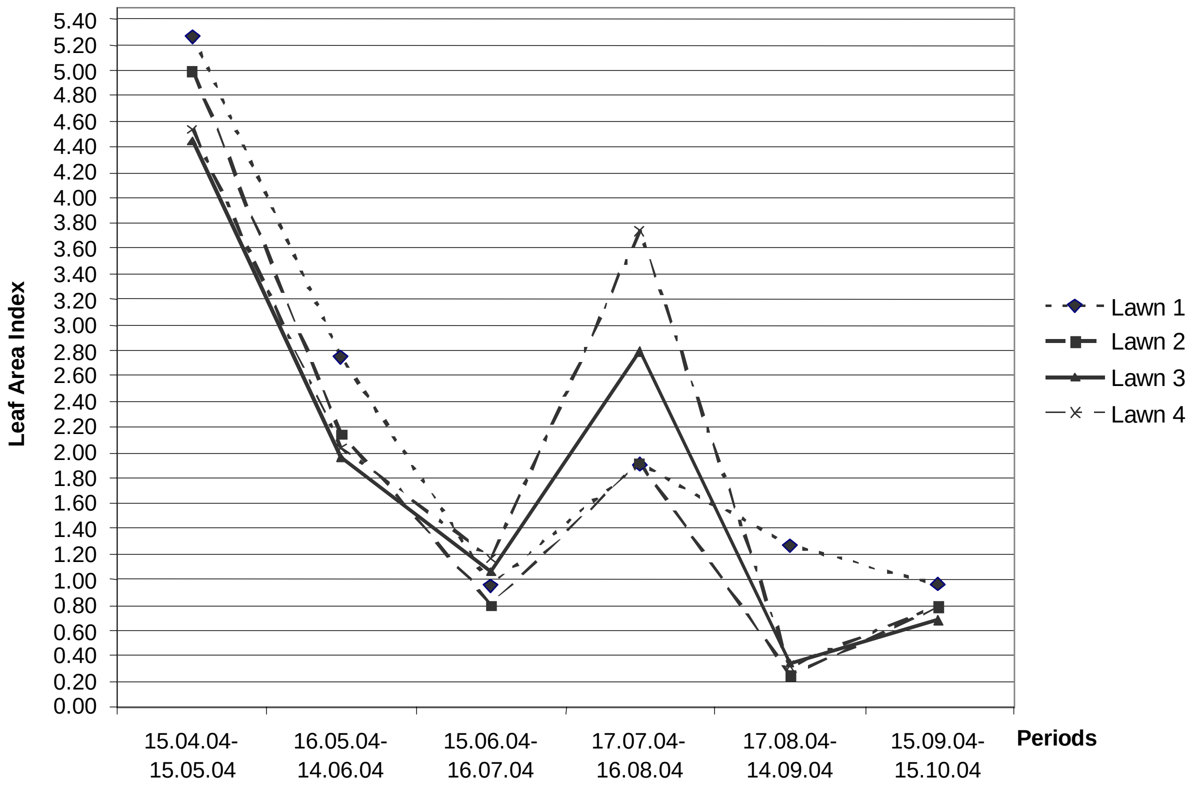

Fig. 4.11. LAI of lawn in the successive periods (<u>Sokolniki (Strominka st.)</u>)

Table 4.6. Summary. Leaf Area Indices of trees and lawn in each period

Object	Values of LAI_{trees}, LAI_{grass}, b_{grass} for each period					
	15.04.04–15.05.04	16.05.04–14.06.04	15.06.04–16.07.04	17.07.04–16.08.04	17.08.04–14.09.04	15.09.04–15.10.04
Habarovskaya st. *alley of trees 1–11*						
S_{area}, m^2	180.0	180.0	180.0	180.0	180.0	180.0
ΣS_{crown}, m^2	37.7	37.7	37.7	37.7	37.7	37.7
$\Sigma S_{crown} / S_{area}$	0.21	0.21	0.21	0.21	0.21	0.21
LAI_{trees}	1.85	2.70	3.52	4.17	3.21	1.80
LAI_{grass}	0.54	0.74	0.81	0.82	1.11	0.86
b^*_{grass}	0.237	0.309	0.333	0.336	0.426	0.349
Saharov pr. *alley of trees 2–4; 6–10*						
S_{area}, m^2	619.0	619.0	619.0	619.0	619.0	619.0
ΣS_{crown}, m^2	347.8	347.8	347.8	347.8	347.8	347.8
$\Sigma S_{crown} / S_{area}$	0.56	0.56	0.56	0.56	0.56	0.56
LAI_{trees}	4.25	5.45	5.94	6.06	5.52	4.24
LAI_{grass}	1.10	1.19	1.24	1.30	1.25	0.81
b_{grass}	0.423	0.448	0.462	0.478	0.465	0.333
alley of trees 1-7 (I-III)						
S_{area}, m^2	281.0	281.0	281.0	281.0	281.0	281.0
ΣS_{crown}, m^2	109.7	109.7	109.7	109.7	109.7	109.7
$\Sigma S_{crown} / S_{area}$	0.39	0.39	0.39	0.39	0.39	0.39
LAI_{trees}	3.18	4.04	4.49	4.36	3.88	2.68
LAI_{grass}	1.17	1.02	1.03	1.14	1.17	0.74
b_{grass}	0.443	0.400	0.402	0.434	0.443	0.309
Sokolniki (Strominka st.) *alley of trees 1*–10**						
S_{area}, m^2	288.0	288.0	288.0	288.0	288.0	288.0
ΣS_{crown}, m^2	82.3	82.3	82.3	82.3	82.3	82.3
$\Sigma S_{crown} / S_{area}$	0.29	0.29	0.29	0.29	0.29	0.29
LAI_{trees}	4.86	5.56	6.05	6.03	5.64	4.68
LAI_{grass}	1.31	1.16	1.01	1.00	1.15	1.14
b_{grass}	0.481	0.440	0.396	0.393	0.437	0.434
bio group of trees 1–4						
S_{area}, m^2	115.0	115.0	115.0	115.0	115.0	115.0
ΣS_{crown}, m^2	59.2	59.2	59.2	59.2	59.2	59.2
$\Sigma S_{crown} / S_{area}$	0.52	0.52	0.52	0.52	0.52	0.52
LAI_{trees}	5.12	6.32	7.11	6.54	5.77	4.20
LAI_{grass}	4.81	2.22	1.00	2.59	0.55	0.81
b_{grass}	0.910	0.670	0.393	0.726	0.240	0.333

* *b* ($f_{c, grass}$) - soil cover fraction by grass.

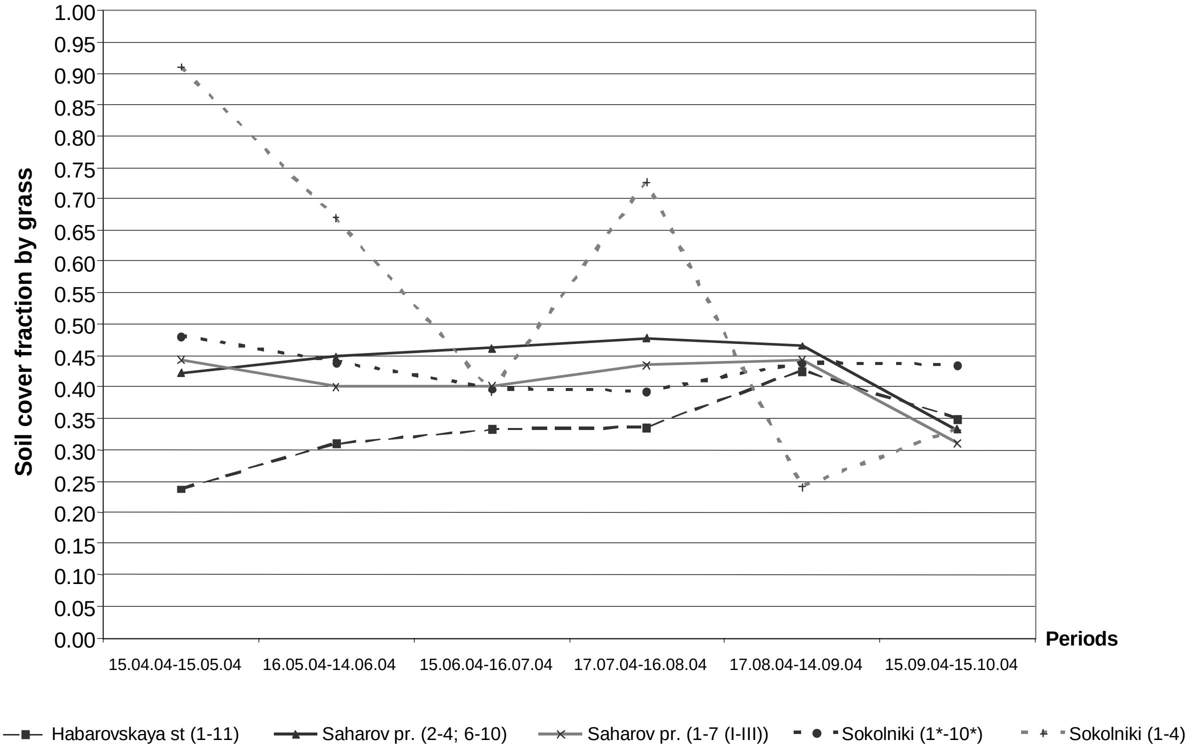

Fig. 4.12. Fraction of soil cover by grass in each period

Habarovskaya st.

(Alley of trees 1-11)

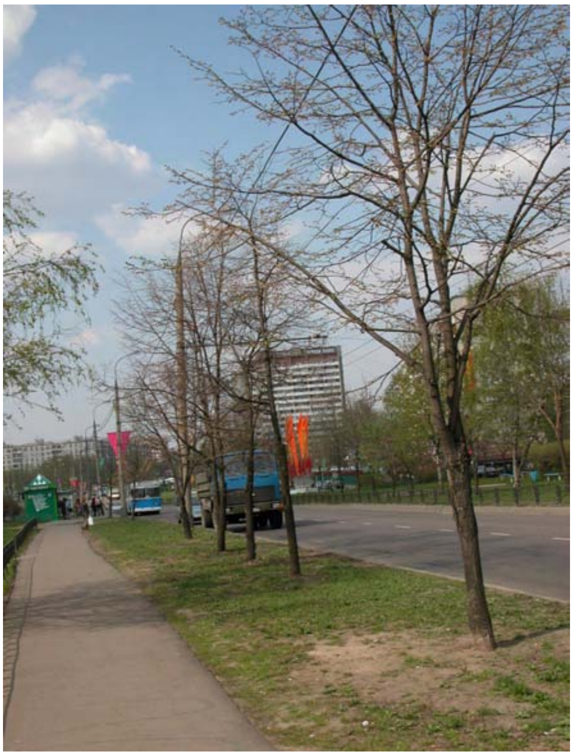

Start of Initial stage

End of Initial stage – Development stage

Mid-season stage

Start of Late season

End of Late season

Winter season

Sokolniki (Strominka st.)

Bio group of trees 1-4

Alley of trees 1-10**

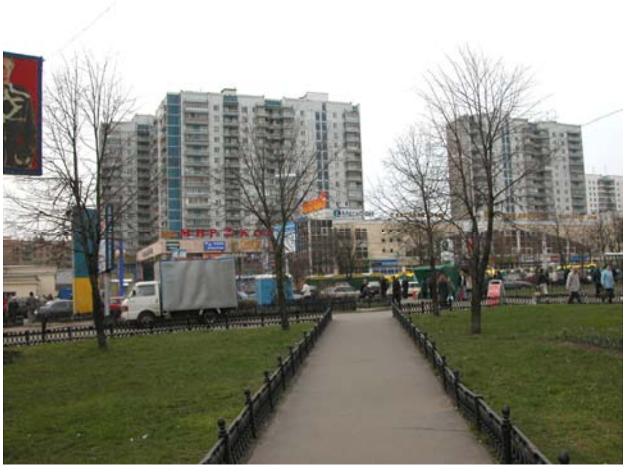

Start of Initial stage

End of Initial stage – Development stage

Mid-season stage

Start of Late season

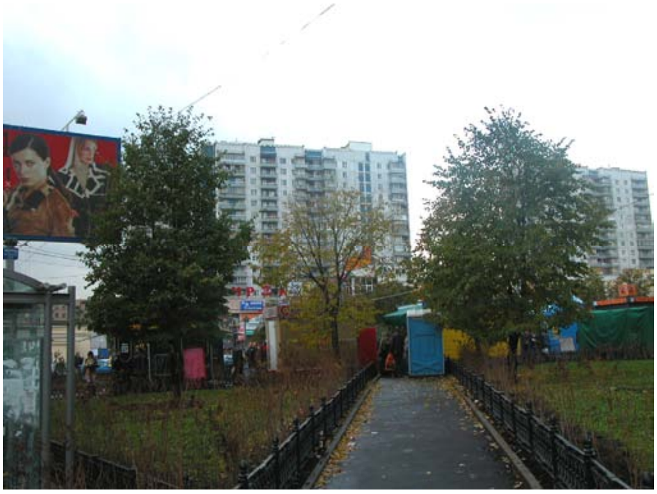


End of Late season


Winter season

Saharov pr.

(Alley of trees 2-4; 6-10)

Start of Initial stage

End of Initial stage – Development stage

Mid-season stage

Start of Late season

End of Late season

Winter season

(Alley of trees I-III)

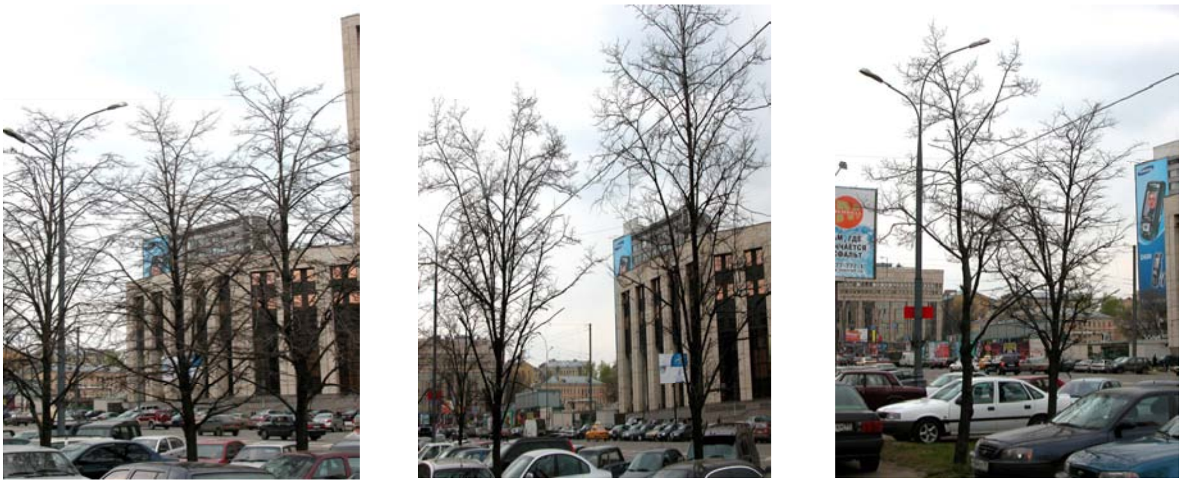

Start of Initial stage

End of Initial stage – Development stage

Mid-season stage

Start of Late season

End of Late season

Winter season

4.3. Calculation of crop coefficients for "Mid-season stage" periods and potential evapotranspiration for trees-lawn combinations in all periods

4.3.1. Calculation of crop coefficients for "Mid-season stage" periods

Crop coefficients for the trees-lawn combinations in Moscow in the "Mid-season stage" periods were calculated according to the FAO guidelines (see sections 2.3.2−2.3.3). The periods are given in Table 4.7. The input data and calculation results are given in Table 4.8.

Table 4.7. "Mid-season stage" periods of linden (Tilia cordata) in Moscow

Periods	Stage
15.06.04−16.07.04	Mid-season
17.07.04−16.08.04	
17.08.04−14.09.04	

1. Measured parameters from Moscow and the Moscow objects

LAI_{trees} = Leaf Area Index of trees [-],

$$LAI_{trees} = \frac{\sum (LAI_{tree} \cdot S_{crown})}{\sum S_{crown}},$$

S_{crown} = projected area of tree crown [m^2],

ΣS_{crown} = total projected area of crowns [m^2],

LAI_{grass} = mean value of Leaf Area Index of grass (lawn) [-],

h = mean height of tree [m],

u_2 = mean value for wind speed at 2 m above ground surface during mid-season [m s^{-1}],

RH_{min} = mean value for minimum daily relative humidity during mid-season [%].

2. Parameters that are required by the model for calculating potential evapotranspiration of the trees-lawn combinations in the "mid-season stage" periods (see section 2.3.5)

$K_{cb, full}$ = estimated basal K_{cb} during the mid-season (at peak plant size or height) for vegetation having full ground cover or LAI>3 [-],

$K_{cb,h}$ = $K_{cb,mid}$ for full cover vegetation (LAI>3) under subhumid and calm wind conditions ($RH_{\min} = 45\%$ and $u_2 = 2$ m s^{-1}. The value for $K_{cb,h}$ is estimated as 1.0 + $0.1h$ for $h \leq 2$ m and as 1.20 for $h > 2$m. The value 1.2 represents a general upper limit on $K_{cb,mid}$ for tall vegetation having full ground cover and LAI > 3 under the sub-humid and calm wind conditions) [-],

f_c = observed fraction of soil surface covered by vegetation as observed from nadir (overhead) [-],

$f_{c,eff}$ = the effective fraction of soil surface covered or shaded by vegetation [-].

For trees, it can be estimated as $f_{c,eff} = f_c / \sin\eta$ where η = the mean angle of the sun above the horizon during the period of maximum evapotranspiration (generally between 11.00 and 15.00).

$K_{c,ini}$ = crop coefficient for the initial stage [-],

$K_{c,end}$ = crop coefficient for the end of the late season stage [-],

$K_{c,ini} = K_{c,end} = 0.45$

$K_{c,mid,trees}$ = crop coefficient for sparse vegetations, considering the trees without grass for the mid-season stage [-],

$K_{c,mid,combination}$ = crop coefficient for the tree-grass combinations for the mid-season stage [-].

3. Results of the data processing per object and per “Mid-season stage” period

Table 4.8. Values of different climate and vegetation parameters and estimation of crop coefficients for tree-lawn combinations for each "Mid-season stage" period

Parameters	Values of parameters for each "mid-season stage" period		
	15.06.04−16.07.04	17.07.04−16.08.04	17.08.04−14.09.04
u_2, m/s	0.95	0.65	0.98
RH_{min}, %	65.6	66.2	65.7
sin η	0.84	0.79	0.67
$K_{c,ini} = K_{c,end}$	0.45	0.45	0.45
Habarovskaya st. *(alley of trees 1−11)*			
S_{area}, m^2	180	180	180
LAI_{trees}	3.52	4.17	3.21
LAI_{grass}	0.81	0.82	1.11
$LAI_{combination}$	1.19	1.22	1.47
h, m	6.71	6.71	6.71
$K_{cb,full}$	1.04	1.02	1.04
$K_{cb,h}$ (h > 2 m)	1.2	1.2	1.2
$K_{c,full}$	1.09	1.07	1.09
$f_{c, combination}$	0.448	0.457	0.521
$f_{c,eff}$	0.533	0.577	0.773
$K_{c,mid,combination}$	0.580	0.586	0.689
Saharov pr. *(alley of trees 2−4; 6−10)*			
S_{area}, m^2	619	619	619
LAI_{trees}	5.94	6.06	5.52
LAI_{grass}	1.24	1.30	1.25
$LAI_{combination}$	2.77	2.83	2.74
h, m	10.29	10.29	10.29
$K_{cb,full}$	1.02	1.00	1.02
$K_{cb,h}$ (h > 2 m)	1.2	1.2	1.2
$K_{c,full}$	1.07	1.05	1.07
$f_{c, combination}$	0.749	0.757	0.746
$f_{c,eff}$	0.891	0.956	1.106
$K_{c,mid,combination}$	0.910	0.902	0.914

(alley of trees 1−7 (I−III))			
S $_{area,}$ m^2	281	281	281
LAI $_{trees}$	4.49	4.36	3.88
LAI $_{grass}$	1.03	1.14	1.17
LAI $_{combination}$	1.89	1.99	1.99
h, m	9.44	9.44	9.44
$K_{cb,full}$	1.02	1.00	1.03
$K_{cb,h}$ (h > 2 m)	1.2	1.2	1.2
$K_{c,full}$	1.07	1.05	1.08
$f_{c, combination}$	0.612	0.631	0.630
$f_{c,eff}$	0.727	0.796	0.934
$K_{c,mid,combination}$	0.775	0.783	0.805
Sokolniki (Strominka st.) *(alley of trees 1*–10*)*			
S $_{area,}$ m^2	288	288	288
LAI $_{trees}$	6.05	6.03	5.64
LAI $_{grass}$	1.01	1.00	1.15
LAI $_{combination}$	1.65	1.64	1.78
h, m	16.12	16.12	16.12
$K_{cb,full}$	0.99	0.97	1.00
$K_{cb,h}$ (h > 2 m)	1.2	1.2	1.2
$K_{c,full}$	1.04	1.02	1.05
$f_{c, combination}$	0.561	0.559	0.589
$f_{c,eff}$	0.667	0.705	0.873
$K_{c,mid,combination}$	0.705	0.688	0.741
(bio group of trees 1−4)			
S $_{area,}$ m^2	115	115	115
LAI $_{trees}$	7.11	6.54	5.77
LAI $_{grass}$	1.00	2.59	0.55
LAI $_{combination}$	2.38	3.96	1.88
h, m	7.10	7.10	7.10
$K_{cb,full}$	1.04	1.02	1.04
$K_{cb,h}$ (h > 2 m)	1.2	1.2	1.2
$K_{c,full}$	1.09	1.07	1.09
$f_{c, combination}$	0.696	0.862	0.609
$f_{c,eff}$	0.828	1.088	0.903
$K_{c,mid,combination}$	0.872	1.003	0.792

4.3.2. Calculation of potential evapotranspiration of trees-lawn combinations

The obtained values of crop coefficients for tree-lawn combinations and the obtained values of reference evapotranspiration were combined in order to estimate the potential evapotranspiration of each trees-lawn combination in each period (Table 4.9 and Fig. 4.13):

$$ET_{combination} = K_{c,\, combination} \cdot ET_0$$

$ET_{combination}$ = potential evapotranspiration of a trees-lawn combination in a period [mm day^{-1}],

$K_{c,\, combination}$ = crop coefficient for a trees-lawn combination in a period [-],

ET_o = reference evapotranspiration in a period [mm day^{-1}].

Table 4.9. Potential evapotranspiration for trees-lawn combinations per period

Object	Values of potential evapotranspiration for each period, mm day^{-1}					
	15.04.04–15.05.04	16.05.04–14.06.04	15.06.04–16.07.04	17.07.04–16.08.04	17.08.04–14.09.04	15.09.04–15.10.04
Habarovskaya st. *alley of trees 1–11*	0.89	1.24	1.51	1.44	1.43	0.50
Saharov pr. *alley of trees 2–4; 6–10*	0.89	1.65	2.38	2.21	1.89	0.50
alley of trees 1–7 (I–III)	0.89	1.49	2.02	1.92	1.67	0.50
Sokolniki (Strominka st.) *alley of trees 1*–10**	0.89	1.41	1.84	1.69	1.53	0.50
bio group of trees 1–4	0.89	1.57	2.28	2.46	1.64	0.50

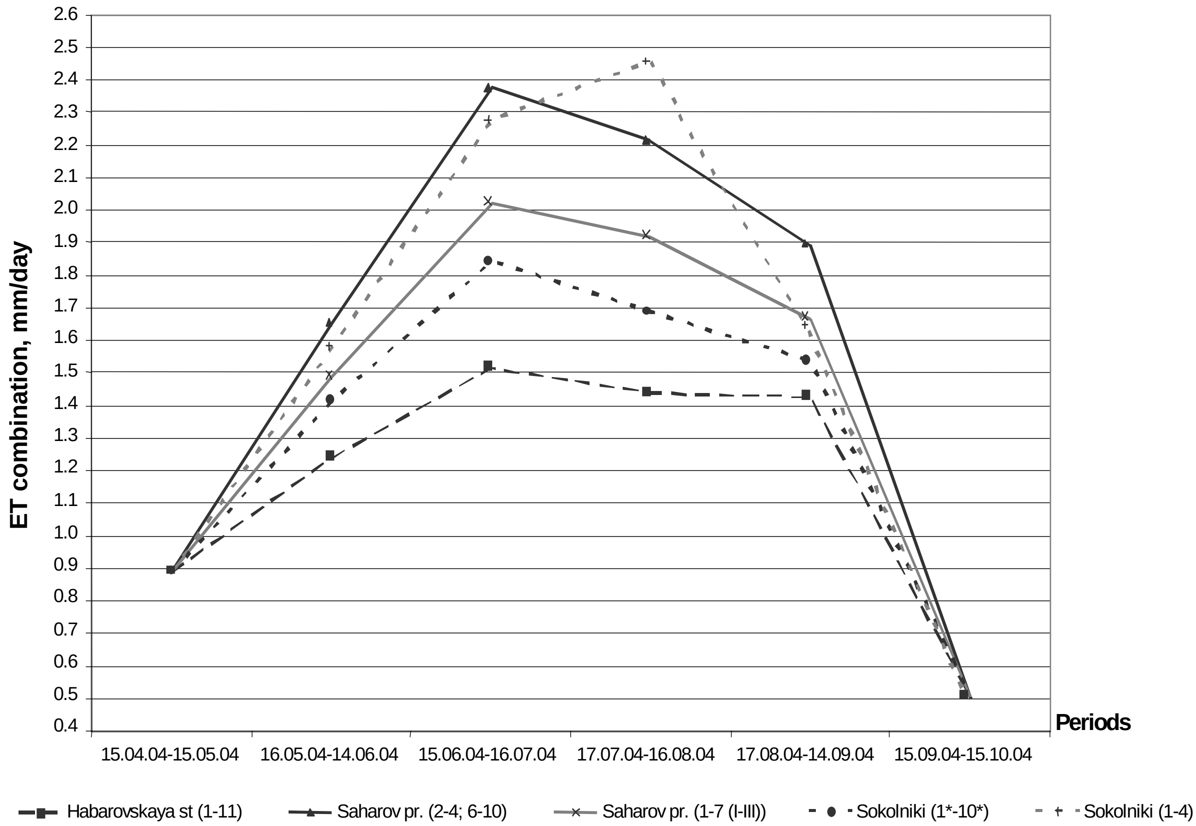

Fig. 4.13. Potential evapotranspiration for trees-lawn combinations per period

CHAPTER 5. CALCULATION OF WATER STRESS AND SALINITY STRESS COEFFICIENTS AND ACTUAL EVAPOTRANSPIRATION FOR TREES-LAWN COMBINATIONS

5.1. Calculation of water stress coefficients

Plants suffer from water stress if the matric suction of the root zone is too low or too high. In very wet conditions (wetter than field capacity θ_{FC}) water stress may occur due to the incidence of oxygen deficiency. If soil dries out to a very dry condition, the roots are not able anymore to take up water from the root zone. Generally, this moisture condition is referred to as wilting point θ_{WP} = water suction of 16000 cm water head = pF 4.2. Water stress already occurs at water contents higher than wilting point, below a critical water content or so-called threshold water content θ_t. This value depends on characteristics of plants, soil properties, climatic parameters and the transpiration process.

The total available soil water (*TAW*) and readily available soil water (*RAW*) in the root zone with depth Z_r can be estimated using the following equations (Allen et al., 1998, p. 162):

$TAW = 1000\ (\theta_{FC} - \theta_{WP})\ Z_r$

$RAW = p\ TAW$

$\theta_t = \theta_{FC} - p \cdot (\theta_{FC} - \theta_{WP})$

θ_{FC} = water content at field capacity [m^3/m^3],

θ_{WP} = water content at wilting point [m^3/m^3],

Z_r = rooting depth [m],

θ_t = threshold soil water content below which transpiration is reduced due to water stress [m^3/m^3],

p = average fraction of Total Available Soil Water that can be depleted from the root zone before moisture stress starts (0.5 according to Allen et al., 1998).

Values of θ_{FC} and θ_{WP} can be estimated from the contents of mineral particles < 0.05 mm and < 0.002 mm and organic matter using pedotransfer functions (Staring series) in Woesten et al. (2001). By comparing the results of our soil survey with the Staring series it was found that our objects have top soils similar to B15 and sub soils similar to O15 in Woesten et al. (2001, pg 18−19; 63; 83). Their pF curves are given in Fig. 5.1. The horizontal lines in each figure indicate the standard deviation from the mean (solid curve) of the results of measurements on a set of samples from one texture class.

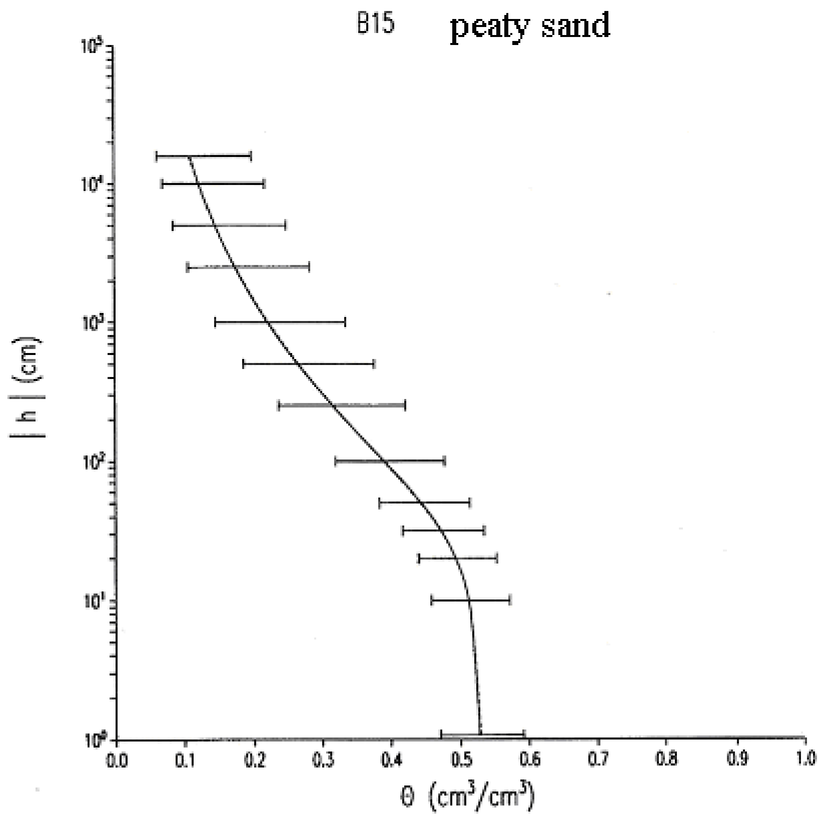

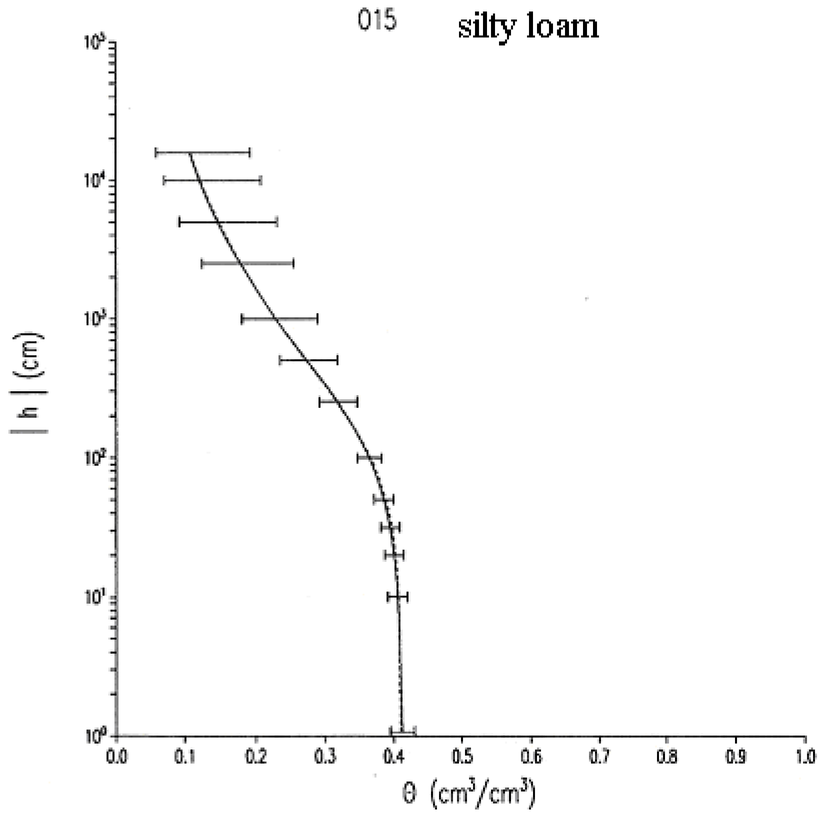

Fig. 5.1. pF curves for top soil (B15) and sub soil (O15)

For B15: θ_{FC} = 0.39; θ_{WP} = 0.11; θ_t = 0.250 (for p = 0.5)
For O15: θ_{FC} = 0.37; θ_{WP} = 0.10; θ_t = 0.235 (for p = 0.5).
Average values: θ_{FC} = 0.38 (38%); θ_{WP} = 0.105 (10.5%); θ_t = 0.24 (24%).

TAW = 1000 · (0.380–0.105) ·1 = 275 mm;
RAW = 138 mm.

A water stress coefficient K_s of a root zone during a period can be found by comparing the actual soil water content θ_a of the root zone during the period with the threshold water content θ_t and by using the following equations:

$$K_S = \frac{\theta_a - \theta_{WP}}{\theta_t - \theta_{WP}} \quad (for\,\theta_a < \theta_t),$$

$$K_s = 1 \ (for\ \theta_a > \theta_t)\ .$$

K_s = water stress coefficient [-],
θ_t = threshold soil water content below which transpiration is reduced due to waterstress [m^3/m^3] or [%],
θ_a = actual soil water content [m^3/m^3] or [%],
θ_{FC} = the water content at field capacity [m^3/m^3],
θ_{WP} = the water content at wilting point [m^3/m^3].

Once the water stress coefficient is known the actual evapotranspiration can by found through multiplying the potential evapotranspiration by the water stress coefficient (Allen et al., 1998).

Table 5.1. Volumetric water contents of the root zones during the various periods

Object	Values of volumetric water content of soil root zones for each period, %					
	15.04.04− 15.05.04	16.05.04− 14.06.04	15.06.04− 16.07.04	17.07.04− 16.08.04	17.08.04− 14.09.04	15.09.04− 15.10.04
Habarovskaya st. *alley of trees 1−11*	23.8±0.58 19.6±1.04 (−4.2)*	19.6±1.04 18.5±0.96 (−1.1)	18.5±0.96 22.2±1.30 (+3.7)	22.2±1.30 18.0±1.16 (−4.2)	18.0±1.16 21.0±1.29 (+3.0)	21.0±1.29 22.8±1.27 (+1.8)
Saharov pr. *alley of trees 2−4; 6−10*	29.3±1.58 24.0±1.57 (−5.3)	24.0±1.57 16.4±1.14 (−7.6)	16.4±1.14 26.2±1.93 (+9.8)	26.2±1.93 22.1±1.24 (−4.1)	22.1±1.24 20.9±1.15 (−1.2)	20.9±1.15 26.0±1.56 (+5.1)
alley of trees 1−7 (I−III)	23.3±1.04 14.3±0.82 (−9.0)	14.3±0.82 10.4±0.22 (−3.9)	10.4±0.22 27.8±0.34 (+17.4)	27.8±0.34 20.1±1.08 (−7.7)	20.1±1.08 16.4±0.80 (−3.7)	16.4±0.80 20.7±1.17 (+4.3)
Sokolniki (Strominka st.) *alley of trees 1*−10**	37.1±1.38 31.6±1.29 (−5.5)	31.6±1.29 22.7±1.18 (−8.9)	22.7±1.18 38.9±1.42 (+16.2)	38.9±1.42 27.6±1.22 (−11.3)	27.6±1.22 24.9±1.19 (−2.7)	24.9±1.19 26.2±1.26 (+1.3)
bio group of trees 1−4	29.7±1.24 27.0±1.15 (−2.7)	27.0±1.15 22.1±1.14 (−4.9)	22.1±1.14 28.0±1.26 (+5.9)	28.0±1.26 20.5±1.21 (−7.5)	20.5±1.21 19.3±1.28 (−1.2)	19.3±1.28 23.9±0.44 (+4.6)

* - difference of volumetric water content between start and end of period.

Table 5.2. Water stress coefficients during the various periods

Object	Values of waterstress coefficient (K_s)					
	15.04.04− 15.05.04	16.05.04− 14.06.04	15.06.04− 16.07.04	17.07.04− 16.08.04	17.08.04− 14.09.04	15.09.04− 15.10.04
Habarovskaya st. *alley of trees 1−11*	0.99−0.67	0.67−0.59	0.59−0.87	0.87−0.56	0.56−0.78	0.78−0.91
Saharov pr. *alley of trees 2−4; 6−10*	1.00−1.00	1.00−0.44	0.44−1.00	1.00−0.86	0.86−0.77	0.77−1.00
alley of trees 1−7 (I−III)	0.97−0.28	0.28−0.00	0.00−1.00	1.00−0.71	0.71−0.44	0.44−0.76
Sokolniki (Strominka st.) *alley of trees 1*−10**	1.00−1.00	1.00−0.90	0.90−1.00	1.00−1.00	1.00−1.00	1.00−1.00
bio group of trees 1−4	1.00−1.00	1.00−0.86	0.86−1.00	1.00−0.74	0.74−0.65	0.65−0.99

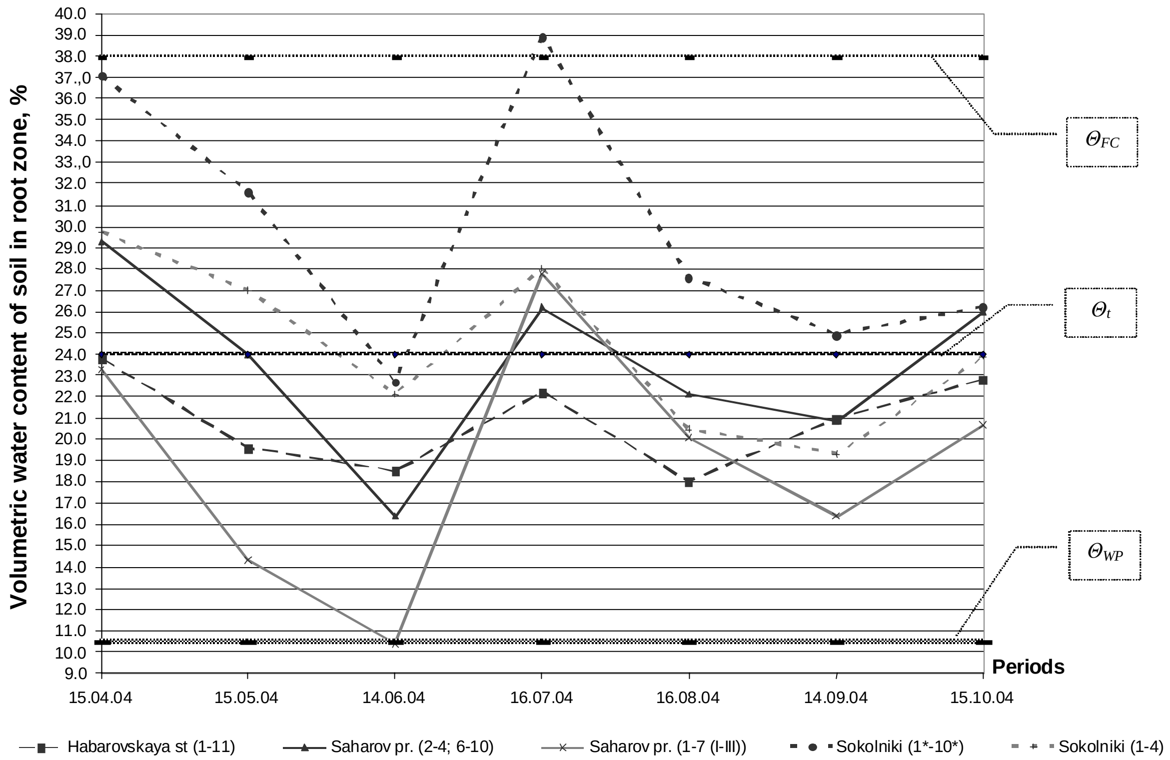

Fig. 5.2. Volumetric water contents of soil root zones during the various periods

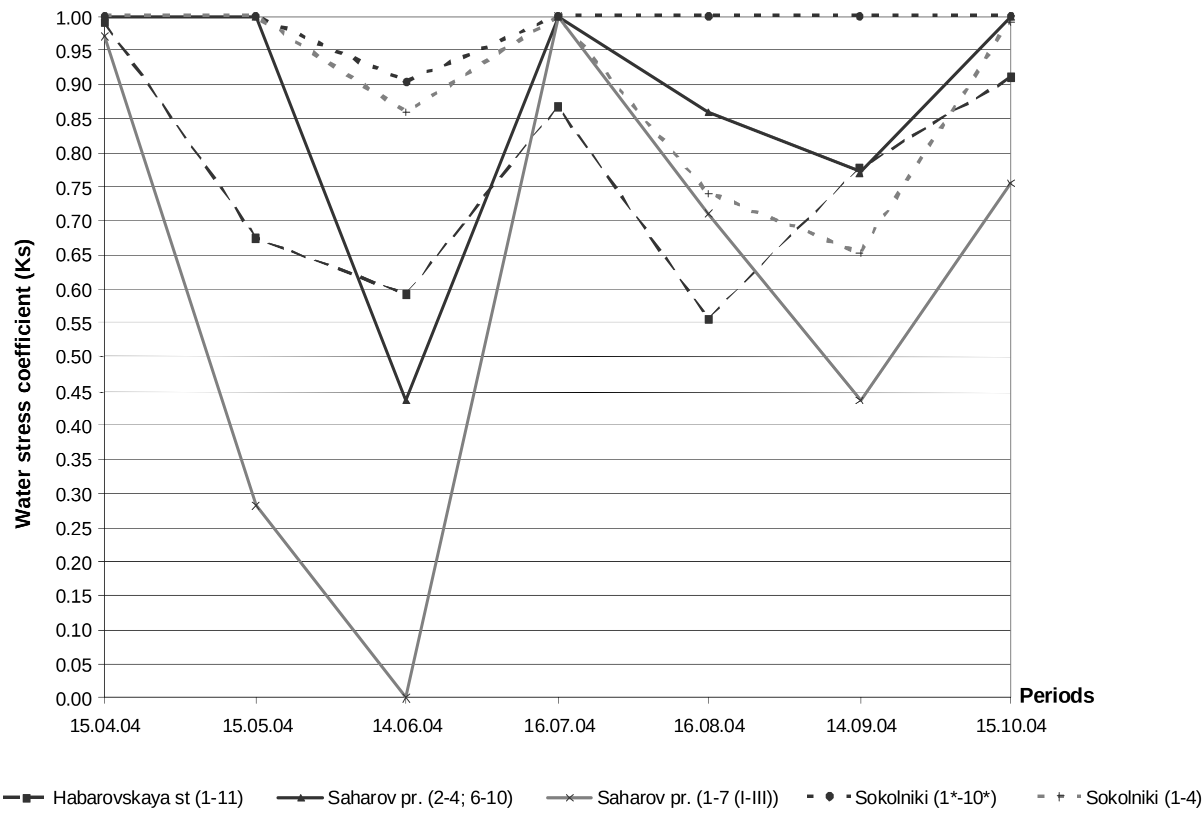

Fig. 5.3. Water stress coefficients during the various periods

5.2. Calculation of salinity stress coefficients

When there is too much salt in the soil, transpiration decreases due to salinity stress. Traditionally, the salt condition of the soil is expressed in EC of the saturation extract, transformed to a temperature of 25 °C (EC depends on water content and temperature; EC of saturation extract, at 25 °C, is not dependent anymore of (incidental) water content and temperature during the measurement). The salinity effect on transpiration is expressed through a salinity stress coefficient, like the effect of drought on transpiration was expressed through a water stress coefficient. The actual evapotranspiration may be calculated through multiplying the potential evapotranspiration not only by the water stress coefficient, but also by the salinity coefficient (Maas and Hoffman, 1977; Maas, 1990; Feddes et al., 2003). The relationship between EC of the saturation extract at 25 °C and the salinity stress coefficient is usually expressed as two straight lines. See Fig. 5.4. The first (horizontal) line represents conditions before salinity stress occurs (salinity stress coefficient K_{ss} = 1). After a threshold EC is exceeded, transpiration decreases linearly with increasing EC, until the coefficient becomes zero (second line). The particular graph in Fig. 5.4 presents experimental data for linden (*Tilia cordata*) from Weissenhorn (2002).

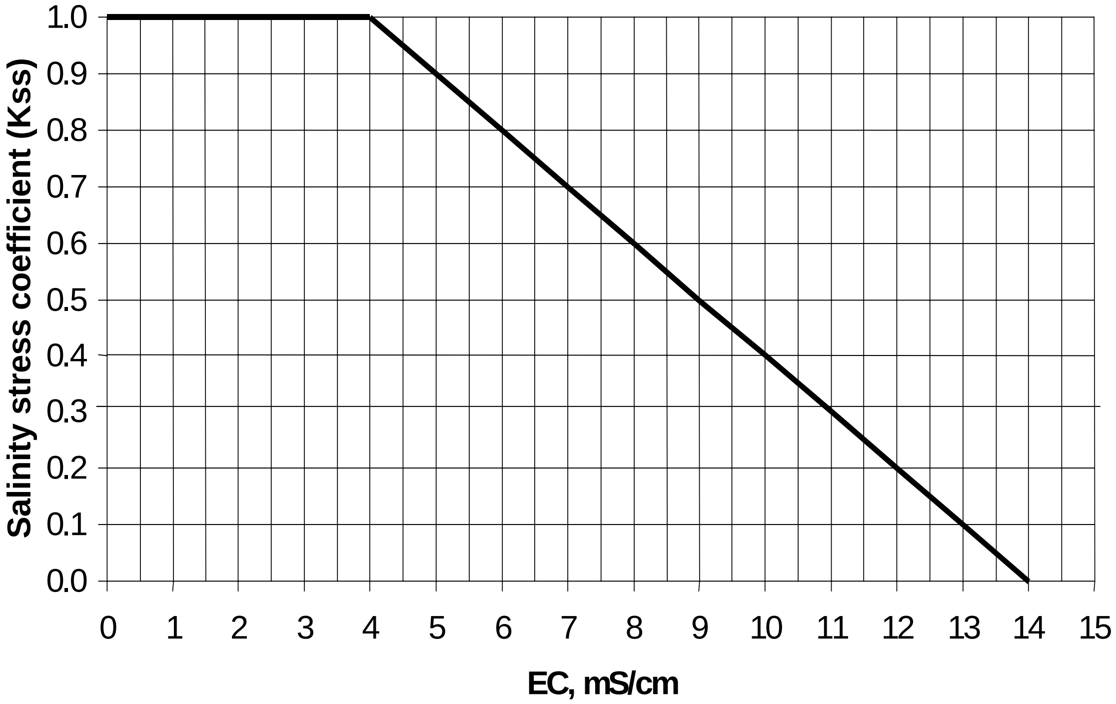

Fig. 5.4. Salinity stress coefficient of *Tilia cordata* and electrical conductivity (EC) of the saturation extract at 25 °C

The two lines in the graph represent

$K_{ss} = 1$ *(for EC = 0 − 4)*
$K_{ss} = -0.1\ EC + 1.4$ *(for EC > 4)*

In order to transform data that are obtained for different soil conditions (temperature, volumetric water content, degree of water saturation), the following set of equations (Heimovaara, 1993; Mualem and Friedman, 1991) can be used:

$$EC_{w,25} = EC_{w,T} \cdot (1 + 0.0216 \cdot (25 - T))$$

$$EC_{SatExt} = EC_{w,25} \cdot \left(\frac{\theta_a}{\theta_{Sat}} \right)$$

$EC_{w,\,25}$ = "soil pore water" electrical conductivity at actual volumetric water content and temperature T = 25 ^{o}C (standard) [mS/cm],
$EC_{w,T}$ = "soil pore water" electrical conductivity at actual volumetric water content and temperature [mS/cm],
EC_{SatExt} = "soil saturation extract" electrical conductivity [mS/cm] (all pores saturated with water),
T = soil temperature [°C],
θ_a = actual soil volumetric water content [cm^3/cm^3],
θ_{Sat} = soil volumetric water content when all pores are saturated with water [cm^3/cm^3],
$\theta_{Sat} \approx 0.55$ for the topsoil and $\theta_{Sat} \approx 0.43$ for the subsoil.

The measuring of the *EC* values was done using a special sensor ("W.E.T. sensor", Eijkelkamp, Giesbeek, The Netherlands), which allows the direct measuring of soil volumetric water content, soil temperature, and pore water electrical conductivity. The final results are presented in Table 5.3 and Fig. 5.5. For all objects and periods $K_{ss} = 1$, because $EC_{SatExt} < 4$. It means that the studied vegetation did not suffer from salinity stress. Water stress appears to be the sole physical stress factor.

Table 5.3. EC of soil saturation extract at 25 ^{0}C for all periods

Object	Values of soil saturation extract electrical conductivity EC_{SatExt}, mS/cm					
	15.04.04−15.05.04	16.05.04−14.06.04	15.06.04−16.07.04	17.07.04−16.08.04	17.08.04−14.09.04	15.09.04−15.10.04
Habarovskaya st. *alley of trees 1−11*	0.38±0.03	0.42±0.03	0.51±0.04	0.36±0.02	0.47±0.02	0.63±0.05
Saharov pr. *alley of trees 2−4; 6−10*	0.39±0.02	0.27±0.01	0.48±0.03	0.35±0.03	0.33±0.02	0.62±0.04
alley of trees 1−7 (I−III)	0.38±0.01	0.36±0.02	0.74±0.05	0.58±0.03	0.57±0.03	0.75±0.02
Sokolniki (Strominka st.) *alley of trees 1*−10**	0.49±0.03	0.34±0.01	0.77±0.04	0.44±0.01	0.41±0.02	0.51±0.03
bio group of trees 1−4	0.57±0.02	0.52±0.01	0.65±0.03	0.43±0.02	0.40±0.01	0.65±0.03

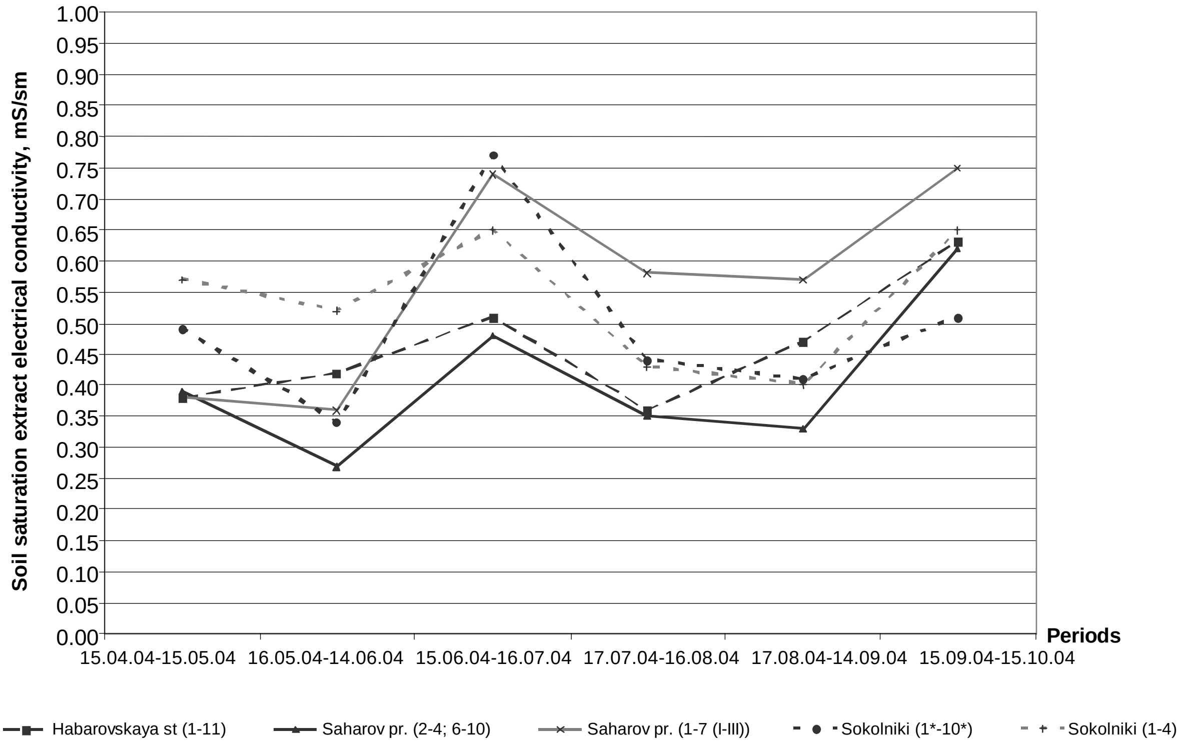

Fig. 5.5. EC of soil saturation extract during all periods

5.3. Calculation of actual evapotranspiration of trees-lawn combinations

After the estimation of the potential evapotranspiration of trees-lawn combinations (see section 4.3.2.) and water stress coefficients (see section 5.1.) the actual evapotranspiration for trees-lawn combinations can be calculated:

$ET_{a,\,combination} = ET_{combination} \cdot K_s$

$ET_{a,\,combination}$ = actual evapotranspiration for a trees-lawn combination in a period [mm day^{-1}],

$ET_{combination}$ = potential evapotranspiration for the trees-lawn combination in a period [mm day^{-1}],

K_s = water stress coefficient [-].

Table 5.4 and Fig. 5.6 present the result of these calculations.

Table 5.4. Actual evapotranspiration of trees-lawn combinations for each period

Object	Values of actual evapotranspiration for each period, mm day^{-1}					
	15.04.04–15.05.04	16.05.04–14.06.04	15.06.04–16.07.04	17.07.04–16.08.04	17.08.04–14.09.04	15.09.04–15.10.04
<u>Habarovskaya st.</u> *alley of trees 1−11*	0.60	0.73	1.31	0.80	1.11	0.46
<u>Saharov pr.</u> *alley of trees 2−4; 6−10*	0.89	0.72	2.38	1.90	1.46	0.50
alley of trees 1−7 (I−III)	0.25	0.00	2.02	1.36	0.73	0.38
<u>Sokolniki (Strominka st.)</u> *alley of trees 1*−10**	0.89	1.28	1.84	1.69	1.53	0.50
bio group of trees 1−4	0.89	1.35	2.28	1.82	1.07	0.50

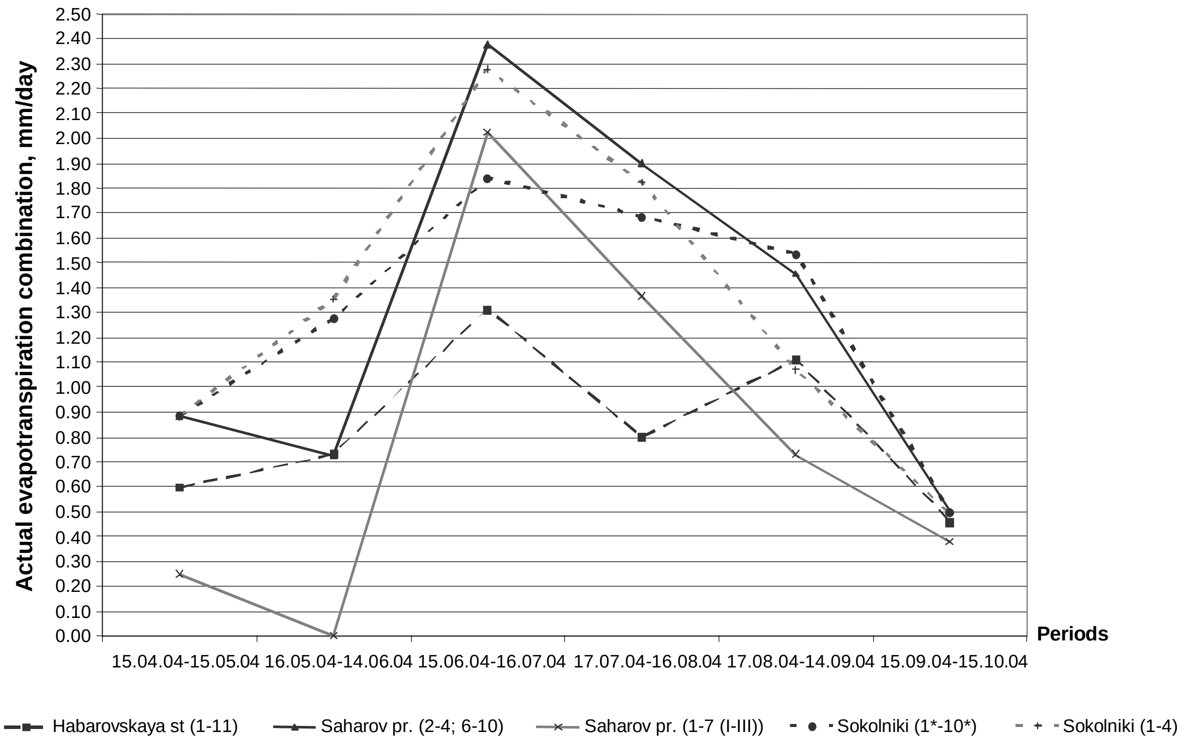

Fig. 5.6. Actual evapotranspiration of trees-lawn combinations for each period

CHAPTER 6. CALCULATION OF RAIN INTERCEPTION BY TREES, LAWNS, AND TREES-LAWN COMBINATIONS

A part of the precipitation cannot reach the soil surface because it is intercepted by the canopy of the trees and grass (Rutter et al., 1975; Gash, 1979; McNaughton and Jarvis, 1983; Landsberg, 1986; Shuttleworth, 1989; Schmugge and Andre, 1991; Bussiere, 1992). The intercepted water evaporates later. Strictly speaking, distinction between intercepted rainwater and throughfall would not be relevant in our calculations because evapotranspiration is defined as the undifferentiated sum of evaporation and transpiration. Evaporation is the process whereby liquid water is converted into water vapor and removed from the evaporating surface. Water evaporates from bare soil and wet vegetation. Transpiration is the process of vaporization of liquid water contained in plants through stomata of the leaves and vapor removal to the atmosphere. Although, strictly speaking, an estimate of the intercepted part would not be necessary, it may be a help in evaluating the consistency of the whole set of calculation results.

The amount of interception may reach 10–15% from the total precipitation (McNaughton and Jarvis, 1983). Landsberg (1986) states that the interception amounts 5−60% from the effective precipitation, i.e., the precipitation that reaches the soil surface and can be used by plants.

The amount of interception strongly depends on amount of precipitation and LAI. Firstly, the interception by the trees within the crown projection areas is calculated. Secondly, the interception by the grass canopy outside the tree crown projections. Finally, the interception of the tree – lawn combinations is estimated.

Aston (1979) and Spittlehouse and Black (1982) present an empirical formula for the estimation of the volume of intercepted precipitation by trees:

$$I_{trees} = P \cdot [1 - (0.0063 \cdot LAI_{trees}{}^2 - 0.1525 \cdot LAI_{trees} + 1.3039)], \qquad (R^2 = 0.97)$$

I_{trees} = intercepted precipitation by trees, [mm],

P = quantity of precipitation, [mm],

LAI_{trees} = leaf area index of trees, [dimensionless].

This formula estimates intercepted precipitations by trees very well when quantity of precipitation is lower than 10−12 mm, and LAI > 2.5. Calculation of I_{trees} was performed for each day with one or more rainfall events, and, after that, summed for each period. A small part of the rainfall events in periods 3, 4 and 5 exceeded 10−12 mm/event (4, 4 and 1 events in periods 3, 4 and 5, respectively). These events were excluded from the calculations.

In 1983, Von Hoyningen-Huene and, in 1985, Braden (Feddes et al., 2003, pp. 5−16 and 5−17) proposed an empirical formula for the estimation of the volume of intercepted precipitations by various agricultural crops. It will be applied to the lawn:

$$I_{grass} = a \cdot LAI_{grass} \cdot \left(1 - \frac{1}{1 + \frac{b \cdot P}{a \cdot LAI_{grass}}} \right)$$

I_{grass} = intercepted precipitation by grass, [mm],

P = quantity of precipitation, [mm],

a = empirical coefficient, a = 0.25 mm,

b = soil cover fraction of grass [-],

LAI_{grass} = leaf area index of grass [-].

Interception by the lawn was calculated for each day with one or more rainfall events. The results were summed for each period.

In order to obtain overall interception values, the calculated interceptions for trees and lawn were summed according to the following weighing equation:

$$I_{combination} = \frac{\sum S_{crown}}{S_{area}} \cdot I_{trees} + \left(1 - \frac{\sum S_{crown}}{S_{area}} \right) \cdot I_{grass}$$

The use of this weighing procedure implies neglecting the interception by the grass canopy underneath trees. This is acceptable because interception by trees is much larger than by grass, and the tree crown projections only cover a fraction of the areas. Application of these formulas needs information on precipitation, LAI_{trees}, LAI_{grass} and b_{grass} for each period. These values are presented in Tables 6.1 and 6.2 and Fig. 6.1. The calculation results are given in Tables 6.3 and 6.4 and Figures 6.2 and 6.3.

Table 6.1. Total quantity of precipitation during all periods

Periods	Total precipitation, mm
15.04.04−15.05.04	33.2
16.05.04−14.06.04	48.3
15.06.04−16.07.04	244.0
17.07.04−16.08.04	109.0
17.08.04−14.09.04	68.2
15.09.04−15.10.04	35.9

The FAO Guidelines by Allen et al. (1998) do not deal with interception explicitly. They account for the sum “interception + soil evaporation” through the difference $K_c - K_{cb}$. This difference is tabulated in their Table 18. For example, it can be derived from this Table that the Guidelines assume for the midseason and late season periods that

$$I + E = (K_c - K_{cb})ET \approx 0.1ET$$

$$I \approx 0.1ET - E$$

ET = potential evapotranspiration [mm d^{-1}],
E = soil evaporation [mm d^{-1}].
Considering the ET values calculated in Chapter 4, it may be concluded that the last equation predicts interception values that are often lower than the values calculated in this chapter (Table 6.3).

Table 6.2. Leaf Area Indices of trees and grass during all periods

Object	Values of LAI_{trees}, LAI_{grass}, b_{grass} for each period, mm					
	15.04.04–15.05.04	16.05.04–14.06.04	15.06.04–16.07.04	17.07.04–16.08.04	17.08.04–14.09.04	15.09.04–15.10.04
Habarovskaya st. *alley of trees 1–11*						
S_{area}, m^2	180.0	180.0	180.0	180.0	180.0	180.0
ΣS_{crown}, m^2	37.7	37.7	37.7	37.7	37.7	37.7
$\Sigma S_{crown} / S_{area}$	0.21	0.21	0.21	0.21	0.21	0.21
LAI_{trees}	1.85	2.70	3.52	4.17	3.21	1.80
LAI_{grass}	0.54	0.74	0.81	0.82	1.11	0.86
b_{grass}	0.237	0.309	0.333	0.336	0.426	0.349
Saharov pr. *alley of trees 2–4; 6–10*						
S_{area}, m^2	619.0	619.0	619.0	619.0	619.0	619.0
ΣS_{crown}, m^2	347.8	347.8	347.8	347.8	347.8	347.8
$\Sigma S_{crown} / S_{area}$	0.56	0.56	0.56	0.56	0.56	0.56
LAI_{trees}	4.25	5.45	5.94	6.06	5.52	4.24
LAI_{grass}	1.10	1.19	1.24	1.30	1.25	0.81
b_{grass}	0.423	0.448	0.462	0.478	0.465	0.333
alley of trees 1–7 (I–III)						
S_{area}, m^2	281.0	281.0	281.0	281.0	281.0	281.0
ΣS_{crown}, m^2	109.7	109.7	109.7	109.7	109.7	109.7
$\Sigma S_{crown} / S_{area}$	0.39	0.39	0.39	0.39	0.39	0.39
LAI_{trees}	3.18	4.04	4.49	4.36	3.88	2.68
LAI_{grass}	1.17	1.02	1.03	1.14	1.17	0.74
b_{grass}	0.443	0.400	0.402	0.434	0.443	0.309
Sokolniki (Strominka st.) *alley of trees 1*–10**						
S_{area}, m^2	288.0	288.0	288.0	288.0	288.0	288.0
ΣS_{crown}, m^2	82.3	82.3	82.3	82.3	82.3	82.3
$\Sigma S_{crown} / S_{area}$	0.29	0.29	0.29	0.29	0.29	0.29
LAI_{trees}	4.86	5.56	6.05	6.03	5.64	4.68
LAI_{grass}	1.31	1.16	1.01	1.00	1.15	1.14
b_{grass}	0.481	0.440	0.396	0.393	0.437	0.434
bio group of trees 1–4						
S_{area}, m^2	115.0	115.0	115.0	115.0	115.0	115.0
ΣS_{crown}, m^2	59.2	59.2	59.2	59.2	59.2	59.2
$\Sigma S_{crown} / S_{area}$	0.52	0.52	0.52	0.52	0.52	0.52
LAI_{trees}	5.12	6.32	7.11	6.54	5.77	4.20
LAI_{grass}	4.81	2.22	1.00	2.59	0.55	0.81
b_{grass}	0.910	0.670	0.393	0.726	0.240	0.333

Table 6.3. Values of interception of tree-grass combinations during all periods

Object	Values of Interception combination for each period, mm					
	15.04.04–15.05.04	16.05.04–14.06.04	15.06.04–16.07.04	17.07.04–16.08.04	17.08.04–14.09.04	15.09.04–15.10.04
Habarovskaya st. *alley of trees 1–11*						
Overall I_{trees}	-*	0.63	7.93	5.09	1.73	-*
Overall I_{grass}	0.69	1.29	2.22	1.16	1.39	1.53
$I_{combination}$	**0.69**	**1.92**	**10.16**	**6.25**	**3.12**	**1.53**
Saharov pr. *alley of trees 2–4; 6–10*						
Overall I_{trees}	4.28	9.20	51.88	23.74	13.21	4.61
Overall I_{grass}	0.90	1.44	2.13	1.17	0.90	0.62
$I_{combination}$	**5.19**	**10.64**	**54.01**	**24.91**	**14.11**	**5.23**
alley of trees 1–7 (I–III)						
Overall I_{trees}	1.52	3.94	24.15	10.26	5.13	0.83
Overall I_{grass}	1.36	1.61	2.34	1.38	1.15	0.75
$I_{combination}$	**2.88**	**5.55**	**26.49**	**11.64**	**6.28**	**1.58**
Sokolniki (Strominka st.) *alley of trees 1*–10**						
Overall I_{trees}	2.78	4.89	27.46	12.22	7.04	2.83
Overall I_{grass}	1.85	2.24	2.66	1.36	1.31	1.59
$I_{combination}$	**4.63**	**7.13**	**30.12**	**13.58**	**8.35**	**4.42**
bio group of trees 1–4						
Overall I_{trees}	5.38	10.25	58.61	24.03	12.99	4.21
Overall I_{grass}	6.11	3.49	1.78	2.86	0.31	0.67
$I_{combination}$	**11.49**	**13.75**	**60.38**	**26.89**	**13.30**	**4.88**

** when LAI_{trees} < 2.5 precipitation is intercepted only by grass and $I_{combination} \sim I_{grass}$*

Table 6.4. Fraction of Intercepted precipitation by tree-grass combinations during all periods

Object	Fraction of Intercepted precipitation for each period, %					
	15.04.04–15.05.04	16.05.04–14.06.04	15.06.04–16.07.04	17.07.04–16.08.04	17.08.04–14.09.04	15.09.04–15.10.04
Habarovskaya st. *alley of trees 1–11*	2.1	4.0	4.2	5.7	4.6	4.3
Saharov pr. *alley of trees 2–4; 6–10*	15.6	22.0	22.1	22.9	20.7	14.6
alley of trees 1–7 (I–III)	8.7	11.5	10.9	10.7	9.2	4.4
Sokolniki (Strominka st.) *alley of trees 1*–10**	13.9	14.8	12.3	12.5	12.2	12.3
bio group of trees 1–4	34.6	28.5	24.7	24.7	19.5	13.6

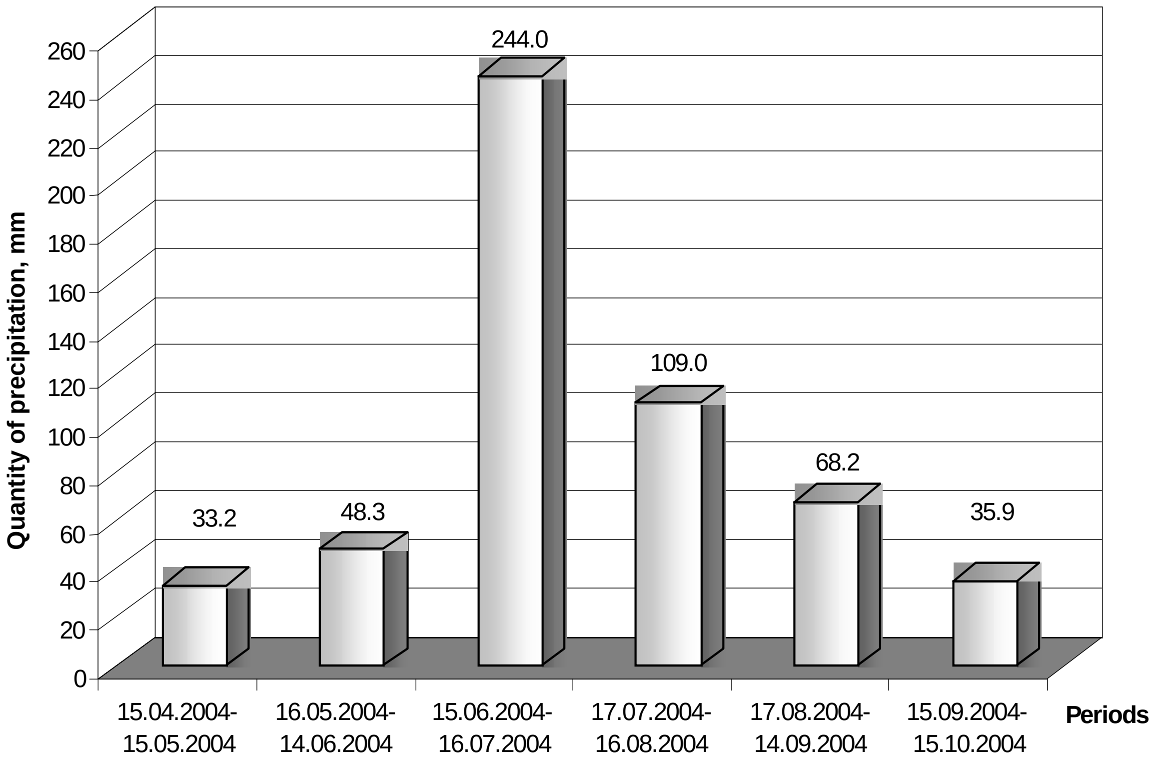

Fig. 6.1. Total quantity of precipitation during all periods

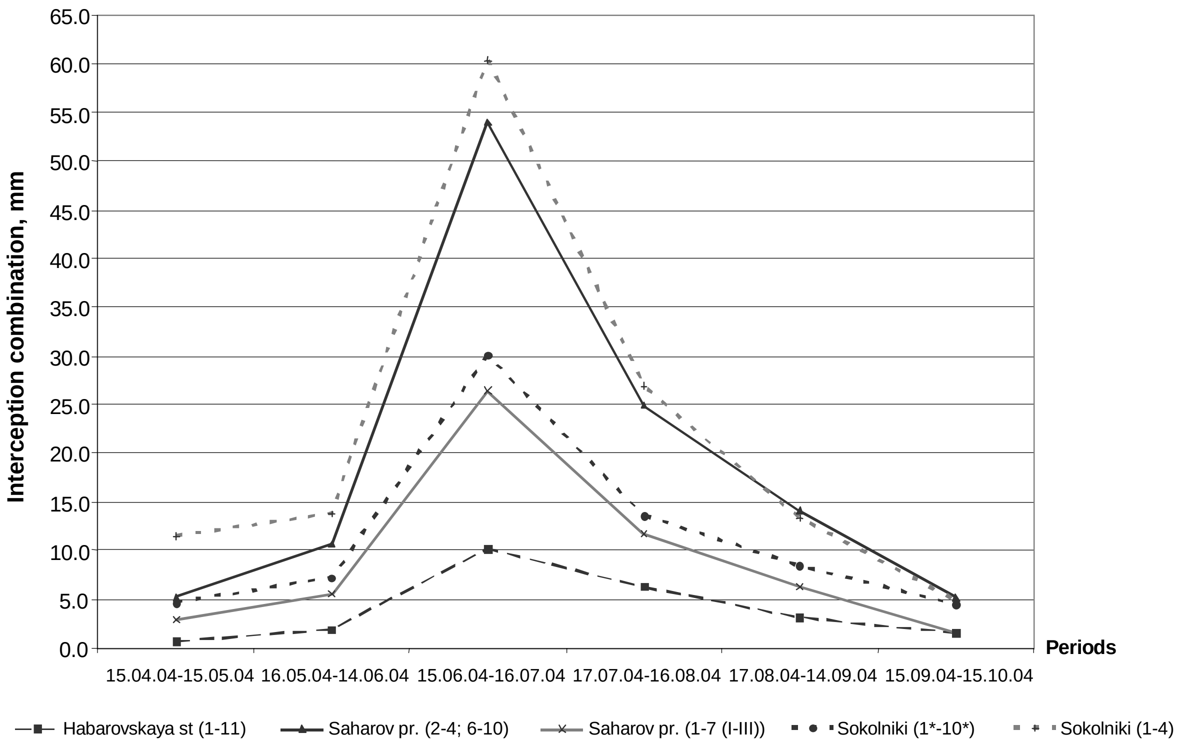

Fig. 6.2. Values of Interception of tree-grass combination during all periods

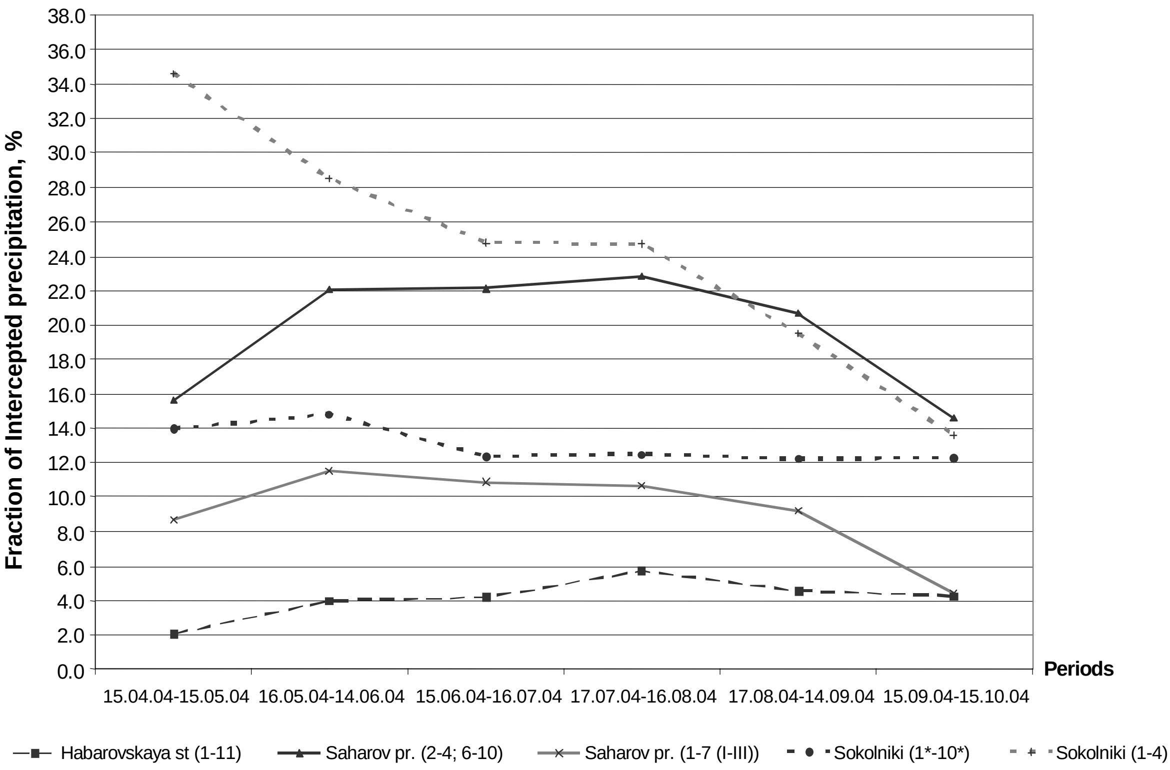

Fig.6.3. Fraction of precipitation that is intercepted by tree-grass combination during all periods

CHAPTER 7. WATER REGIMES OF ROOT ZONES

A vegetation zone may be defined as the system of above-ground parts of the vegetation and the soil root zone. It may further be assumed that the water content of the vegetation is the same at all measuring days, and that the root-zone thickness is 1 m. This chapter concentrates on the water regime of the vegetation zone. A water balance may be written for each object and each period between two subsequent measuring routines of soil water content, as well as for each object and the total period between the measuring routines at the start of the first period and at the end of the last period:

Initial water content of the root zone + rainfall + inflow from runoff elsewhere + watering incidents = actual evapotranspiration + runoff + deep percolation + final water content of the root zone.

Table 7.1 presents rainfall amounts for each period and, for each object and period, the initial and final water contents of the root zones, potential evapotranspiration and actual evapotranspiration. Cases where precipitation exceeds potential evapotranspiration have, by definition, a rainfall surplus. Table 7.1 shows that most cases had a rainfall surplus. The table indicates a number of periods of objects which suffer from water stress (actual evapotranspiration smaller than potential evapotranspiration). Cases without water stress are shaded in the table.

Rates of deep percolation may be estimated from the water contents of the 90 – 100 cm deep soil layers of the root zones. Rate of deep percolation by gravity is equal to the unsaturated water conductivity, which depends on water content. If the 90 − 100 cm soil layer is very dry, deep percolation may be neglected. If the layer is very wet, the rate may be very high. The root zones are similar to soil O15 from the Staring series. Woesten et al. (2001) present for this soil unsaturated water conductivities as a function of water content: 1.2; 6.3; 39; 96; 159; 222; 333; 1110 mm/month at soil water contents of 27.3; 31.8; 36.7; 38.9; 39.8; 40.3; 40.7; 41.0%, respectively. We assumed that deep percolation may be neglected if it is less than 1.2 mm/month. Now we return to Table 7.1. Measuring values of the water contents of the lowest soil layer are available from the measuring routines between periods 1 and 2, 2 and 3, 3 and 4, 4 and 5, 5 and 6, and at the end of period 6, for Habarovskaya st., Saharov pr., and Sokolniki (Strominka st). In addition, the values are available for Sokolniki (strominka st), site (1−4), at the start of period 1, and for Habarovskaya st. at 25.10.04, a date later than the end of the last period. The water contents of the lowest layers at the beginning of the first period are not available for most of the objects. It is only available for Sokolniki (Strominka st.), site (1−4): locally as high as 39%. This is equivalent to a deep percolation rate of 100 mm/month at the measuring day. The highest measured water contents of the lowest layer of this object between period 1 and 2 and between period 2 and 3 were 33 and 33%, implying deep percolation rates of 20 mm/month at the measuring days. The water contents of the lowest layers of the sites of Habarovskaya st. that were measured some days after the last period at 25.10.04, had as highest measuring value 36%, indicating a deep percolation rate of 35 mm/month at day 25.10.04. For all further measured lowest-layer water contents of objects and measuring times the value of the water content of the lowest layer was so low that rate of deep percolation could be neglected. It may be concluded that deep percolation occurs early spring and late autumn, but not in the remaining part of the growing season.

The possibilities for rain to infiltrate the soil surface may be estimated from the saturated water conductivity (permeability) of the upper soil layers. The part of the rainfall that is not intercepted by the canopy reaches the soil surface. If the intensity of this part is larger than the maximum infiltration rate at the soil surface, runoff will occur. The order of magnitude of the maximum infiltration rate is the same as that of the water permeability (saturated hydraulic conductivity). Well structured soils have permeabilities that are largely determined by inter-aggregate pores, biopores, etc. Such pores are large and provide excellent infiltration possibilities. The upper parts of the soils of the objects are highly degenerated. They contain much dust rather than aggregates (Chapter 3). Their permeability is more related to size of individual mineral particles than to size of aggregates and large pores. Most of the particles of the soils are between 0.01 – 0.05 mm. This size fraction has a permeability of 0.0004 cm/s. It means that the order of magnitude of the infiltration rate of the degenerated, dusty, upper soil parts is 0.24 mm/min. Rainfall intensities often exceed this value. The above reasoning means that, when rainfall reaches the soil surface, a nonzero but very limited infiltration rate develops.

The amount of runoff from each object during the entire period may be estimated from a simplified water balance. If we neglect inflow from runoff elsewhere, watering incidents and deep percolation, and assume that the water content of a root zone at the start of the growing season is equal to its water content at the end of the growing season, then:

Runoff = rainfall – actual evapotranspiration

Using this equation, runoff was estimated for each object. The estimated values were 385, 297, 391, 301 and 295 mm for Habarovskaya st., Saharov pr. site (2 − 4; 6 − 10), Saharov pr. site (I − III), Sokolniki (Strominka st.) (1* − 10*) and Sokolniki (Strominka st.) site (1 − 4), respectively. This is, on average, 62% of the rainfall. The values deviate a little due to neglecting deep percolation.

The water balance equation may also be applied to single periods. Then, the water contents at the start and at the end of a period cannot be neglected and must be included in the balance. It appears that now anomalies arise: calculated runoff is often higher than rainfall in cases with a drying regime and calculated runoff is often negative in cases with a wetting regime. These anomalies disappear if one uses much smaller root-zone volumes in the balance calculations. It indicates that the effective root-zone volume is less than 1 m^3/m^2 object area.

The root-zone water contents at the start of the first period are plotted against the values of the total evapotranspiration in Fig. 7.1. The graph suggests that an optimal value of this water content is 280–300 mm in the top 1 m soil layer.

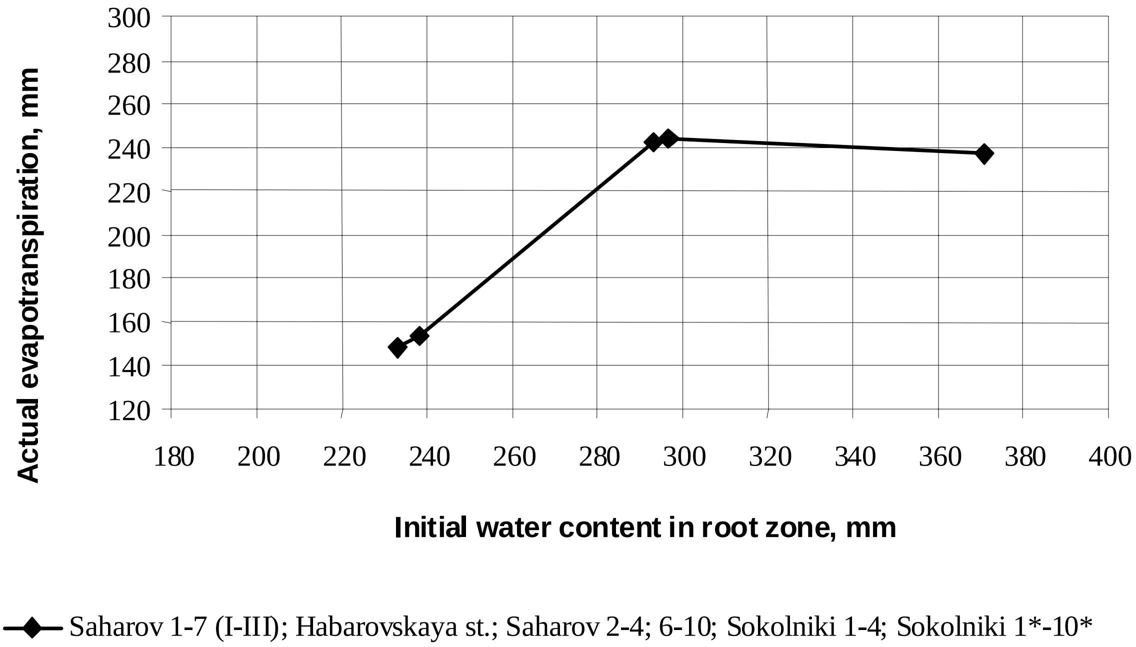

Fig. 7.1. Initial water content in root zone (at start of period 15.04.04–15.05.04) and actual evapotranspiration (sum for all periods). Dots from left to right: Saharov 1–7 (I–III); Habarovskaya st.; Saharov 2–4; 6-10; Sokolniki 1–4; Sokolniki 1*–10*

Table 7.1. For each object and period: precipitation, initial water content, end water content, potential and actual evapotranspiration (see text)

Object	Precipitation, water content $_{ini}$, water content $_{end}$, *water loss*					
	15.04.04–15.05.04	16.05.04–14.06.04	15.06.04–16.07.04	17.07.04–16.08.04	17.08.04–14.09.04	15.09.04–15.10.04
Precipitation, mm	33.2	48.3	244.0	109.0	68.2	35.9
Duration of period, days	31	30	32	31	29	31
Habarovskaya st. *alley of trees 1–11*						
Water content $_{ini}$, mm	238	196	185	222	180	210
Water content $_{end}$, mm	196	185	222	180	210	228
$ET_{combination}$, *mm/day*	0.89	1.24	1.51	1.44	1.43	0.50
$ET_{a, combination}$, *mm/day*	0.60	0.73	1.31	0.80	1.11	0.46
Saharov pr. *alley of trees 2–4; 6–10*						
Water content $_{ini}$, mm	293	240	164	262	221	209
Water content $_{end}$, mm	240	164	262	221	209	260
$ET_{combination}$, *mm/day*	0.89	1.65	2.38	2.21	1.89	0.50
$ET_{a, combination}$, *mm/day*	0.89	0.72	2.38	1.90	1.46	0.50
alley of trees 1–7 (I–III)						
Water content $_{ini}$, mm	233	143	104	278	201	164
Water content $_{end}$, mm	143	104	278	201	164	207
$ET_{combination}$, *mm/day*	0.89	1.49	2.02	1.92	1.67	0.50
$ET_{a, combination}$, *mm/day*	0.25	0.00	2.02	1.36	0.73	0.38
Sokolniki (Strominka st.) *alley of trees 1*–10**						
Water content $_{ini}$, mm	371	316	227	389	276	249
Water content $_{end}$, mm	316	227	389	276	249	262
$ET_{combination}$, *mm/day*	0.89	1.41	1.84	1.69	1.53	0.50
$ET_{a, combination}$, *mm/day*	0.89	1.28	1.84	1.69	1.53	0.50
bio group of trees 1–4						
Water content $_{ini}$, mm	297	270	221	280	205	193
Water content $_{end}$, mm	270	221	280	205	193	239
$ET_{combination}$, *mm/day*	0.89	1.57	2.28	2.46	1.64	0.50
$ET_{a, combination}$, *mm/day*	0.89	1.35	2.28	1.82	1.07	0.50

CHAPTER 8. DISCUSSION OF MODEL RESULTS

8.1. Reference evapotranspiration

In order to estimate the reference evapotranspiration (ET_0) in Moscow, two radiation models were used: the very universal FAO guidelines and the semi-empirical Makkink's radiation model that has been developed in The Netherlands (Table 4.2 and Fig. 4.1). The estimations were carried out for the growth stages (periods) of combined vegetations of Linden trees (*Tilia cordata*) and grass (lawn) on the basis of data on climatic parameters. The FAO model contains more parameters and is less empirical than Makkink's model, so that one might expect that it estimates the unknown evapotranspiration more exactly. Therefore, we accepted the FAO model as "base" (standard). However, we found that Makkink's model (with factor C_1 = 0.65) gave ET_0 values that are the same as the values obtained through the FAO model. Hence, in cases where the availability of climatic parameters for conditions of Moscow is limited, it is possible to use the simpler Makkink's model.

The evapotranspiration values are relatively low because of urban influences (low wind speeds and high cloudiness and humidity). The maximal level of the reference evapotranspiration (ET_0) was observed during the periods 15.06.04−16.07.04 and 17.07.04−16.08.04, with values equal to 2.61 (Makkink: 2.62) and 2.45 (2.42) mm/day, respectively. This can be explained by the increase of air temperature in these periods because of the reception of a maximum solar radiation. The complex interrelation of climatic parameters resulted in similarity of values for the periods 15.04.04−15.05.04 and 17.08.04−14.09.04. Values of ET_0 in these periods are equal to 1.97 (1.94) and 2.07 (2.01), respectively. Note that the first period is the Initial stage, and the other period is the last time-step of the Mid-season stage. The importance of this will be specified later at the discussion of trees-lawn combinations.

A further essential feature is the distinct "uniformity of change" of the ET_0 values. From the Initial stage the reference evapotranspiration gradually increases, followed by an also gradual decrease to the final period of the Mid-season stage. Further on, a sharp reduction of ET_0 values is observed during late season. This is connected to a change of climatic parameters (especially change of air temperature), strongly slowing down the process of evapotranspiration. The ET_0 value for the period 15.09.04−15.10.04 is reduced two times in comparison with the period 17.08.04−14.09.04, and equals 1.11 (0.97) mm/day.

One might argue that the application of the evapotranspiration models to the urban objects may be not quite correct because of shading by buildings and the relatively small size of the objects. But Moscow is very widely planned, and the period of maximum evapotranspiration is generally between 11.00 and 15.00 hours (Allen et al., 1998, p. 188). And the selected objects are surrounded by similar greening objects and further objects like road signs, traffic lights, above-ground cables, statues, etc., all making the aerodynamic roughness more uniform.

8.2. Leaf Area Indices of individual trees and lawn areas

Considering city conditions, we can surely observe the dependency of the various vegetation conditions on a complex of factors. A first step on the way towards an estimation of the state of plants can be the use of a universal indicator quantity that allows studying not only a “status quo” but also dynamic processes. Accordingly, we used, for trees and lawn, the quantity Leaf Area Index (LAI), because it is possible to draw conclusions about the presence of plant stress and the consequences of its influence from the development of leaf surface and crown as a whole.

City plantings of *Tilia cordata* and lawn areas at different locations of Moscow were involved in studying these questions. Using a specific algorithm (see section 3.2), values of LAI were obtained for each tree and lawn area at these objects. We shall consider the obtained data at the level of an individual tree and at the level of a planting (alley or biogroup).

Object: Habarovskaya st. (Table 4.3 and Figs 4.2 and 4.3)

During the Initial stage (15.04.04−15.05.04) the majority of trees have a LAI of 1.65−2.27 (max = 2.63−2.67; min = 0.67−0.79). From that, LAI increases and during 17.07.04−16.08.04 the maximal LAI values of the majority of trees are 3.48−4.69 (max = 5.17−5.08; min = 1.92). Thus, the LAI values of the "leader trees" in the Initial stage are levelled with those of the other trees during Mid-season. During the further periods decrease of LAI is observed, and again, during 15.09.04−15.10.04, there is a change of “leader trees”. Values of LAI in this period are 1.07−2.13 (max = 3.22−3.75; min = 0.63). Trees with a rather high LAI at Initial stage can improve or keep their positions up to the end of the vegetative period. The trees with lowest initial values of LAI do not show an essential increase. Their values remain rather low. The given example shows specific features of each tree (groups of trees), reacting not only on the general climatic factors, but also on site-specific anthropogenic factors like: technology of planting and size of planting hole; mechanical damages to stem; different degrees of soil density near the surface and change of water-air regimes under the surface in the root zone; a non-uniform care (watering, application of fertilizers); etc.

Analyzing the condition of the lawn on various sites of this object a rather non-uniform development is observed. Periods of increasing LAI are unexpectedly interrupted by decrease. At Initial stage the LAI values of the lawn are 0.18−0.78 (max = 1.06−1.18; min = 0.09). In this case it is impossible to speak about a general natural increase of LAI values, reaching maximum in the optimum period. At each site, more than one peak LAI value is reached, in different periods. Thus, there can be several maximal LAI values at each site. The absolute-maximal value for the lawn of this object is LAI = 2.51 and the absolute-minimal is LAI = 0.08 (in the period 17.07.04−16.08.04). The unstable condition of the lawn during almost the entire vegetative period can be attributed to the realization of actions for lawn improvement and repeated local damages.

Object: Saharov pr. (Table 4.4 and Figs 4.4−4.7)

On this object the change of the LAI of trees was considered separately for two parts (2−4; 6−10) and (I−III).

For the majority of trees (2−4; 6−10) LAI typically increased gradually from Initial stage (15.04.04−15.05.04) with LAI = 3.47−5.12 (max = 6.04; min = 3.39) to mid-season (17.07.04−16.08.04) with LAI = 5.60−7.12 (max = 8.12; min = 5.01−5.05). The period 15.09.04−15.10.04 is characterized by LAI = 3.23−5.66 (max = 6.18; min = 1.46). In this case the "leader" (tree 4) keeps its position. The sharp decrease of LAI of tree 9 may be explained by intensive anthropogenic influence like, for example, repair of underground communications in the root zone and significant damage of the root system. Other trees kept stable values of LAI.

Change of LAI of trees at I−III occurs differently. Each of the sites I−III is surrounded by a highway and secondary roads, all paved with an asphalt covering, leaving very small areas for lawn. At Initial stage (15.04.04−15.05.04) LAI = 2.58−3.61 (max = 4.19; min = 1.92). The further increase of the LAI values, up to a maximum, occurs during the period 15.06.04−16.07.04, and reaches values of LAI = 3.69−4.81 (max = 5.22−5.29; min = 2.55). Only one tree has kept ability to increase LAI during the following period 17.07.04−16.08.04. This value, LAI = 5.65, is also the absolute-maximal value for trees of site I−III. The period

15.09.04−15.10.04 is characterized by LAI = 1.80−3.24 (max = 3.95; min = 0.93). Thus, it is similar to the situation of object Habarovskaya st. If trees had rather high LAI values at the initial stage they can increase these values or keep the values at a high level during the whole vegetative period, and trees with lowest values of LAI typically do not significantly increase their LAI values.

The condition of the lawn on this object is also unstable during the vegetative period, at site (2−4; 6−10) and as well as at site (I−III). A comparison may be made. Initial stage LAI is 0.62−1.47 (max = 2.25; min = 0.40) at site (2−4; 6−10) and is 1.15−1.84 (max = 1.94; min = 0.25−0.26) at site (I−III). The absolute maximum of site (2−4; 6−10) is LAI = 2.54−2.60, being observed in the periods (17.07.04−16.08.04) and (17.08.04−14.09.04), and of site (I−III) it is LAI = 3.03, being observed in an earlier period (15.06.04−16.07.04). For two lawns in these periods average values of lawn LAI did not exceed 2.1−2.2. Late Season LAI values are 0.37−1.05 (max = 1.85; min = 0.29) and 0.26−0.94 (max = 1.89; min = 0.09) at sites (2−4; 6−10) and (I−III), respectively. These values are similar for the two sites, and reflect the general condition of lawn in this period.

Object: Sokolniki (Strominka st.). (Table 4.5 and Figs 4.8-4.11)

This object is also presented by two parts: alley (1*−10*) and biogroup (1−4). The first values belong to site (1*−10*). Initial stage (15.04.04−15.05.04) LAI = 3.74−5.44 (max = 5.68; min = 3.51). These are the greatest values of this period from all considered sites. Further development of LAI of the majority of trees is sufficiently uniform and reaches maximum levels in periods 15.06.04-16.07.04 and 17.07.04-16.08.04, during which LAI = 4.87−6.51 (max = 7.48; min = 4.09) and LAI = 4.81−6.36 (max = 7.57; min = 4.11). Late Season is characterized by LAI = 3.77−5.48 (max = 5.84; min = 3.29). We can see again the tendency of preservation of the level of LAI values of each of the trees, both for well and for a slowed-up way of developing.

It is also interesting to analyze LAI of trees in biogroup (1−4). Initial stage (15.04.04−15.05.04) LAI = 4.34−5.44. Maximal values LAI are characteristic for the period 15.06.04−16.07.04 and equal 5.42−8.96. Late Season LAI = 2.60−6.08. In this case the LAI values of the tree with minimal initial LAI value remain the minimum values during all periods.

The LAI values of lawns on site (1*−10*) at Initial stage (15.04.04−15.05.04) are not so large: LAI = 1.20−1.65 (max = 2.06; min = 0.49−0.58). Considering the whole vegetative period the lawn areas show also non-uniform development. It is interesting that the absolute maximum and minimum observed LAI occurred in one period. It is 17.07.04−16.08.04 with maximum LAI = 2.51 and minimum LAI = 0.28. Late Season values are LAI = 0.71−1.52.

LAI values of lawn areas at site (1−4) for Initial stage (15.04.04−15.05.04) are sufficiently high and equal to 4.45−5.26, which is three times higher than at site (1*−10*). From that there is a sharp decrease of LAI. So during 15.06.04−16.07.04 it has already fallen to 0.80−1.17. After that there is an increase to LAI = 1.91−3.74 in the period 17.07.04−16.08.04, and LAI is reduced again to a minimal size of 0.25 in period 17.08.04−14.09.04. During Late Season the values of LAI equal 0.68−0.96.

Thus, this object being an example, we could see some dynamics of the condition of lawns, which is rather indicative and reflects influences of such factors as: compaction of soil; damage as a result of construction work and subsequent soil erosion; restoration of lawns; lawn care activities, including trimming, watering, aeration, application of fertilizers. Besides, the state of a lawn is influenced substantially by its appropriateness: incidence of shading from parts of buildings and large trees; properties of soil substrate on which the lawn grows (including optimum composition of the substrate); degree of drainage of the territory; climatic factors (favorable or unfavorable combinations of temperature and quantity of precipitation); i.e., a complex influence of the components of the system «tree – lawn – growing conditions».

8.3. Leaf Area Indices of objects

The original data were obtained for individual trees and specific lawn sites. In order to be able to compare the set of trees and lawn of an object with those of others, and in order to formulate a complete/overall representation of LAI, it was necessary to take into account the areas of the tree crown projections and to determine a weighted average LAI value for the trees of each object. The results made it possible to compare objects (Table 4.6 and Fig. 4.12).

Initial stage (15.04.04-15.05.04)

Maximal values of LAI of trees are characteristic for object Sokolniki (Strominka st.), and equal to 4.86 at site (1*−10*) and 5.12 at site (1−4). Average values are observed on object Saharov pr.: LAI = 4.25 at site (2−4; 6−10), and 3.18 at site (I−III). Minimal values are observed for object Habarovskaya st. where LAI = 1.85, which is 2.6−2.8 times less than for object Sokolniki (Strominka st.).

Development (16.05.04−14.06.04) and

Mid-season (15.06.04−16.07.04; 17.07.04−16.08.04; 17.08.04−14.09.04)

During these periods there is an increase of LAI values at all objects. However, the maximal values and the periods of their occurrence can be various. For objects Sokolniki (Strominka st.) and Saharov pr. LAI is 6.05−7.11 and 5.94−4.49, respectively, for the period 15.06.04−16.07.04; and LAI is 6.03−6.54 and 6.06−4.36, respectively, for the period 17.07.04−16.08.04. For Habarovskaya st., maximal LAI = 4.17 occurring in the period 17.07.04−16.08.04. Thus, objects Sokolniki (Strominka st.) and Saharov pr. kept not only higher LAI values than Habarovskaya st., but also during a longer term.

Late Season (15.09.04−15.10.04)

The given period is characterized by the following values: Sokolniki (Strominka st.) LAI = 4.68−4.20; Saharov pr. LAI = 4.24−2.68; Habarovskaya st. LAI = 1.80 (the minimal value in comparison with other objects).

Thus, on Habarovskaya st. there was a situation at which even a favorable combination of climatic factors is not capable to improve significantly its usual growing conditions (including soil). The condition of *Tilia cordata* can worsen significantly at negative combinations of climatic factors (for example, at insufficient precipitation).

Analyzing the average LAI values for lawn during the period 15.04.04−15.05.04 we can draw the conclusion that Habarovskaya st. again shows the lowest LAI: 0.54 (fraction of soil cover by grass only 0.237). Other objects show rather uniform values: Saharov pr., site (2−4; 6−10), LAI = 1.10 (0.423); site (I−III), LAI = 1.17 (0.443); Sokolniki (Strominka st.) (1*−10*), LAI = 1.31 (0.481, i.e. more than 50% of the area is exposed bare soil). Much greater values were observed for object Sokolniki (Strominka st.), site (1−4): LAI = 4.81 (0.910).

Change of LAI of a lawn during the vegetative period has no clear regularity and is characterized by various periods of increase and decrease of values. The maximal values for different objects during the periods of an observably maximum follow. Habarovskaya st. LAI = 1.11 (0.426) - the period 17.08.04−14.09.04. Saharov pr. site (2−4; 6−10) LAI = 1.30 (0.478) - the period 17.07.04−16.08.04; site (I−III) LAI = 1.17 (0.443) - the periods 15.04.04−15.05.04 and 17.08.04−14.09.04; Sokolniki (Strominka st.) site (1*−10*) LAI = 1.31 (0.481) - the period 15.04.04−15.05.04, site (1−4) LAI = 4.81 (0.910) - the period 15.04.04−15.05.04.

LAI values of the period 15.09.04–15.10.04 on all objects vary 0.74–1.14 (0.309-0.434).

According to our research sufficiently high values of LAI of lawn are observed during the Initial stage. It may be explained by several reasons. In conditions of Moscow, the start of the development of grass (lawn) is earlier than of other vegetation in the spring, and, accordingly, the grass has no competitors for light, water and nutrients. Besides, in the city conditions, the air temperature is some degrees higher; the snow cover disappears earlier; and the surface of soil warms up faster (also because of significant contents of organic matter having dark color in the soil top layer); - all this enabling the lawn to develop more intensively than in suburbs of the city. It should be noted, that "life" of lawn under conditions of Moscow stops in the winter period and does not proceed before the spring starts. In this case the quality of the soil conditions in the spring period is a potentiality for the entire vegetative period.

8.4. K_c values and potential evapotranspiration

In our calculations of crop coefficients (section 2.3.4.), we adopted the value K_c = 0.45 for all Initial and Late stages. Using this value we derived Initial and Late stage values of potential evapotranspiration for the tree-grass combination $ET_{combination}$ from the Initial and Late stage reference evapotranspiration. The derived value for Initial stage is $ET_{combination}$ = 0.89 mm/day, which appeared to be 1.8 times more than the derived Late Season $ET_{combination}$ = 0.50 mm/day (Table 4.9, Fig. 4.13). Certainly, approximation of these values for all objects without differentiation may be questioned. However, we know that in the Initial stage the stable part of the vegetation transpiration is transpired by the lawn grass. LAI of lawn in this period is not so high on the majority of the sites. Only by the end of the period (practically for one week) trees show sufficiently intensive development of leaf surface. In Late Season the transpiration is reduced, since climatic factors significantly slow down biological processes.

For the calculation of values of evapotranspiration of all Mid-season periods, appropriate K_c values were derived (Table 4.8). This derivation was based on the definitions of fraction of soil surface covered by trees (as observed from overhead) and fraction of soil surface covered by grass (as observed from above). The obtained data indicate low values of grass LAI. Therefore, when objects as a whole are considered, decrease of fraction of soil surface covered by the combined vegetation can be observed. Certainly, our data show rather significant tree LAI values, but tree crowns only represent a part of the transpiring surfaces, not occupying all object territory. In spaces between trees the basic transpiring surface is grass, the projected cover of which is not stable during the vegetative period.

Values of Mid-season evapotranspiration (Table 4.9, Fig. 4.13) are maximal during 15.06.04−16.07.04: Habarovskaya st. $ET_{combination}$ = 1.51 mm/day; Saharov pr. site (2−4; 6−10) $ET_{combination}$ = 2.38 mm/day; site (I−III) $ET_{combination}$ = 2.02 mm/day; Sokolniki (Strominka st.) site (1*−10*) $ET_{combination}$ = 1.84 mm/day; site (1−4) $ET_{combination}$ = 2.28 mm/day. Later (the period 17.07.04−16.08.04) almost all objects show gradual decrease of evapotranspiration. Only Sokolniki (Strominka st.), site (1−4), is characterized by an increase of $ET_{combination}$ = 2.46 mm/day. The obtained results may be explained by comparing them with the information about LAI, the values of which are large, and by taking into account that conditions (climatic factors; insignificant shading; location of surrounding buildings; etc.) are favourable for evapotranspiration as well.

8.5. Soil water contents

In order to transform potential evapotranspiration values into actual evapotranspiration values it is necessary to analyze the parameter “volumetric water content of soil” and to estimate its change during the various periods of the vegetation process. Besides, such an analysis can evidently show whether plants suffered from water stress or not, and provide factors of water stress (section 5.1).

The analysis of the values of the volumetric water content that were obtained for each object (Table 5.1 and Fig. 5.2) shows that, after snow thawing and water accumulation in the root zone, an unequal situation is already present. During Initial stage (15.04.04−15.05.04), objects Sokolniki (Strominka st.), sites (1*−10*) and (1−4), and Saharov pr., site (2−4; 6−10), have volumetric water content values that are higher than the critical value: 29.7; 37.1; 29.3 > critical value = 24.0% at the beginning of the period and 31.6; 27.0; 24.0 ≥ 24.0% at the end of the period. Volumetric soil water contents of root zones of other objects are already below critical level in this period: Habarovskaya st. and Saharov pr., site (I−III): 23.8 and 23.3 < 24.0% at the beginning of the period and 19.6 and 14.3 < 24.0% at the end of the period. But the reasons of these conditions are various. The soil profile of Habarovskaya st. has water shortage because significant runoff occurs, and Saharov pr., site (I−III), has, besides significant runoff, a more intensive development of tree LAI and grass LAI, i.e. its area of transpiration surface is larger than at Habarovskaya st.

During the following period (15.05.04−14.06.04), all objects show decreases of volumetric soil water contents, to values below the critical value, 16.4−22.7 < 24.0% , and, in the case of Saharov pr., site (I−III), volumetric water content becomes even lower than the water content at wilting point: 10.4 < wilting point = 10.5%. The reasons are: insufficient amount of precipitation, intensive development of leaf surface.

Later (period 15.06.04−16.07.04), volumetric soil water contents increase up to values of 26.2−28.0%, which are higher than critical, and for one of the objects, Sokolniki (Strominka st.) site (1*−10*), even to a value that is a little higher than field capacity: 38.9 > 38.0%, despite the significant tree LAI value (4.49−7.11) of this object during this period. But the precipitation in this period is 244 mm. It is rather favorable allowing the significant area of transpiration surfaces to receive sufficient water from the soil. It is especially important for *Tilia cordata*, because this species of wood plants reaches its maximal development in this period (15.06.04−16.07.04). Only Habarovskaya st. has volumetric soil water contents again below critical level (22.2% < 24.0%).

Then there is a decrease of volumetric water content of soil, proceeding up to the period 17.08.04−14.09.04 when value of water content is again below critical level and equals 16.4−21.0%. Only on one object Sokolniki (Strominka st.), site (1*−10*) this value is a little more and about 24.9%.

During the period 15.09.04−15.10.04 air temperature, LAI and evapotranspiration decrease, which allows a large amount of water to reach the root zone and to be stored in it. It is interesting that even in this period objects Habarovskaya st. and Saharov pr., site (I−III), have volumetric water contents (22.8 and 20.7%) below critical value.

8.6. Water stress coefficients

Similar regularity is observed when we consider water stress coefficients K_s (Table 5.2 and Fig. 5.3). On all objects there is a reduction of this parameter. This can especially be seen during 16.05.04−14.06.04, because of several reasons: development of the leaf surface, insufficient amount of precipitation and, in some cases (Habarovskaya st. and Saharov pr., site (I−III)), low initial volumetric water content of the soil after snow thawing. Thus, during Development stage, K_s = (0.90-0.44) < 1 on almost all objects, and even = 0 (water content at wilting point) on Saharov pr., site (I−III).

During the period with maximum precipitation (15.06.04−16.07.04) K_s = 1 on all objects, except for Habarovskaya st., where K_s = 0.87. Then again the water stress factors decrease, and, at the end of period (17.08.04−14.09.04), K_s = 0.44−0.78. Only the factor of Sokolniki (Strominka st.), site (1*−10*), is stable and remains 1.

Then, certainly, K_s values start to increase, but do not always reach the maximal value. Thus, before the formation of a snow cover, the soil profile cannot receive enough water to reach its water holding capacity. Because of the city practice of gathering and taking out most part of snow, the soil in the spring period is not completely saturated by water again, which may be considered suboptimal. Besides, if the amount of precipitation in spring is insignificant, and water runoff is significant, it happens that the water storage in the root zone soil is not sufficient. In addition, appearing grass (lawn) also requires water. Accordingly, the tree in the city develops in stressful conditions already in the beginning of the vegetative period, and its state depends to a greater extent on a favorable combination of climatic factors or a duly care.

8.7. Actual evapotranspiration

On the basis of the obtained data we determined values of actual evapotranspiration for the tree-grass combinations, $ET_{a,\ combination}$ (see section 5.3.). The values are given in Table 5.4 and Fig. 5.6. Minimal values of Initial Stage were observed for Habarovskaya st. and Saharov pr., site (I−III), where $ET_{a,\ combination}$ = 0.60 and 0.25 mm/day, respectively. For the period 16.05.04−14.06.04 volumetric water content has decreased to the water content at wilting point at Saharov pr., site (I−III), and trees experience strong water stress, by which the process of evapotranspiration practically stopped.

During 15.06.04−16.07.04 maximal values of actual evapotranspiration were observed: 1.31−2.38 mm/day (minimal value applies to Habarovskaya st.). At this time significant amounts of precipitation provide the soil profiles with water, which then transpire through the leaf surface. Thereafter, actual evapotranspiration is gradually reduced, already to $ET_{a,\ combination}$ = 0.73 mm/day on object Saharov pr., site (I−III), in period 17.08.04−14.09.04, which is two times less than on Saharov pr., site (2−4; 6−10), with $ET_{a,\ combination}$ = 1.46 mm/day and Sokolniki (Strominka st.), site (1*−10*), with $ET_{a,\ combination}$ = 1.53 mm/day.

This tendency of object Saharov pr., site (I−III), remains during Late stage when its $ET_{a,\ combination}$ = 0.38 mm/day, which is the minimal value from all objects of study.

8.8. Interception

An interesting aspect at studying the distribution of water by plants in the city is the interception of some part of precipitation by the leaf surface of trees and lawn, $I_{combination}$. This parameter depends on the value of LAI (Table 6.2) and amounts of precipitations (Table 6.1 and Fig. 6.1). The parts of the precipitations intercepted by trees do not reach the level of the lawn (under tree crowns) and cannot be intercepted by the grass leaves or reach the soil at the surface of the root zone (Tables 6.3 and 6.4).

The calculated interception values for periods 1, 2, and 6 are small relative to the corresponding evapotranspiration values. Note that evapotranspiration is defined as the sum of the evaporation from soil and wet vegetation and transpiration of vegetation, which means that interception is included in evapotranspiration. It should also be noted that the evaporation from wet vegetation is not uniquely related to precipitation: the evaporation from wet vegetation is relatively small if the same amount of rainfall is distributed over a small number of events with intensive rainfall. In other words, the intercepted water part at precipitations of intensive character (storms) is less than at uniform, small, precipitations.

The minimal interception during Initial stage was found for site Habarovskaya st.: $I_{combination}$ = 0.69 mm (2.1% from total amount of precipitations), which is in this case basically due to the leaf surface of the grass. The maximal value for this stage was found for Sokolniki (Strominka st.), site (1−4): $I_{combination}$ = 11.49 mm (34.6% from total amount of precipitations). In this case values of LAI of trees and grass are high.

The absolute maximum of the intercepted precipitations was observed during 15.06.04−16.07.04. In this period, maximum quantity of precipitations and maximum LAI of trees occurred (LAI values of lawns were not so high). The $I_{combination}$ values in this period were 60.38 mm and 54.01 mm on Sokolniki (Strominka st.), site (1−4) and Saharov pr., site (2−4; 6−10), respectively. These amounts represent 24.7 and 22.1% of the total quantity of precipitations, respectively. When the precipitations had an intensive character (storms), the part of the intercepted water is less than when precipitations were uniform and small.

During Late Season the amount of intercepted water decreases, since the leaf surface of trees becomes less, and the amount of precipitations is not so large. Fractions of interception in this period are 4.3−14.6%, depending on the LAI values of trees and grass, and also on the ability of trees to keep the leaf surface in this period.

8.9. Water regimes

Chapter 7 indicates an extreme runoff value for the objects during the measuring period: 62% of the rainfall. Part of this excessive value may be explained by systematic errors. Evapotranspiration is calculated from LAI values that were obtained through image processing. This method provides LAI values that are a little too low if the canopy parts are clustered. The introduced error can only be small as evapotranspiration is only a weak function of LAI. By definition, the evapotranspiration includes evaporation of intercepted rain. This may not affect the evapotranspiration value when evaporating wet canopy surface (in case of wet canopy) is identical to transpiring dry canopy surface (in case of dry canopy). But in the case of sparse woody plants this evaporating wet surface is much larger than the dry transpiring surface. Then, the real evapotranspiration increases with the time that the wooden parts are wet. A maximum value of the introduced error may be estimated from Chapter 6 (Interception). The maximum error is limited. The significant runoff is due to the very limited infiltration possibilities. The infiltration rate is nonzero, so that there is a yearly refill of the water that the vegetation withdraws from the root zones. But the refill is very slow and often does not reach field capacity. The limited infiltration possibilities are accompanied by excessive runoff.

The results may be interpreted for rainfall in other years. The rainfall in Moscow during the distinguished six periods of the growing season of 2004 was 33.2, 48.3, 244.0, 109.0, 68.2, and 35.9 mm, respectively. Norm values are 46.5, 55.5, 72.5, 79.0, 64.5, and 51.5 mm, respectively. Rainfall in the 2004 growing season was 538.6 mm (norm: 369.5 mm). The difference, 169 mm, is mainly caused by a few peak rainfall events in periods three and four of the 2004 growing season. It may be assumed that this difference ran off the surface. Estimated runoff values in the 2004 growing season ranged from 295 to 385 mm. In order to obtain an estimate for the runoff in a growing season with a rainfall of 369.5 mm (norm), we may correct this range by subtracting 169 mm. Then we find the range 126 – 216 mm. This is a substantial part of the norm rainfall summed over the six periods (369.5 mm): 34 – 58 %. The norm values of the rainfall in the distinguished periods (1.50, 1.85, 2.27, 2.55, 2.22, and 1.66 mm/day, respectively) may be compared with the values of potential evapotranspiration of the sites and periods of the 2004 growing season in Table 7.1. Norm rainfall for most of the periods would be enough to support the calculated potential evapotranspiration of most of the distinguished sites and periods. Only period three of Saharov pr. and period three of biogroup of trees 1–4 of Sokolniki (Strominka st.) are exceptions. For both cases deficits are small (0.11 and 0.01 mm/day, respectively). If the sites would be improved, evapotranspiration would increase. An upper bound for the evapotranspiration may be estimated as the reference evapotranspiration in the growing season (386.7 mm) multiplied by the factor 1.2, which is 464 mm. The norm rainfall is 369.5 mm. The root-zone soil can supply the difference of 94.5 mm if the zone is sufficiently rewetted before the start of the growing season.

The results may also be compared with literature on similar vegetation types. McIntyre et al. (2002) review runoff studies for grassy woodlands, and Arnaez et al. (2007) for vineyards. The runoff coefficient is strongly connected to the degree of soil cover by the smaller plants, and may range between zero and values that exceed 70%. Degree of soil cover by the grass, averaged over the six periods, can be derived from Table 4.6 for each site. These values are 0.332, 0.435, 0.405, 0.430, 0.545 for Habarovskaya st., Saharov pr. 2–4; 6–10, Saharov pr. 1–7 (I–III), Sokolniki (Strominka st. 1*–10* and Sokolniki (Strominka st. 1–4, respectively. The corresponding runoff values are 385, 297, 391, 301, and 295 mm (Chapter 7). The correlation coefficient, r, of both series of values is –0.731. It may be expected that the estimated runoff for the growing season correlates negatively with the soil water content at the start of the growing season (Water content$_{ini}$ for the first period in Table 7.1.). The correlation coefficient r of this runoff and this initial water content is –0.808. The saturated water conductivity value, estimated in Chapter 7, is in the lower part of the range of reported values for new and old, compacted and non-compacted, residential lawns (Partsch et al., 1993; Ferguson, 2005).

Chapter 7 indicates that the assumed root-zone volume of 1 m^3/m^2 is much too large, and that the effective root-zone volume is much smaller. It is indeed very plausible that, in reality, the root zone volumes are severely reduced by: road foundations extending under the vegetated areas; over-compacted spots; debris; utilities like tubes, cables; incomplete exploration of potential root zones by the roots, etc. The effective root depth should be interpreted as the average root-zone volume under a unit of vegetated area. Note that, when the whole growing season is considered and based on our calculations, it counter-intuitively appears that the root-zone volume has little influence on the runoff. This could because:

* the amount of water in the root zone is small in comparison with the rainfall during the growing season;

* the measured fractional water contents at the beginning and the end of the growing season are similar; and

* the amount of deep percolation during the growing season is neglible.

We may carry out a sensitivity analysis using some data derived from Table 7.1: rainfall during the whole growing season; actual evapotranspiration during the whole growing season; initial and final fractional water contents of the root zone (mm water per 1000 mm root zone), and applying the following balance equation:

*runoff = rainfall – actual evapotranspiration – ((final – initial fractional water content) * root zone volume)*

Considering a variation of 0.75 – 1.25 m^3 root zone volume/m^2soil surface, we find that the resulting runoff variations are 371 – 362, 259 – 233, 359 – 338, 290 -283 and 249 – 237 mm for the Habarovskaya st., Saharov pr. 2-4; 6-10, Saharov pr. 1-7 (I-III), Sokolniki (Strominka st. 1*-10* and Sokolniki (Strominka st. 1-4 data, respectively. It can be seen that the assumed large variation in root-zone volume produces only small variations in runoff.

In Chapter 7, the runoff data of the whole growing season were calculated from the simplified balance equation

runoff = rainfall – actual evapotranspiration

These runoff data (385, 297, 391, 301, and 295 mm) are an overprediction because the amount of water in the root zones at the end of the growing season is not precisely equal to, but slightly higher than the amount at the start of the growing season. If we apply the balance equation that includes root-zone water content, using a root-zone volume of 1 m^3/m^2 and the initial and final water contents in Table 7.1, we find the runoff values 367, 246, 349, 287, and 249 mm. These data are an under-prediction because the root-zone volumes are much less than 1 m^3/m^2.

The depth to which the roots extend has been set at 1 m. This is in agreement with urban greening practice in Moscow where standard planting holes have a depth of 1 m, and in agreement with rooting behaviour of *Tila cordata* (Kutschera and Lichtenegger, 2002). So, we have the situation that the roots reach to a depth of 1 m, but the root-zone volume is much less than 1 m^3/m^2, due to reasons mentioned above. This is not a drawback for the calculation of the stress factors, because these factors are not derived from the total amount of root-zone water, but from the fractional soil water content of the root zone. This procedure is widely accepted. Gregory (2006) includes a review of this.

Chapter 7 also indicates that the assumed root depth of 1m is much too large, and that the effective root depth of the root zones is much smaller. It is indeed very plausible that, in reality, the root zone volumes are severely reduced by: road foundations extending under the vegetated areas; over-compacted spots; debris; utilities like tubes, cables, incomplete exploration of potential root zones by the roots, etc. The effective root depth should be interpreted as the average root-zone volume under a unit of vegetated area. Note that, when the whole growing season is considered, the root zone volume has no influence on the calculated runoff, because the amounts of water in the root zones at the beginning of the growing period and at the end of the growing period are similar. It means that the runoff as calculated in Chapter 7 is not influenced by uncertainties in root zone volumes.

Under conditions of excessive runoff and reduced root zones the level of the soil water content at the start of the growing period plays a significant role. It is clearly demonstrated in Fig. 7.1. Real urban conditions are very irregular and variable. Nevertheless, the data show clearly that vegetation frequently suffers from water stress although there is a surplus of rainfall. The incidence of excessive runoff is connected with a number of negative factors: soil structure degeneration at the surface of the soil, which is very sensitive to soil structure deterioration by anthropogenic influences; absence of large pores; hydrophobic soil behaviour; small fraction of soil surface covered by vegetation; little micro-relief. These factors are closely related to urban conditions and urban activities.

8.10. Conclusion

This chapter considered the basic aspects of the dynamics of the condition of the soil and plantings at different objects in the city. From this, conclusions are drawn and presented in the next chapter. The conclusions make it possible to find solutions that can help to improve the very frequent suboptimal situations. These solutions should be based on an appropriate substrate technology and Russian component materials.

9. CONCLUSIONS

1. Reference evapotranspiration (ET_0) in Moscow was calculated according to the FAO Penman-Monteith method. This calculation needed: cloudiness, temperature, wind speed, relative humidity of air. It appeared that Makkink's method to calculate reference evapotranspiration gave the same values as the FAO Penman-Monteith method. The calculation according to Makkink does not need values of wind speed and relative humidity. The calculated reference evapotranspiration values are low because of urban influences. Evapotranspiration periods could be chosen according to FAO guidelines: Initial stage, Development stage, 3 Mid-season stages, Late Season stage.

From the Initial stage the reference evapotranspiration gradually increases, followed by an also gradual decrease to the final period in the Mid-season stage. Further on, a sharp reduction of ET_0 values is observed during Late Season.

The FAO-Penman-Monteith reference calculation method likely produces correct estimations of the evapotranspiration in Moscow.

2. The majority of researched objects trees (*Tilia cordata*) and lawn (trees-lawn combination) had water stress, which was demonstrated by the obtained values of water stress coefficients. For the period from the middle of April up to the middle of June (Initial and Development stages), a decrease in the values of the factors of water stress ($K_s < 1$) was observed on all objects.

In most cases, values of actual evapotranspiration in this period were 0.60–0.89 mm per day, while the potential evapotranspiration for the trees-lawn combinations (unstressed conditions) in this period could be 1.24–1.65 mm per day.

The Leaf Area Index (LAI) of trees in conditions of water stress at the end of the Development stage had smaller values, in comparison with optimal conditions ($K_s = 1.0$). This decrease in values of LAI corresponds with a degeneration of the state of the trees (by visual estimation, category 0 changes into category 1 or even 2).

Trees with rather high LAI at Initial stage can improve or keep their positions up to the end of the vegetative period. The trees with lowest initial values of LAI do not show an essential increase.

State of lawn was unsatisfactory, because the fraction of bare soil was more than 50% in most cases.

3. A principal cause of water stress for trees-lawn combinations in Moscow is

deficiency of water content in soil during significant periods of vegetation, especially during Initial and Development stages. In this time mean quantity of precipitation is about 50 mm per month, and measured volumetric water content of soil was 22.7–10.4%, being lower than threshold value (24%).

A large fraction of the not-intercepted rainfall runs off from the surface of soil. This extreme runoff is connected with a very limited possibility for rainwater to infiltrate into the soil, due the high dust content, a dry condition of the soil top layer, and incidence of unstructured bare soil.

Total actual evapotranspiration highly depends on the amount of water that is present in the root zone at the start of the growing season. In this period the optimal value of water content in the top 1 m soil layer is 280–300 mm for trees-lawn combinations in Moscow.

The suboptimal condition of the vegetation can be improved by diminishing the water stress, which can be realised by improving the infiltration capacity of the top soil and quality of soil substrates.

PRINCIPAL SYMBOLS AND UNITS

a = empirical coefficient in interception equation, a = 0.25 mm

b = fraction of soil surface covered by grass [-]

b-value = blue channel intensity of pixel, 0-255 [-]

C_f = foliage surface drag coefficient [-]

c_p = specific heat of air [cal g^{-1} K^{-1}]

D = fraction of sky that can be seen on a photo that is taken from beneath a tree crown in a vertical direction (or fraction of bare soil on a photo towards lawn in a vertical direction) [-]

d_0 = zero-plane displacement height [-]

E = vapour flux (mass of water vapour per unit of surface per unit of time) [kg m^{-2} s^{-1}]

E_0 = potential evaporation [mm day^{-1}]

E_{RC} = evaporation of a reference crop [mm day^{-1}]

E_T = transpiration [mm day^{-1}]

EC = soil electrical conductivity [mS cm^{-1}]

EC_{SatExt} = electrical conductivity of soil saturation extract [mS cm^{-1}]

$EC_{w, 25}$ = soil pore water electrical conductivity at a given volumetric water content and temperature T = 25 ^oC (standard) [mS cm^{-1}]

$EC_{w,T}$ = soil pore water electrical conductivity at given volumetric water content and temperature [mS cm^{-1}]

E_{refM} = potential evapotranspiration of a surface with a closed dry grass canopy with height 8 − 15 cm and well supplied with water (Massop et al., 2005) [mm day^{-1}]

ET = evapotranspiration [mm day^{-1}]

ET_0 = reference evapotranspiration [mm day^{-1}]

$ET_{combination}$ = potential evapotranspiration for trees-grass combination [mm day^{-1}]

$ET_{a, combination}$ = actual evapotranspiration for trees-grass combination [mm day^{-1}]

e = vapour pressure [kPa]

$e^0 (T_{max})$ = saturation vapour pressure at maximum air temperature [kPa]

$e^0 (T_{min})$ = saturation vapour pressure at minimum air temperature [kPa]

e_a = actual vapour pressure at screen height [kPa]

e_a = actual vapour pressure at screen height [mbar]

e_d = saturation vapour pressure at air temperature at screen height [mbar]

e_s = saturated vapour pressure, prevailing at the surface [mbar]

e_s = saturation vapour presure [kPa]

F_r = resistance correction factor [-]

f_1 = total fraction of ground under crowns that is covered by trees and/or grass [-]

f_2 = fraction of lawn outside the tree crown projections that is covered by grass canopy (1-fraction of “bare soil”) [-]

$f_{1,g}$ = fraction of lawn covered by grass canopy, in spots within tree crown projections that are not covered by tree canopy. $f_2 = f_{1,g}$ [-]

$f_{1,t}$ = fraction of lawn (grass + “bare soil”) under tree crown projections that is covered by tree canopy [-]

f_c = fraction of soil surface covered by vegetation as observed from nadir (overhead) [-]

$f_{c,eff}$ = effective fraction of soil surface covered or shaded by vegetation [-]

f_{ew} = fraction of the soil that is both exposed and wetted, i.e., the fraction of soil surface from which most evaporation occurs [-]

$f(u)$ = wind function

G = soil heat flux density [MJ m^{-2} day^{-1}]

g-value = green channel intensity of pixel, 0-255 [-]

H = sensible heat loss [J m^{-2} day^{-1}]

h = plant height, mean plant height, mean maximum plant height [m]

h_{canopy} = mean vertical height of canopy area [m]

h_{crop} = crop height [m]

h_s = height of crown base above surface [m]

h_u = sensible heat transfer coefficient [J m^{-2} day^{-1} $^oC^{-1}$]

I = intercepted precipitations [mm]

$I_{combination}$ = intercepted precipitations by trees-grass combination [mm]

I_{grass} = intercepted precipitations by grass [mm]

I_{trees} = intercepted precipitations by trees [mm]

I_s = direct solar radiation along path of a solar beam in canopy [J s^{-1}]

I_{so} = direct solar radiation of a solar beam just above canopy [J s^{-1}]

K_c = crop coefficient [-]

$K_{c,ini}$ = crop coefficient during initial growth stage [-]

$K_{c,mid}$ = crop coefficient during mid-season growth stage [-]

$K_{c,end}$ = crop coefficient at end of late season growth stage [-]

$K_{c,full}$ = $K_{cb,full} + 0.05$ (p. 143 in (Allen et al., 1998)) [-]

$K_{c,combination}$ = crop coefficient for tree-grass combination [-]

$K_{c,mid,combination}$ = crop coefficient for tree-grass combination for mid-season stage [-]

$K_{c,mid,trees}$ = crop coefficient for sparse vegetation, considering the trees without grass, for mid-season stage [-]

$K_{c,\max}$ = maximum value of K_c following rain or irrigation [-]

K_{cb} = basal crop coefficient [-]

$K_{cb,ini}$ = basal crop coefficient during initial growth stage [-]

$K_{cb,mid}$ = basal crop coefficient during mid-season growth stage [-]

$K_{cb,end}$ = basal crop coefficient at end of late season growth stage [-]

$K_{cb,full}$ = estimated basal K_{cb} during mid-season (at peak plant size or height) for vegetation having full ground cover or LAI>3 [-]

$K_{cb,h}$ = $K_{cb,mid}$ for full cover vegetation (LAI>3) under subhumid and calm wind conditions ($RH_{\min} = 45\%$ and $u_2 = 2$ m s^{-1}) [-]

K_e = soil evaporation coefficient [-]

K_m = kinematic eddy viscosity [cm^2 s^{-1}]

K_r = soil evaporation reduction coefficient [-]

K_s = water stress coefficient [-]

K_{ss} = salinity stress coefficient [-]

k = von Kármán’s constant [-]

k_s = extinction coefficient [-]

L = latent heat of vaporization [2.45 MJ m^{-3}]

L , LAI = Leaf Area Index = one-sided leaf area per unit of basal area [-]

L_t = foliage area index = upper-sided area of all foliage elements per unit of basal area [-]

$LAI_{combination}$ = overall Leaf Area Index of trees – lawn combination [-]

LAI_{grass} = Leaf Area Index of grass [-]

LAI_{trees} = Leaf Area Index of trees [-]

LAI_{path} = LAI along path length of radiation beam through canopy (fractional surface area of leaves projected on a plane perpendicular to the path) [-]

M = canopy cover (i.e., fraction of total ground surface covered by vegetation) [-]

m = exponent relating shear stress on foliage to horizontal wind velocity and having the nominal value 0.5 for the foliage elements of trees [-]

N = maximum possible sunshine duration in a day [hour]

n = actual duration of sunshine in a day [hour]

n = number of sides of each foliage element producing surface resistance to wind and having the nominal value 2 for the foliage elements of trees [-]

P = quantity of precipitation [mm]

p = average fraction of Total Available Soil Water that can be depleted from the root zone before moisture stress [-]

$q(z)$ = air specific humidity at height z (mass of water vapour per unit mass of dry air) [-]

q_s = saturation air specific humidity (mass of water vapour per unit mass of dry air) [-]

R_a = extraterrestrial radiation (solar radiation received at the top of the Earth's atmosphere on a horizontal surface) [MJ m^{-2} day^{-1}]

R_G = global radiation [MJ $m^{-2}day^{-1}$]

R_N = net radiation [J m^{-2} day^{-1}]

R_n = net radiation at the crop surface [MJ m^{-2} day^{-1}]

R_{nl} = net long-wave radiation [MJ m^{-2} day^{-1}]

R_{ns} = net solar or short-wave radiation [MJ m^{-2} day^{-1}]

R_s = solar or short-wave radiation [MJ m^{-2} day^{-1}]

R_{so} = clear-sky solar or clear-sky short-wave radiation [MJ m^{-2} day^{-1}]

RAW = Readily Available soil Water in root zone [mm]

RH_{max} = average daily maximum relative humidity [%]

RH_{min} = average daily minimum relative humidity [%]

r_a = atmospheric or aerodynamic resistance [s m^{-1}]

r_c = canopy resistance [s m^{-1}]

r_{ex} = excess resistance [s m^{-1}]

r_i = interleaf layer resistance [s m^{-1}]

r_{lb} = leaf boundary layer resistance per unit area of leaf surface [s m^{-1}]

r_{ls} = stomatal resistance per unit area of leaf surface [s m^{-1}]

r-value = red channel intensity of pixel, 0-255 [-]

S_{area} = total area of object [m^2]

S_{crown} = area of projection of crown of tree [m^2]

T = soil temperature, ^oC;

T = mean daily air temperature at 2 m height [ºC]

T_a = air temperature at screen height

T_s = (air) temperature at the surface

T_d = the dewpoint of air at screen height [ºC]

T_{max} = average daily maximum air temperature at 2 m above ground surface [°C]

T_{min} = average daily minimum air temperature at 2 m above ground surface [°C]

T_{mean} = daily mean air temperature at screen (2 m) height [°C]

TAW = Total Available soil Water in the root zone [mm]

threshold_blue = threshold value of blue channel intensity of pixel, 0–255 [-]

threshold_green = threshold value of blue channel intensity of pixel, 0–255 [-]

threshold_red = threshold value of blue channel intensity of pixel, 0–255 [-]

$u(z)$ = mean horizontal wind velocity at height z [m s^{-1}]

u_* = shear velocity [m s^{-1}]

u_2 = mean horizontal wind speed at 2 m height [m s^{-1}]

z_0 = surface roughness length [m]

(z_{0h}) = roughness length for vapour and heat [m]

(z_{0m}) = roughness length for momentum [m]

Z_r = rooting depth [m]

z_h = height of temperature and humidity measurements [m]

z_m = height of wind speed measurements [m]

α_v = ratio of the von Kármán constants for water vapour and momentum, ≈ 1 [-]

β = momentum extinction coefficient = cosine of angle leaf surface makes with horizontal [-]

$\gamma = mn\beta$ = extinction parameter for horizontal wind velocity [-]

γ, γ_0 = psychrometer constant, expressing the physical connection between sensible heat transport and vapour transport by moving air [kPa $^oC^{-1}$]

Δ = slope of saturation vapour pressure curve [kPa $^oC^{-1}$]

θ_{FC} = water content at field capacity [$m^3\,m^{-3}$]

θ_{Sat} = soil volumetric water content when all pores are saturated with water [$m^3\,m^{-3}$]

θ_{WP} = water content at wilting point [$m^3\,m^{-3}$]

θ_a = actual soil volumetric water content [$m^3\,m^{-3}$]

θ_t = threshold soil water content below which transpiration is reduced due to water stress [$m^3\,m^{-3}$]

λ = latent heat of vaporization per unit mass of liquid water [MJ kg^{-1}]

$\xi = \frac{h-z}{h-h_s}$, relative distance down from the crown top [-]

ρ = air (fluid) mass density [g cm^{-3}]

σ = Stefan-Boltzmann constant [$4.903 \cdot 10^{-9}$ MJ $K^{-4}\,m^{-2}\,day^{-1}$]

τ_0 = shear stress at the top of the canopy [N m^{-2}]

REFERENCES

Allen, R.G., Jensen, M.E., Wright, J.L., Burman D., 1989. Operational estimates of reference evaporation. Agronomy Journal 81, 650-662.

Allen, R.G., Pereira, L.S., Raes, D., Smith, M., 1998. Crop evaporation. Guidelines for computing crop water requirements. Irrigation and Drainage Paper 56, FAO, Rome, Italy, 300 pp.

Arnaez, J., Lasanta, T., Ruiz-Flano, P., Ortigosa, L., 2007. Factors affecting runoff and erosion under simulated rainfall in Mediterranean vineyards. Soil & Tillage Research 93: 324-334.

Aston, A.R., 1979. Rainfall interception by eight small trees. Division of Plant Industry, CSIRO, Canberra, pp. 383-395.

Auclair, D., Dupraz, C. (Eds), 1999. Agroforestry for sustainable land-use: fundamental research and modelling with emphasis on temperate and Mediterranean applications: selected papers from a workshop held in Montpellier, France, 23−29 June 1997. Kluwer, Dordrecht, The Netherlands, pp. 272.

Bakker, J.W., 1992. Techniques to promote plant growth applied to urban sites. Water Saving Techniques for Plant Growth, Kluwer Academic Publishers, Dordrecht, The Netherlands, pp. 223-228.

Bakker, J.W., Van den Akker, J.J.H., Cornelissen, P., 1995. Oorzaak en preventie van schade aan wegen door vochtonttrekking door bomen. Rapport 318, DLO-Staring Centrum, Wageningen, 103 pp.

Barry, R.G., Chorley, R.J., 2003. Atmosphere, weather and climate. Routledge, London, UK, 421 pp.

Beetz, A., 2002. Agroforestry overview. ATTRA (Appropriate Technology Transfer for Rural Areas), Fayetteville Arkansas, 16 pp.

Black, T.A., Kellihier, F.M., 1989. Processes controlling understorey evapotranspiration. Phil. Trans. R. Soc. Lond. B 324: 207-231.

Bockheim J.G., 1974. Nature and properties of highly disturbed urban soils, Philadelphia, Pa. Paper presented before Div. S-5, Soil Science Soc. Am. Annual meeting, Chicago, IL.

Bruin de, H.A.R., 1987. From Penman to Makkink. In: Hooghart, J.C. (Ed.), Evaporation and weather, TNO Committee on Hydrological Research, Proceedings and Information No. 39, The Hague, The Netherlands, pp. 5-31.

Brutsaert, W.H., 1982. Evaporation into the atmosphere, Reidel, Dordrecht, Holland, 299 pp.

Bussiere, F., 1992. Rainfall interception by plant canopies, consequences for water partitioning in intercropping systems. Ecophysiology of Tropical Intercropping, Paris, INRA, pp. 163-174.

City-ecosystem, 1996. Lihacheva E.A., Timofeev D.A., Zhidkov M.P. (Eds.). IGRAN, Moscow, pp. 94-231.

Condition of green plantations in Moscow (according to monitoring 2002), 2003. The Analytical Report, 6, Prima-M, Moscow, 200 pp.

Condition of green plantations in Moscow (according to monitoring 2003), 2004. The Analytical Report, 7, Prima-M, Moscow, 224 p.

Eagleson, P.S., 2002. Ecohydrology. Darwinian expression of vegetation form and function. Cambridge University Press, Cambridge, U.K., 443 pp.

Feddes, R.A., Van Dam, J.C. and Witte, J.P.M., 2003. Soil Physics and Agrohydrology. Lecture Notes, Chair Soil Physics, Agrohydrology and Groundwater Management. Wageningen University, Wageningen, The Netherlands, pp. 9-11.

Ferguson, B.K., 2005. Porous Pavements. CRC Press, Boca Raton, Florida, 577 pp.

Frere, M. A., 1979. Method for the practical application of the Penman formula for the estimation of potential evapotranspiration and evaporation from a free water surface. Rome, FAO, 26 pp.

Frere, M., Popov, G.F., 1979. Agrometeorological crop monitoring and forecasting, Rome, FAO, 64 pp.

Gash, J.H.C., 1979. An analytical model of rainfall interception by forests. Quart. J. Royal Meteorol. Soc. 105, 43-55.

Gerasimova M.I., Stroganova M.N., Mozharova N.V., Prokofeva T.V., 2003. Anthropogenic soil: genesis, geography, reclaiming. Oykumena, Smolensk, 268 pp.

Goudriaan, J., 1977. Crop micrometeorology: a simulation study. Wageningen, Pudoc, 249 pp.

Gregory, P.J., 2006. Plant roots: growth, activity, and interaction with soils. Blackwell, Oxford, 318 pp.

Grey, G.W., 1996. The urban forest. Comprehensive management. New York, John Wiley & Sons, INC, 156 pp.

Hardin, P.J., Jensen, R.R., 2007. The effect of urban leaf area on summertime urban surface kinetic temperatures: A Terre Haute case study. Urban Forestry and Urban Greening 6: 63-72.

Hromov, S.P., Petrosynz M.A., 2001. Meteorology and climatology. Moscow State

University, Moscow, 450 pp.

Huinink, J.T.M., 1998. Neerslag, Verdamping en Neerslagoverschotten. Regionale verschillen binnen Nederland. Informatie- en KennisCentrum Landbouw, Ede, The Netherlands, 42 pp. *In Dutch.*

Isaev, A.A., 2001. Ecological climatology. Scientific World, Moscow, 456 pp.

Isaev, A.A., 2002. Atmospheric precipitation. Part I. Variability of characteristics of precipitations in territory of Russia and the neighboring countries. Moscow State University, Moscow, 191 pp.

Janson, T.J.M., 1994. Stadsbomen Vademecum. Deel 4: Boomsoorten en gebruikswaarde (City trees handbook. Part 4: Tree species and practical value). IPC Groene Ruimte, Arnhem, The Netherlands, 375 pp.

Jensen, M.E., Burman, R.D., Allen, R.G., 1990. Evapotranspiration and irrigation water requirements. ASCE manuals and reports on engineering practice no. 70, ASCE, New York. 332 pp.

Kareva, M., 2005. April 2005 conditions of trees and substrates at selected sites in The Hague. City Management Department of Municipality The Hague, The Netherlands / Moscow State forest University, Russia / Wageningen University, The Netherlands, pp. 79 + appendix.

Kellihier, F.M., Black, T.A., Price, D.T., 1986. Estimating the effects of understory removal from a Douglas fir forest using a two-layer canopy evapotranspiration model. Water Resources Research, vol. 22, no 13, 1891-1899.

Kramer, P.J., Kozlowski, T.T., 1979. Physiology of woody plants. New York, Academic Press, 811 pp.

Kroes J.G., Van Dam, J.C., Huygen, J., Vervoort, R.W., 2002. User’s Guide of SWAP version 2.0. Simulation of water flow, solute transport and plant growth in the soil – water – atmosphere – plant environment. Alterra-report 610, Alterra, Wageningen, The Netherlands, 137 pp.

Kroes, J.G., Van Dam, J.C. (Eds.), 2003. Reference Manual SWAP version 3.0.3. Alterra-report 773, Alterra, Wageningen, The Netherlands, 210 pp.

Kutschera, L., Lichtenegger, E., 2002. Wurzelatlas: mitteleuropäischer Waldbäume und Sträucher. Stocker, Graz, 604 pp. *In German*.

Landsberg, H.E., 1981. The urban climate. Academic press, New York, 275 pp.

Landsberg, J.J., 1986. Physiological ecology of forest production.Academic press, London, pp. 133-164.

Landsberg, J.J., McMurtrie, R., 1984. Water use by isolated trees. Agricultural Water Management, 8, 223-242.

Larcher, W., 1995. Physiological Plant Ecology, 3rd edition. Springer Verlag, Berlin, Germany, 506 pp.

Lhomme, J.-P., 1997. A theoretical basis for the Priestley-Taylor coefficient. Boundary-Layer Meteorology, 82, 179-191.

Lihacheva, E.A., Smirnova, E.B., 1994. Environmental problems of Moscow for 150 years. Moscow, pp. 10-16.

Lihacheva, E.A., Timofeev, D.A., Zhidkov, M.P. (Eds.), 1996. City-ecosystem. IGRAN, Moscow, pp. 94-231.

Lindsey, P.A., Bassuk, N.L., 1992. A nondestructive image analysis technique for estimating whole-tree leaf area. HortTechnology 2(1): 66-72.

Lvovich, M.I., Chernogaeva, G.M., 1977. The water balance of Moscow. Symposium Effects of urbanization and industrialization on the hydrological regime and on water quality, IAHS-AISH Publication, 123, 48-51.

Maas, E.V., 1990. Crop salt tolerance. In: K.K. Tanji (Ed.), Agricultural salinity assessment and management. ASCE Manuals and Reports on Engineering practice, 71, New York, 619 pp.

Maas, E.V., Hoffman, G.J., 1977. Crop salt tolerance-current assessment. J. Irrig. and Drainage Div., 103, 115-134.

Makarova, O.V., 2003. Soil technological and other ecological aspects of state of trees in Moscow. PhD Thesis Wageningen University, 140 pp.

Makkink, G.F., 1957. Ekzameno de la formulo de Penman. Neth. J. Agric. Sci., 5, 290-305.

Makkink, G.F., 1962. Vijf jaren lysimeteronderzoek. Verslagen van landbouwkundige onderzoekingen nr 68.1, PUDOC, Wageningen, The Netherlands, 241 pp.

Massop, H.T.L., Van Bakel, P.J.T., Kroon, T., Kroes, J.G., Tiktak, A., Werkman, W., 2005. Op zoek naar de “ware” neerslag en verdamping. Alterra-rapport 1158. Alterra, Wageningen, The Netherlands, 108 pp. In Dutch.

Mayus, M., Millet growth in windbreak-shielded fields in the Sahel. PhD Thesis Wageningen University, 259 pp.

McIntyre, S., McIvor, J.G., 2002. Managing and Conserving Grassy Woodlands. CSIRO, Collingwood, Victoria, 253 pp.

McMurtrie, R., Wolf, L., 1983. A model of competition between trees and grass for radiation, water and nutrients. Annals of Botany, 52, 449-458.

McNaughton, K., Jarvis, P.G., 1983. Predicting effects of vegetation changes on transpiration and evaporation. In: Koslowski, T.T. (Ed.), Water deficits and plant growth, Vol. VII, Academic press, New York, pp. 1-47.

Mohren, G.M.J., 1987. Simulation of forest growth, applied to douglas fir stands in The Netherlands. PhD-Thesis Wageningen University, Wageningen, The Netherlands, 184 pp.

Mohren, G.M.J., Van Laar, H.H., Scarascia-Mugnozza, G, 1994. Systems analysis and simulation in forest ecology and silviculture. A simulation course. Trento, Italy, 2-12 November 1994. Dept Theoretical Production Ecology, Wageningen Agricultural University, Wageningen, The Netherlands, 237 pp.

Monteith, J.L., 1965. Evaporation and the environment. Symp. Soc. Exptl. Biol., 19, 205-234.

Monteith, J.L., 1981. Evaporation and surface temperature. Quart. J. Royal Meteorol. Soc., 107, 1-27.

NN, 1965. De bodem van Nederland (The soils of The Netherlands). Stiboka, Wageningen, The Netherlands, 292 pp.

NN, 1996a. Ermittlung der Verdunstung von Land- und Wasserflaechen. Deutscher Verband fuer Wasserwirtschaft und Kulturbau e.V. (DVWK), Merkblaetter zur Wasserwirtschaft 238/1996. Bonn, Germany, 135 pp. *In German.*

NN, 1996b. Hydrology handbook. Second edition. ASCE, New York. 784 pp.

NN, 2003. Condition of green plantations in Moscow (according to monitoring 2002). The analytical report, 6, Prima-M, Moscow, 200 pp.

NN, 2004. Condition of green plantations in Moscow (according to monitoring 2003). The analytical report, 7, Prima-M, Moscow, 224 pp.

NN, 2005. The report about condition of environment of Moscow for the year 2004. Department of Nature Management and Protection of Environment of City of Moscow, Moscow.

Norman, J.M., Campbell, G.S., 1989. Canopy structure. In: Pearcy, R.W., Ehleringer, J.R., Mooney, H.A. and Rundel, P.W. (Eds). Plant Physiological Ecology. Field methods and instrumentation. Chapman and Hall, London, New York, pp. 301-325.

Ogink-Hendriks, M.J., 1995. Modelling surface conductance and transpiration of an oak forest in The Netherlands. Agricultural and Forest Meteorology, 74, 99-118.

Oke, T.R., 1987. Boundary layer climates. Methuen, London, New York, pp. 154-157.

Oker-Blom, P., 1988. Models of light interception in forest stands. Simulation of forest growth: a course on basic aspects of simulation of plant growth, applied to forest growth in Finland, University of Joensuu, Mekrijävi, Finland, 44 pp.

Partsch, C.M., Jarrett, A.R., Watschke, T.L., 1993. Infiltration characteristics of residential lawns. Transactions of the ASAE 36 (6): 1695-1701.

Penman, H.L., 1948. Natural evaporation from open water, bare soil and grass. Proc. Roy. Soc. London, Ser. A, 193, 120-145.

Penman, H. L. 1963. Vegetation and hydrology. Tech. Comm. No. 53, Commonwealth Bureau of Soils, Harpenden, England. 125 pp.

Pratt, W.K., 2007. Digital Image processing. Wiley, Hoboken, New Jersey, USA, 782 pp.

Priestley, C.H.B., Taylor, R.J., 1972. On the assessment of surface heat flux and evaporation using large-scale parameters. Monthly Weather Rev., 100(2), 81-92.

Rauner, J.L., 1976. Deciduous forests. In: Monteith, J.L. (Ed.), Vegetation and the Atmosphere. Case Studies, Vol. 2. Academic press, New York, pp. 241-264.

Ritchie, J.T., 1972. Model for predicting evapotranspiration from a row crop with incomplete cover. Water Resources Research, 8, 1208-1213.

Ritchie, J.T., Johnson, B.S., 1990. Soil and plant factors affecting evaporation. In: Stewart, B.A., Nielsen, D.R., Bruce, R.R., Kanemasu, E.T., Niehaus, M.H., Mickelson, S.H. (Eds), Irrigation of agricultural crops. ASA, Madison, pp. 363–390.

Roloff, A., 1989. Kronenentwicklung und Vitalitaetsbeurteilung ausgewaehlter Baumarten der gemaessigten Breiten. J.D. Sauerlander's Verlag, Frankfurt am Main, Deutschland, 258 pp. *In German.*

Rowntree, P.R., 1991. Atmospheric parameterization schemes for evaporation over land: basic concepts and climate modeling aspects. In: Schmugge, T.J. and André, J.C. (Eds.), Land Surface Evaporation. Measurement and Parameterization, Springer Verlag, Heidelberg, Germany, pp. 5-29.

Rutter, A.J., Morton, A.J., Robins, P.C., 1975. A predictive model of rainfall interception in forests. II: Generalization of the model and comparison with observations in some coniferous and hardwood stands. J. Appl. Ecol., 12, 367-384.

Schachtschabel, P., Blume, H.P., Bruemmer, G., Hartge, K.H., Schwertmann, U., 1989. Lehrbuch der Bodenkunde (Textbook of Soil Science). Ferdinand Enke Verlag, Stuttgart, Germany, 491 pp.

Schmugge, T.J., Andre, J.C., 1991. Land surface evaporation: measurement and parameterization. New York, Springer, 424 pp.

Scholes, R.J., Archer, S.R., 1997. Tree-grass interactions in savannas. Annu. Rev. Ecol. Syst., 28, 517-544.

Shaw, R.H., Pereira, A.R., 1982. Aerodynamic roughness of a plant canopy: A numerical experiment. Agric. Meteorol., 26, 1498-1501.

Shuttleworth, W.J., 1989. Micrometeorology of temperate and tropical forest. Phil. Trans. R. Soc. Lond., B 324, 299-334.

Shuttleworth, W.J., 1991. Evaporation models in hydrology. In: Schmugge, T.J., André, J.C. (Eds.), Land Surface Evaporation. Measurement and Parameterization. Springer Verlag, Heidelberg, Germany, pp. 93-120.

Shuttleworth, W.J.,Wallace, J.S., 1985. Evaporation from sparse crops – an energy combination theory. Quarterly Journal of the Royal Meteorological Society, 111, 839-855.

Sinoquet, H., Cruz, P. (eds), 1995. Ecophysiology of tropical intercropping. INRA, Paris, France, 483 pp.

Spittlehouse, D.L., Black, T.A., 1982. A growing season water balance model used to partition water use between trees and understorey. In: Proceedings of the Canadian Hydrology Symposium. Associate Committee on Hydrology, National Research Council of Canada, Ottawa, pp. 195-214.

Stroganova, M.N., Agarkova, M.G., 1992. City soils: experience of studying and systematization (on example soils of southwest part of Moscow). Soil Science, 7, 16-24.

Stroganova, M.N., Agarkova, M.G, Miagkova, A.D., 1997. Soils and soil cover of Moscow. In: Dobrovolskiy, G.V. (Ed.), Soil, city, environment. Fund «For economic literacy», Moscow, pp. 181-265.

Van Keulen, H., Wolf, J. (Eds.), 1986. Modelling of agricultural production: weather, soils and crops. Simulation Monographs, Pudoc, Wageningen, The Netherlands, 479 pp.

Vrecenak, A.J., Herrington, L.P., 1984. Modeling transpiration from selected urban shade tree species. J. Environ. Hort., 2(4), 130-135.

Weissenhorn, I., 2002. Mycorrhiza and Salt Tolerance of Trees. Final report of EU-project Mycorem, Nederland, 36 pp.

Welles, J.M., Norman, J.M., 1991. Instrument for indirect measurement of canopy structure. Agronomy Journal, 83, 818-825.

Woesten, J.H.M., Veerman, G.J., DeGroot, W.J.M., Stolte, J., 2001. Waterretentie- en doorlatendheidskarakteristieken van boven- en ondergronden in Nederland: de Staringreeks, Vernieuwde uitgave 2001, Alterra, Research Instituut voor de Groene Ruimte, Alterra-rapport 153, Wageningen,pp. 18-19; 62-83. In Dutch.

Zubov, V.I. (Ed), 1998. Sketches about ecology of Moscow region, 1998. MPU, Moscow, 240 pp.

SUMMARY

Moscow is a very large megalopolis and the politic, cultural and financial center of Russia. Moscow is located between 55^{o} and 56^{o} northern latitude and 37^{o} and 38^{o} east longitude, between the rivers Oka and Volga. The territory of the city is located at a height of 150 m above sea level. Average duration of the vegetative period is 175 days. The average temperature of January is –9.4 ^{0}C and of July is +18.4 ^{0}C. In the last years the air mid-annual temperature has increased. The amount of precipitations in Moscow is usually 540−650 mm per year. Monthly average wind speed is equal to 1.8−2.2 m/s, but frequency of winds of 0−1 m/s (38%) and of calms (18%) has increased. The current relief map of Moscow is substantially formed by sediments from the glacial epoch (Moscowskaya and Dneprovskaya moraines), erosive activity of the rivers, and anthropogenic sediments. The anthropogenic influence caused an intensive transformation of natural peat soil, floodplain soil, podzolic and sod-podzol soils into specific soil: anthropogenic-superficial-reformed natural soil called «urbo-soil»; anthropogenic deep-reformed soil called «urbanozem»; and a specific soil called «technozem». The total size of the green areas of the city (trees, shrubs, lawns) equals about 16785.8 ha. About 19.5% of the trees are *Tilia cordata.* The largest part of the green sites is occupied by "tree –lawn" combinations.

Anthropogenic factors like intensive increase of urban buildings and communications and large areas of roofs and asphalt coverings etc. influence the natural cycle of climate parameters and discomforts the urban vegetation.

In order to estimate these changes the concept of evapotranspiration was used as a basic informative parameter. This quantity makes it possible to unite data on climate parameters, state of trees and lawn, expressed as Leaf Area Index (LAI), and conditions of the soil in the city. Evapotranspiration is the undifferentiated sum of the evaporation and transpiration process. Evaporation is the process whereby liquid water is converted into water vapour and removed from the evaporating surface (rivers, bare soil, wet vegetation). Transpiration is the process of vaporization of liquid water contained in plants through stomata of the leaves and the vapour removal to the atmosphere. When soil water content is lower than the optimum range or rate of transpiration is very high, plants are in a stress situation.

Many evapotranspiration models exist, but, for tree-lawn combinations in Moscow, we applied a system of calculations based on FAO guidelines. Additionally, for reference

evapotranspiration, we applied Makkink's radiation model. Besides, an algorithm was developed for the estimation of LAI values through digital photos of tree crowns and lawn areas and digital image analysis with computer.

Values of water stress coefficient, salinity stress coefficient, actual evapotranspiration, part of precipitations that is intercepted by the canopy, and water loss from root zones were also calculated. The values were obtained for sites with trees (*Tilia cordata*) and lawn for the vegetation stages (periods): Initial (15.04.04-15.05.04); Development (16.05.04-14.06.04); Mid-season (15.06.04−16.07.04; 17.07.04−16.08.04; 17.08.04−14.09.04); Late season (15.09.04−15.10.04).

The value of the reference evapotranspiration (ET_0) in the Initial stage (15.04.04−15.05.04) is 1.97 mm/day. Maximal ET_0 values were observed during the Mid-season (periods 15.06.04−16.07.04 and 17.07.04−16.08.04), being 2.45−2.61 mm/day.

Values of LAI were obtained for individual trees and for plantings (alley or biogroup) of *Tilia cordata* and for lawn on different objects of Moscow: Habarovskaya st., Saharov pr., Sokolniki (Strominka st.).

During the Initial stage majority of trees have LAI values of 1.65−5.44 (max = 6.04; min = 0.67) and lawns have LAI values of 0.18−1.84 (max = 5.26; min = 0.09).

Typically, maximum values of LAI of trees occur for the Mid-season periods 15.06.04−16.07.04 and 17.07.04−16.08.04 and equal 3.48−7.12 (max = 8.96; min = 1.92). For lawn these periods were different (15.06.04−16.07.04 and 17.08.04−14.09.04) and absolute maximum and minimum LAI could be observed in one and the same period. Maximum LAI = 3.03 and minimum LAI = 0.08.

On the level of individual trees and lawn-plots maximal values were observed on Sokolniki and minimal values on Habarovskaya st. If trees have rather high LAI at initial stage they increase LAI or keep it at a high level during the whole further vegetative period. Trees with lowest LAI values typically have insignificant increase of the parameter. The lawns had non-uniform development during the whole vegetative period.

Considering LAI of set of trees (alley or biogroup), the objects had during the Initial stage on average LAI = 1.85−5.12 and during Mid-season 4.17−7.11. For lawn during the Initial stage average values of LAI = 0.54−4.81 were observed (soil fraction covered by grass 0.237−0.910). Change of LAI of lawn during the vegetative period has no clear regularity and is characterized by the "incidental" occurrence of periods with increasing or decreasing values. The maximal values for Mid-season are 1.11−1.30 (soil fraction covered by grass

0.426–0.478). Consequently, in most cases, more than 50% of the area is exposed (bare soil).

Based on calculations of crop coefficients evapotranspiration values were obtained for tree-grass combinations, $ET_{combination}$. In Initial stage $ET_{combination}$ = 0.89 mm/day; during Mid-season this value increases to $ET_{combination}$ = 1.51–2.46 mm/day; for Late season $ET_{combination}$ = 0.50 mm/day. The differences of $ET_{combination}$ between objects during Mid-season were equal to a factor of 1.6.

In order to find reasons for the differences in the state of trees, volumetric water contents of the root zones were estimated from soil water content measurements at a range of depths and a number of points of time. During the Initial stage, already two objects from a total of five had water contents lower than the critical level (24%). During Development stage, a similar situation was observed on all objects (even a "wilting point" water content occurred). When the amount of precipitation was high (244 mm), i.e. in the Mid-season period 15.06.04–16.07.04, most objects were in an even more critical state.

Later, in 17.08.04–14.09.04, the water content decreased again below 24%. Here, water stress coefficients were often < 1. Only during 15.06.04–16.07.04 the coefficient reached 1 for all objects. The stressful situation could be explained by the dry state of the soil, high runoff values and development of larger transpiration surface (LAI).

Consequently, values of actual evapotranspiration $ET_{a,\ combination}$ decreased and were 0.25–0.89 mm/day during Initial stage, up to 1.35 mm/day during Development stage, 1.31–2.38 mm/day during Mid-season 15.06.04–16.07.04, the last value being the maximum.

During the vegetative period some parts of the precipitations were intercepted by canopies of trees and grass, $I_{combination}$. This parameter is 0.69–11.49 mm for the Initial stage, which is 2.1–34.6% from the total precipitation in that period. It is 1.92–13.75 mm for the Development stage (4.0–28.5%). The interception during Mid-season was not estimated because of incidence of extreme rainfall events. $I_{combination}$ is low for Late season 15.09.04–15.10.04.

Losses of water from root zones per object and period were calculated using water characteristics of the soil and an assumed root depth of 1 m. The calculations pointed to important features. Deep percolation occurred in early spring and late autumn, but not in late spring, summer and early autumn. Runoff was high due to a limited infiltration capacity. Volume of root zones was reduced. The rainfall would be enough to support a potential evapotranspiration.

The obtained data show the need for the development of a new procedure for the estimation of the condition of urban plantings, a procedure that takes into account the seasonal dynamics of the conditions of growth: climatic, soil-hydrological and anthropogenic conditions. In this procedure, special attention should be given to the Initial and Development stages for Moscow conditions. The current assessment procedure estimates the condition of the city plantings during the second part of Mid-season, which is a period of stabilization without a possibility to change the consequences of stress factors. The new approach will allow to project actions for improvement of conditions of growth: preparation of optimum soil mixes; duly watering; a complex care.

SAMENVATTING

Moskou is een zeer grote megalopolis en het politieke, culturele en financiële centrum van Rusland. Moskou is gesitueerd tussen 55^o en 56^o noorderbreedte en 37^o en 38^o oosterlengte, tussen de rivieren Oka en Wolga. Het territorium van de stad ligt op een hoogte van 150 m boven zeeniveau. De gemiddelde duur van de periode waarin plantengroei kan plaats vinden is 175 dagen. De gemiddelde temperatuur van januari is –9,4 ^oC en van juli +18,4 ^oC. Gedurende de laatste jaren is de temperatuur van het jaarmidden gestegen. De neerslaghoeveelheid in Moskou is meestal 540 − 650 mm per jaar. Het maandgemiddelde van de windsnelheid is gelijk aan 1.8 – 2.2 m/s, maar de frequentie van windsnelheden van 0 − 1 m/s (38%) en van windstilte (18%) is toegenomen. Het huidige reliëf van Moskou is hoofdzakelijk gevormd door sedimenten uit de glaciale periode (Moscowskaya en Dneprovskaya moraines), erosieve activiteit van de rivieren, en anthropogene sedimenten. De anthropogene invloed veroorzaakte een intensieve transformatie van natuurlijke veengronden, overstromingsvlaktes, podsolen en gras-podsolen in specifieke bodems: anthropogeen-oppervlakkig-veranderde natuurlijke bodem, genaamd «urbo-soil»; anthropogeen-diep-veranderde bodem, genaamd «urbanozem»; en een specifieke bodem genaamd «technozem». De totale oppervlakte van de groene gebieden van de stad (bomen, struiken, gazon) is ongeveer gelijk aan 16785,8 ha. Ongeveer 19,5% van de bomen is *Tilia cordata.* Het grootste deel van deze gebieden bestaat uit “bomen-gazon” combinaties.

Anthropogene faktoren zoals een intensieve toename van stedelijke bebouwing en communicatievoorzieningen en grote oppervlaktes daken en asfalt-dekken etc. beïnvloeden de natuurlijke cyclus van klimaatparameters en hinderen de stedelijke vegetatie.

Teneinde dit te onderzoeken is het evapotranspiratie-concept gebruikt als basale informatieparameter. Deze grootheid maakt het combineren mogelijk van waardes van: klimaatparameters, de conditie van bomen en gazon, uitgedrukt in de bebladeringsindex (LAI), en de conditie van de bodem in de stad. Evapotranspiratie is de ongedifferentieerde som van de evaporatie en transpiratie processen. Evaporatie is het proces waarbij water in vloeibare vorm wordt omgezet in waterdamp en afgevoerd wordt van het verdampende oppervlak (rivieren, onbegroeide grond, natte vegetatie). Transpiratie is het proces van verdamping van zich in planten bevindend vloeibaar water via stomata van de bladeren en de afvoer van de waterdamp naar de atmosfeer. Indien het vochtgehalte van de bodem lager is dan het optimale traject, of indien de transpiratiesnelheid zeer hoog is, verkeren planten in een

stress situatie.

Er bestaan vele evapotranspiratiemodellen, maar voor de boom-gazon combinaties in Moskou is een berekeningssysteem gebaseerd op FAO richtlijnen gebruikt. Daarnaast is ook het stralingsmodel van Makkink voor referentie-evapotranspiratie toegepast. Bovendien is een algoritme ontwikkeld voor de schatting van LAI-waardes middels digitale foto's van boomkronen en gazon-delen en digitale beeldverwerking met pc.

Ook zijn berekend: waardes van de waterstress factor, de zoutstress factor, actuele evapotranspiratie, het deel van de neerslag dat is onderschept door de bovengrondse plantendelen (interceptie), en het waterverlies van wortelzones. De waardes zijn verkregen voor locaties met bomen (*Tilia cordata*) en gazon voor de volgende vegetatie stadia (periodes): Initieel (15.04.04−15.05.04); Ontwikkeling (16.05.04−14.06.04); Middenseizoen (15.06.04 − 16.07.04; 17.07.04 − 16.08.04; 17.08.04 − 14.09.04); Laatseizoen (15.09.04 − 15.10.04).

De waarde van de referentieverdamping (ET_0) in het Initiële stadium (15.04.04 − 15.05.04) is 1,97 mm/dag. Maximale ET_0 waardes werden waargenomen gedurende het Middenseizoen (periodes 15.06.04 − 16.07.04 en 17.07.04 − 16.08.04): 2,45 − 2,61 mm/dag.

Waardes voor LAI werden verkregen voor individuele bomen en voor plantsoen (allee of biogroep) van de soort *Tilia cordata*, en voor gazon, op verschillende objekten van Moskou: Habarovskaya st., Saharov pr., Sokolniki (Strominka st.).

Gedurende het Initiële stadium hebben de meeste bomen een LAI van 1,65 − 5,44 (max = 6,04; min = 0,67), en de gazons een LAI = 0,18 − 1,84 (max = 5,26; min = 0,09).

Maximale waardes voor LAI van de bomen zijn karakteristiek voor de Middenseizoen periodes 15.06.04 − 16.07.04 en 17.07.04 − 16.08.04 en gelijk aan 3,48 − 7,12 (max = 8,96; min = 1,92). Voor gazon waren deze periodes verschillend (15.06.04 − 16.07.04 en 17.08.04 − 14.09.04) en konden de absolute maximum en minimum LAI waargenomen worden in dezelfde periode. Maximum LAI = 3,03 en minimum LAI = 0,08.

Op het niveau van individuele bomen en gazon-delen werden maximale waardes waargenomen op Sokolniki en minimale waardes op Habarovskaya st. Indien bomen een nogal hoge LAI hebben in het Initiële stadium, dan verhogen zij hun LAI of houden deze op een hoog niveau gedurende de gehele verdere vegetatieve periode. Bomen met de laagste LAI waardes kenmerken zich door een slechts insignificante toename van de parameter. De gazons vertoonden niet-uniforme ontwikkeling gedurende de gehele vegetatieve periode.

Op het niveau van boomgroepen (allee of biogroep) hadden de objekten gedurende het

Initiele stadium een gemiddelde LAI van 1,85 − 5,12 en gedurende het Middenseizoen van 4,17 − 7,11. Voor gazon gedurende het Initiële stadium werden gemiddelde LAIs van 0,54 − 4,81 waargenomen (bedekkingsgraad van het gras 0,237 − 0,910). De verandering van LAI van gazon gedurende de vegetatieve periode vertoonde geen duidelijke regelmatigheid en is gekarakteriseerd door een "toevallig" optreden van periodes met toenemende of afnemende waardes. De maximale waardes voor het Middenseizoen zijn 1,11 − 1,30 (graad van bedekking van grond door gras 0,426 − 0,478). Het betekent dat in de meeste gevallen meer dan 50% van het oppervlak bestaat uit onbegroeide grond.

Gebaseerd op berekeningen van gewasfaktoren zijn evapotranspiratie-waardes verkregen voor boom-gras combinaties, $ET_{combination}$. In het Initiële stadium heeft deze de waarde 0,89 mm/dag; gedurende het Middenseizoen neemt deze toe tot 1,51 − 2,46 mm/dag; voor het Laatseizoen is de waarde: 0,50 mm/dag. De verschillen van $ET_{combination}$ tussen de objekten gedurende het Middenseizoen waren gelijk aan een faktor 1,6.

Teneinde oorzaken te vinden voor de verschillen in boomconditie zijn vochtgehaltes van de wortelzones geschat uit vochtgehaltes die gemeten zijn op een reeks van dieptes en op een reeks van tijdstippen. Gedurende het Initiële stadium hadden al twee objekten (uit een totaal van vijf) vochtgehaltes lager dan het kritische niveau (24%). Gedurende het Ontwikkelingsstadium is eenzelfde situatie waargenomen voor alle objekten (zelfs een vochtgehalte overeenkomend met het verwelkingspunt). Toen de hoeveelheid neerslag erg hoog was (244 mm, in de Middenseizoen-periode 15.06.04 − 16.07.040), hadden de meeste objekten een nog meer kritieke toestand. Later, in de periode 17.08.04 − 14.09.04, daalde het vochtgehalte weer onder 24%. Toen waren de waterstress faktoren vaak < 1. Alleen gedurende 15.06.04 − 16.07.04 bereikte de waterstress faktor de waarde 1 voor alle objekten. De stress-volle situatie kon verklaard worden uit de droge toestand van de grond, het oppervlakig afstromen van veel regenwater, en de ontwikkeling van meer transpirerend oppervlak (LAI).

Dientengevolge was de actuele evapotranspiratie $ET_{a,\ combination}$ veelal kleiner dan de potentiële en was 0,25 − 0,89 mm/dag gedurende het Initiële stadium, bereikte waardes tot 1,35 mm/dag gedurende het Ontwikkelingsstadium, en was 1,31 − 2,38 mm/dag gedurende Middenseizoen 15.06.04 − 16-07.04. De laatste waarde is tevens het maximum.

Gedurende de vegetatieve periode is een deel van de neerslag onderschept door de bovengrondse delen van de bomen en het gras, $I_{combination}$. Deze parameter is 0,69 − 11,49 mm voor het Initiële stadium, wat neerkomt op 2,1 − 34,6% van de totale neerslag in die periode.

De interceptie is 1,92 − 13,75 mm voor het Ontwikkelingsstadium (4,0 − 28,5%). De interceptie gedurende het Middenseizoen is niet geschat vanwege de extreem grote regenval in die periode. $I_{combination}$ is laag voor het Laatseizoen 15.09.04 − 15.10.04.

Waterverliezen per object en periode zijn berekend uit de vochtkarakteristieken van de bodem onder aaname van een bewortelingsdiepte = 1 m. De berekeningen wezen naar belangrijke aspekten. Wegzijging naar diepere bodemlagen trad op in het vroege voorjaar en late najaar, maar niet in het late voorjaar, zomer en vroege najaar. De oppervlakkige afstroming was hoog, tengevolge van een beperkte infiltratiecapaciteit. Het volume van de wortelzones was gereduceerd. De regenval zou voldoende zijn voor een potentiële evapotranspiratie.

De verkregen gegevens tonen de behoefte aan de ontwikkeling van een nieuwe procedure voor de schatting van de conditie van stedelijke beplantingen, een procedure die rekening houdt met de seizoensgebonden dynamiek van de groeicondities: klimatologische, bodem-hydrologische en anthropogene condities. In deze procedure behoort speciale aandacht gegeven te worden aan de Initiële en Ontwikkelings-stadia voor de condities van Moskou. De huidige procedure voor vegetatie-beoordeling houdt in dat de conditie van het stedelijk groen geschat wordt in het tweede deel van het Middenseizoen. Deze periode vertoont een conditie die gestabiliseerd is, zonder de mogelijkheid tot verandering van stressfaktoren. De nieuwe benadering maakt het mogelijk om plannen voor verbetering van groeicondities mogelijk te maken: het prepareren van optimale grondmengsels; tijdig water geven; een complex van boom- en gazonverzorgingsmaatregelen.

ACKNOWLEDGEMENTS

This research project was supported by Dr. Olga V. Makarova-Kormilitsyna, Moscow State Forest University (Daily supervisor); Dr. Ir. A.J. Koolen, Wageningen University (Daily supervisor) and Prof. Dr. Ir. P.C. Struik, Wageningen University (Principal supervisor). Technical assistance was provided by the Soil Laboratory of the Moscow State Forest University. Special gratitude for help goes to Y. L. Shmelkin, Research-and-production centre "Map Maker" of GIS Meteo, and to Ir J. Meuleman, Wageningen University. The research was funded by the Netherlands Organisation for Scientific Research (NWO) and the Russian Foundation for Basic Research (RFBR).

CURRICULUM VITAE

Vasily Valentinovich Bondarenko was born in Schelkovo, Moscow Region, Russia, on the 2nd of November, 1975. In 1993, he finished High School and entered the Moscow State Forest University.

In 1998, he received the qualification of engineer of forestry management, with a specialization in landscape management. In that year he entered post-graduate education. During 3 years he studied different aspects of the influence of climate parameters, soil properties and anthropogenic factors on apical growth of forest stands.

On the 27th of April, 2001, he defended a thesis entitled "Estimation of ecological consequences of anthropogenic influence on forest soil in the Moscow Region". On the 5th of October, 2001, he obtained the scientific degree of Candidate of Biological Science, and, on the 1st of June, 2001, the qualification of engineer-researcher. From that time until present, he worked as a docent at the Soil Science Department of the Moscow State Forest University.

In October, 2003, he was invited to participate in a joint project of the Netherlands Organisation for Scientific Research (NOW) and the Russian Foundation for Basic Research (RFBR) and to prepare a PhD-thesis in urban soil technology within the Farm Technology Chair of the Wageningen University. During the years 2003–2007 he was a member of a Netherlands-Russian scientific group for research on the influence of climate, soil, hydrology, and anthropogenic activities on the state of urban soils and stands.